ISTANBUL TECHNICAL UNIVERSITY ★ GRADUATE SCHOOL OF SCIENCE ENGINEERING AND TECHNOLOGY

IDENTIFICATION EFFECTS OF PROTEIN KINASE C ACTIVATION IN NEURONS UNDER PHYSIOLOGICAL AND DEGENERATIVE CONDITIONS

Ph.D. THESIS

Şirin KORULU KOÇ

Department of Advanced Technologies

Molecular Biology – Genetics and Biotechnology Programme

NOVEMBER 2012

ISTANBUL TECHNICAL UNIVERSITY ★ GRADUATE SCHOOL OF SCIENCE ENGINEERING AND TECHNOLOGY

IDENTIFICATION EFFECTS OF PROTEIN KINASE C ACTIVATION IN NEURONS UNDER PHYSIOLOGICAL AND DEGENERATIVE CONDITIONS

Ph.D. THESIS

Şirin KORULU KOÇ
(521062206)

Department of Advanced Technologies

Molecular Biology – Genetics and Biotechnology Programme

Thesis Advisor: Prof. Dr. Arzu KARABAY KORKMAZ

NOVEMBER 2012

İSTANBUL TEKNİK ÜNİVERSİTESİ ★ FEN BİLİMLERİ ENSTİTÜSÜ

NÖRONLARDA FİZYOLOJİK VE DEJENERATİF KOŞULLAR ALTINDA PROTEİN KİNAZ C AKTİVASYONUNUN ETKİLERİNİN ARAŞTIRILMASI

DOKTORA TEZİ

Şirin KORULU KOÇ
(521062206)

İleri Teknolojiler Anabilim Dalı

Moleküler Biyoloji – Genetik ve Biyoteknoloji Programı

Tez Danışmanı: Prof. Dr. Arzu KARABAY KORKMAZ

KASIM 2012

Şirin Korulu Koç, a **Ph.D.** student of ITU **Graduate School of Science Engineering and Technology** student ID **521062206** successfully defended the **thesis** entitled **"IDENTIFICATION EFFECTS OF PROTEIN KINASE C ACTIVATION IN NEURONS UNDER PHYSIOLOGICAL AND DEGENERATIVE CONDITIONS",** which she prepared after fulfilling the requirements specified in the associated legislations, before the jury whose signatures are below.

Thesis Advisor : **Prof. Dr. Arzu KARABAY KORKMAZ**
İstanbul Technical University

Jury Members : **Prof. Dr. Melek ÖZTÜRK** .....
Istanbul University

Assoc.Prof. Dr. Eda TAHİR TURANLI .....
Istanbul Technical University

Prof. Dr. Selma YILMAZER .....
Istanbul University

Assist.Prof. Dr. Gizem DİNLER DOĞANAY .....
Istanbul Technical University

Date of Submission : 7 September 2012
Date of Defense : 19 November 2012

To my father,

FOREWORD

I would like express my most sincere gratitude to my supervisor Prof. Dr. Arzu Karabay Korkmaz for invaluable guidance, advice, and also for her motivation and morale support at difficult times. Her understanding, encouraging, stimulating advices and personal guidance have provided a strong basis for this thesis.
I want to express my deep appreciation to Ayşegül Yıldız-Ünal for her valuable friendship.
I would like to express my special gratitude to my family starting with my dear father, rest in peace, Seyit Korulu, my mother Şafiye Korulu and my sister Şermin Korulu who have always been my biggest inspirations. They have always been there for me.
Finally, my husband Ersin Koç and my little son, Ersin Kaan Koç, who are the most important and enjoyable part of my life.
I would also like to acknowledge the funding agencies. I was funded by scholarship from The Scientific and Technological Research Council of Turkey, TUBİTAK-BİDEB-2211 and this study was funded by grants to Arzu Karabay from The Turkish Academy of Sciences (TUBA)-GEBIP, TUBITAK-TBAG (108T811) and İTÜ BAP.

November 2012 Şirin KORULU KOÇ

TABLE OF CONTENTS

Page

ABBREVIATIONS

BCA	: Bicinchoninic acid
BSA	: Bovine serum albumin
cDNA	: Complementary deoxyribonucleic acid
DAPI	: 4',6-diamidino-2-phenylindole
DIV	: Day in vitro
DMSO	: Dimethyl sulfoxide
DNA	: Deoxyribonucleic acid
dNTP	: Deoxyribonucleotide
FBS	: Fetal bovine serum
GAPD	: Glyceraldehyde 3-phosphate dehydrogenase
Gö6976	: 12-(2-Cyanoethyl)-6,7,12,13-tetrahydro-13-methyl-5-oxo-5H-indolo [2,3-a]pyrrolo[3,4-c]
HEPES	: 4-(2-hydroxyethyl)-1-piperazineethanesulfonic acid
HRP	: Horse radish peroxidase
NFTs	: Neurofibrillary tangles
PKC	: Protein kinase C
PMA	: Phorbol 12-myristate 13-acetate
pRb	: Retinoblastoma protein
ppRb	: Phosphorylated retinoblastoma protein
RNA	: Ribonucleic acid
SDS	: Sodium dodecyl sulfate
SDS-PAGE	: Sodium dodecyl sulphate-polyacrylaimde gel electrophoresis
SPSS	: Statistical package for the social sciences statistical analysis program
Tris	: Tris(hydroxymethyl)aminomethane
µg	: Microgram
µl	: Microliter
µM	: Micromolar

LIST OF TABLES

Page

LIST OF FIGURES

Page

IDENTIFICATION EFFECTS OF PROTEIN KINASE C ACTIVATION IN NEURONS UNDER PHYSIOLOGICAL AND DEGENERATIVE CONDITIONS

SUMMARY

Neurons are highly differentiated cells and specialized for the processing and transmission of cellular signals. Neurons develop from mitotic cells of ectodermal origin and after several divisions, these cells begin to express neuron specific proteins and stop dividing early in development and hence, neurons direct their efforts of division towards the formation of axonal and dendritic processes, instead.

Under normal circumstances, neurons are expected to reside in G_0 phase of the cell cycle. However, recent studies showed that under neurodegenerative conditions such as Alzheimer's disease (AD) – which is a progressive brain disorder and characterized by extracellular deposition of amyloid beta (Aβ) peptide, intracellular neurofibrillary tangles (NFTs) which primarily contain tau protein, and synaptic and neuronal loss – neurons basically leave G_0, avoid G_1/S checkpoint and continue to cell cycle, they even replicate their DNA. Why neurons bypass this checkpoint is still unknown. It has been found that some cyclins, like in cdk1-cyclinB1 complex, are re-activated in degenerating neurons of AD patients. Another reason that gives rise to cell cycle re-activation in Alzheimer's neurons is increased activity of cyclinD1. Re-activation of cyclinD1 results in activation of its partner cdk4 and Alzheimer's neurons re-enter G_1 phase of the cell cycle. However, there is evidence demonstrating that several of these cell cycle proteins in neurons can also play role in neuronal differentiation.

Protein Kinase C (PKC) is a member of Ser/Thr protein kinase family. Activation of PKC generally depends on its targeting to the membrane compartments. Targeting to membrane compartments is promoted by second messengers such as diacylglycerol and arachidonic acid. However, there is also a growing body of evidence attributing nuclear functions for PKC such as DNA replication, RNA synthesis and processing, and gene expression. Hence, its precise subcellular distribution and roles especially in neurons are still unclear.

Several alterations of many signal transduction pathways in AD have been reported and PKC is one of the proteins that have altered expression and activation levels in AD. PKC activity has been found to be altered in AD patients' fibroblasts; altered activity and expression of particular PKC isoforms have also been demonstrated in postmortem brain cortex of AD subjects. Furthermore, amyloid beta has been shown to contain putative PKC pseudosubstrate domain and directly interact with PKC and alter its activity. PKC is also the upstream effector of many signaling pathways like Erk, GSK3β which have role in tau hyperphosphorylation where it is also associated with neurodegeneration. For instance, in AD neurons, tau dissociates from microtubules and form NFTs upon hyperphosphorylation via kinases like GSK3β. However, tau has also a key role in regulating microtubule dynamics, axonal transport and neurite outgrowth through site-specific phosphorylation events. For

instance p-tauSer199 is known to take a role in axonogenesis which is important for neuronal differentiation.

Besides its role in signaling pathways which are associated with neurodegeneration, PKC has also been associated with proliferation and even differentiation. Expression of catalytically active PKC-α constructs was found to activate the expression of cyclinD1, via the AP-1 element of the cyclinD1 promoter, thus enhancing cell cycle progression. PKC-α activation can also promote cell cycle progression in glioma cells by up-regulating cyclinD1 and cyclin dependent kinase inhibitor, p21waf1/cip1. However, PKC-α can also play an inhibitory role during the regulation of the cell cycle through inactivation of cyclins. For instance, in crypt region of intestines, where differentiating, proliferating and stem cells are all present and where regulation of cell cycle arrest is strictly necessary, PKC activation resulted in cell cycle withdrawal into G_0 phase due to a PKC-α mediated down regulation of cyclinD1 and increased expression of p21waf1/cip1 and p27kip1, which targets the inhibition of CDK complex activity. Therefore, PKC-α, has the ability to act as a growth stimulator or inhibitor depending on the cell system. When it comes to its role in differentiation, Western blot analysis of nuclei isolated from fully differentiated rat pheochromocytoma (PC12) cells demonstrated an increase in PKC-α levels, which indicated a role for nuclear PKC-α in neuronal differentiation.

The purpose of this study was to investigate the effects of PKC activation by Phorbol 12-myristate 13-acetate (PMA), a general PKC activator, on cell cycle re-activation in neurons under non-degenerative (in physiological) and degenerative (Aβ treated) conditions. Quantitative Real Time Polymerase Chain Reaction (qRT-PCR), immunofluorescence and Western blotting analysis was performed to reveal expressional changes and distribution of PKC-α and cyclins in primary hippocampal neurons based on implications of cell cycle re-activation and PKC's involvement in neurodegeneration. Furthermore, to reveal downstream effects of PMA directed PKC activation in neurons in terms of differentiation or de-differentiation, pRb and ppRb protein levels were also analyzed in order to understand how PKC activation would affect them in the pendulum of proliferation and differentiation in control and Aβ treated neurons. Since differentiation and de-differentiation states in neurons would be related to re-organization of cytoskeletal structure, microtubule structures in neuronal processes in PMA treated neurons were also analyzed. Changes in hyper-phosphorylated tau and p60-katanin protein levels were also analyzed, since they are important players of microtubule stability and hence, crucial factors in neuronal branching. Finally, knowing that there are studies demonstrating up-regulation of cell cycle proteins like cyclinD1 in nucleus causing neurodegeneration; PMA and amyloid beta treated neurons were further analyzed for any potential activation of apoptosis or changes in proliferation.

Results in this study showed that PMA mediated PKC activation elevates nuclear PKC-α and cyclinD1. These increases are accompanied by an increase in phosphorylation of pRb. Furthermore, PMA mediated PKC activation caused shorter process lengths and an increase in process numbers together with elevated p-tau and p60-katanin levels in hippocampal neurons which may indicate impairment from differentiation. However, in Aβ treated neurons (degenerative condition) there was no significant change observed in mRNA levels of cyclins; yet, cyclinA and cyclinB protein levels were elevated according to immunofluorescence analysis. pRb, p-tau, p60-katanin and p-GSK3β protein levels were also similar with control groups. Although there was no indication for apoptosis in any of the experimental conditions

in terms of cleaved PARP, there was an inclease in Bax/Bcl-2 ratio in Aβ conditions. However, in only PMA treated neurons Bax/Bcl-2 ratio was found to decrease.

In conclusion, in addition to its previously known roles in cell cycle regulation, nuclear PKC may have effects causing withdrawal from differentiation in neurons by increasing nuclear cyclinD1 and promoting microtubule re-organization. Furthermore, Aβ seems to be obstacle for this designated role of PKC.

NÖRONLARDA FİZYOLOJİK VE DEJENERATİF KOŞULLAR ALTINDA PROTEİN KİNAZ C AKTİVASYONUNUN ETKİLERİNİN ARAŞTIRILMASI

ÖZET

Nöronlar ileri derecede farklılaşmış, sinyal iletimi ve sinyal işleme üzerine özelleşmiş hücrelerdir. Bu hücreler ektoderm kökenli mitotik hücrelerden gelişirler ve hayatlarının ilk evrelerinde bölünme özelliğine sahiptirler. Gelişimlerinin erken evrelerinde ise nörona özgü proteinler eksprese etmeye başlayarak bölünme yeteneklerini kaybederler; enerjilerini bölünmek yerine akson, dendrit gibi nöronal uzantılar oluşturmada kullanırlar.

Normal koşullar altında nöronların hücre fazının G_0 evresinde kalmaları beklenir. Ancak, hücre dışı amiloid beta (Aβ) plakları, tau proteininden oluşan hücre içi NFT ve nihayetinde sinaptik ve nöronal kayıplarla karakterize Alzheimer hastalığı (AH) gibi nörodejeneratif durumlarda nöronların G_0 evresini terk ettiği, G_1/S kontrol noktasını atlayarak hücre siklusuna devam ettiği, hatta DNA'sını replike ettiği gösterilmiştir. Nöronların bu kontrol noktasını neden atladığı tam olarak bilinmemektedir. Bununla beraber, Alzheimer hastalarının nöronlarında cdk1-siklinB1 kompleksi gibi bazı siklinlerin tekrardan aktive edildiği bulunmuştur. Alzheimer nöronlarında hücre siklusun yeniden akivasyonunda etken olan başka bir sebep ise artan siklinD1 aktivitesidir. SiklinD1'deki aktivite artışı beraberinde partneri cdk4'ün aktivitesini de arttırır. Bundan dolayı da Alzheimer nöronları hücre siklusunun G_0 fazını terk ederek tekrardan G_1 fazına girebilir. Bununla birlikte, nöronlarda var olan hücre siklus proteinlerinin nöronal farklılaşmada görevleri olduğuna dair de bulgular mevcuttur.

Protein Kinaz C (PKC) Ser/Thr protein kinaz ailesinin üyesi olup aktivasyonu genellikle bu proteinin hücrenin membran kompartmanlarına lokalizasyonu ile sağlanır. PKC'nin membran kompartmanlarına lokalizasyonu ise diaçilgliserol, araşidonik asit gibi ikincil mesajcı sinyal moleküllerince tetiklenir. Bununla birlikte, PKC'ye DNA replikasyonu, RNA sentezi ve işlemesi, gen ekspresyonu gibi nükleusta meydana gelen olaylarda görevler atfeden bulgular ve görüşler de artmaktadır. Kısacası PKC'nin hücre içi konumu ve görevleri özellikle nöronlar için henüz net olarak tanımlanamamıştır.

AH'nda sinyal iletim yolaklarının birçoğu değişime uğramaktadır. PKC de AH'nda ekspresyon ve aktivasyon düzeyleri değişime uğrayan proteinler arasında yer almaktadır. Örneğin Alzheimer hastalarının fibroblast hücrelerinde PKC'nin aktivasyonunda değişimler olduğu görülmektedir. Benzer şekilde, AH sebebiyle yaşamını kaybedenlerin beyin korteks dokuları incelendiğinde belirli PKC izoformlarının hem aktivitesinde hem de ekspresyonun seviyesinde farklılıklar olduğu gösterilmiştir. Buna ilaveten, amiloid beta'nın PKC ile etkileşimi sağlayan substrat bağlanma bölgesi içerdiği, böylelikle de doğrudan PKC'nin aktivitesini etkileyebildiği gösterilmiştir. PKC, ayrıca tau proteininin aşırı fosforlanmasında görevli olan Erk, GSK3β gibi yolakların öncesinde yer alması bakımından da

önemlidir. Bilindiği gibi tau aşırı fosforlanması nörodejenerasyonla ilişkilidir. Fosforlanmamış halde mikrotubuller üzerinde tutunmuş halde bulunan tau proteini, Alzheimer nöronlarında da olduğu üzere, GSK3β gibi kinazlarca aşırı fosforlanmayı mütakiben mikrotubullerden ayrılır ve NFT (Neuro-Fibrillary Tangle) oluşturur. Nörodejenerasyondaki rolünden farklı olarak tau proteininin, fosforilasyon mekanizmasının da yardımıyla, mikrotubul dinamiklerini düzenlemede ve nörit uzamasını sağlamada da kilit görevleri bulunmaktadır. Örneğin Ser199'tan fosforlanan tau nöronal farklılaşmada da son derece önemli bir olay olan aksonogenezde görevlidir.

PKC, nörodejenerasyon ile ilişkili yolaklardaki görevinin yanı sıra, hücre bölünmesi ve hatta hücre farklılaşması gibi olaylar ile de ilişkilendirilmektedir. Katalitik olarak aktif PKC-α konstrakları eksprese edildiğinde, siklinD1'in espresyonu dolayısı ile hücre siklusunun da aktive edildiği bulunmuştur. Benzer şekilde, gliyoma hücrelerinde de PKC-α, siklinD1 ve siklin bağımlı kinaz inhibitör (p21waf1/cip1) miktarını arttırmak suretiyle hücre siklusunda ilerlemeye sebep olmaktadır. Bu görevlerine ilaveten, PKC-α'nın siklinleri inaktive etmek suretiyle hücre siklusunun düzenlenmede negatif bir rolü de mevcuttur. Örneğin barsak kriptlerinde, ki bu bölgede bölünen, farklılaşan ve de kök hücrelerin tamamı mevcuttur, ve hücre siklus kontrolü çok sıkı gerçekleştirilir, PKC aktivasyonunun hücreleri G_0 fazına çekilmeye tetiklediği gösterilmiştir. Bunun sebebi olarak da siklinD1'in PKC-α kaynaklı negatif regülasyonu, p21waf1/cip1 ve p27kip1'in ise artışı gösterilmektedir. Kısacası, PKC-α, hücre bölünmesinde, hücre sistemine göre pozitif ya da negatif regülatör olarak görev yapabilmektedir. Diğer yandan PKC-α'nın hücre farklılaşmasındaki görevine örnek olarak ise PC12 hücreleri ile yapılan bir çalışma gösterilebilir. Bu çalışmada tamamen farklılaşması sağlanan PC12 hücrelerinin nükleusları izole edilmiş ve Western blotlama yöntemi ile PKC-α düzeyleri araştırılmıştır. Sonuçlar farklılaşma ile birlikte PKC-α düzeylerinde artışa işaret etmiştir.

Tüm bu veriler ışığında, bu çalışmanın amacı nöronlarda fizyolojik ve dejeneratif koşullar altında Phorbol 12-myristate 13-acetate (PMA) kaynaklı PKC aktivasyonunu etkilerini nöronlarda hem dejeneratif (amiloid kaynaklı) hem de dejeneratif olmayan (fizyolojik) koşullar altında araştırmaktır. Bu amaca yönelik olarak gerçek zamanlı kantitatif PCR (qRT-PCR), immünflöresan boyama ve Western blotlama yöntemleri kullanılarak PKC-α ve siklinlerin ekspresyon düzey ve protein lokalizasyon farklılıkları bu iki farklı koşul altında primer hipokampal nöron hücreleri kullanılarak araştırılmıştır. Buna ilaveten, nöronlarda PMA kaynaklı PKC aktivasyonunun farklılaşma ya da geri-farklılaşma bakımından etkilerini araştırmak adına pRb ve ppRb protein düzeyleri de araştırılmıştır. Nöronlarda meydana gelen farklılaşma ya da geri-farklılaşma süreçleri sitoiskelet yapısının yeniden organizasyonu ile ilişkili olduğundan, PMA ile muamele edilen nöronlarda mikrotubul yapıları da detaylı incelenmiştir. Ayrıca, mikrotubul bütünlüğünü sağlamada ve nöronal dallanmanın oluşumunda önemli oyunculardan olan p-tau ve p60-katanin protein düzeylerindeki değişimler de PMA muamelesini mütakiben tesbit edilmiştir. Son olarak, siklinD1 gibi hücre siklus proteinlerinin artışını nörodejenerasyonla ilişkilendiren çalışmalar mevcut olduğundan, yaptığımız muamemelerin olası apoptoz ya da proliferasyon yolağı tetiklemesine sebep olup olmadığı araştırılmıştır.

Sonuçlar PMA kaynaklı PKC aktivasyonunun nükleer PKC-α ve siklinD1 seviyelerinde artışa sebep olduğunu göstermiştir. Bu artışa pRb'nin fosforilasyonundaki artış eşlik etmiştir. Dahası, PMA kaynaklı PKC aktivasyonu

nöronlarda daha kısa uzantıların oluşumuna yol açarken uzantı sayılarında, p-tau ve p60-katanin düzeylerinde de artışa sebep olmuştur, ki tüm bu veriler nöronlardaki farklılaşmada bir bozulmaya işaret etmektedir. Bununla birlikte, Aβ muamelesi içeren koşullarda siklin mRNA düzeylerinde anlamlı farklılıklara rastlanmamıştır. İmmünfloresan boyamalara istinaden sadece siklinA ve siklinB protein düzeylerinde artış görülmüştür. Çeşitli deneysel muamelelere tabi tutulan nöronlardaki pRb, p-tau, p60-katanin ve p-GSK3β protein düzeyleri de kontrol nöronları ile benzerlik göstermektedir. Deneysel grupların hiçbiri kesilmiş PARP bakımından analiz edildiğinde apoptoza işaret etmemektedir; ancak hücreler Bax/Bcl-2 oranı bakımından incelendiğinde Aβ muamelesi içeren koşullarda bu oranın arttığı gözlemlenmiştir. Halbuki sadece PMA ile muamele edilen nöronlarda Bax/Bcl-2 oranı düşüş göstermektedir.

Sonuç olarak, bu çalışma ile, hücre siklusuyla ilişkili hali hazırda bilinen görevlerine ilaveten nükleer PKC'nin nöronlarda nükleer siklinD1 artışı ve mikrotubullerin yeniden organizasyonu yardımı ile farklılaşmada gerilemeye yol açabileceği gösterilmiştir. Ancak, Aβ mevcut deney şartlarında nörodejenerasyonu tamamen tetiklememiş olsa da, PKC'nin kendisine atfedilen bu görevi yerine getirebilmesinde engeldir.

1. INTRODUCTION

1.1 Neurons

Neurons are the primary cells of the nervous system. They develop from ectodermal origin mitotic cells. Although early in development neurons have ability to divide, after several divisions, they begin to express neuron specific proteins, stop dividing and become highly specialized for the processing and transmission of cellular signals (Figure 1.1) (Baas, 1999; Galderisi, 2003).

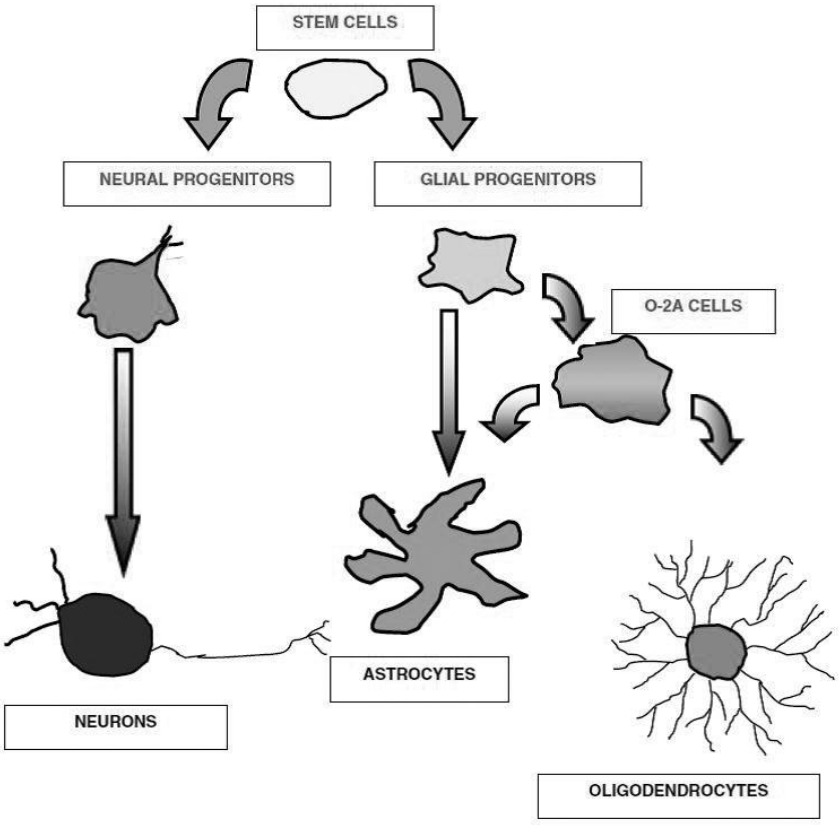

Figure 1.1 : Simplified model of a neural stem cell. (Galderisi, 2003)

Typical neuron has an enlarged cell body that contains a nucleus and most of the cytoplasmic organelles (Figure 1.1). Cell body is also the place where all the neuronal proteins are synthesized.

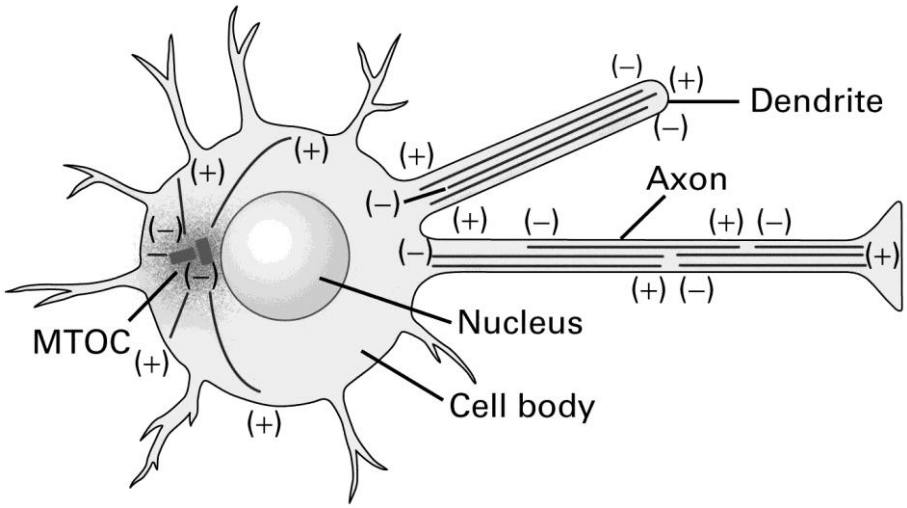

Figure 1.2 : Microtubule orientation in a typical neuron. (Lodish, 2003)

Since neurons stop dividing, they direct their efforts of division towards the formation of axonal and dendritic processes, instead. They contain one axon and multiple dendrites (Figure 1.2). Axon sends information over long distances, whereas dendrites act as receptors for incoming information. Neurons are the most polarized cells in nature and this event is supposed to be maintained by neuronal cytoskeleton, especially microtubules. Axons contain long microtubules and their plus ends are oriented away from the cell body and microtubule polarity is uniform; whereas microtubules in the dendrites are short and they have mixed polarity orientation (Figure 1.2) (Baas, 1989; 1999; 2002).

1.1.1 Cell cycle markers in mitotic cells and in neurons

Eukaryotic cell cycle contains four main phases: G_1, S, G_2 and M phase (Figure 1.3). During G_1 phase (first gap), mitogenic signals trigger synthesis of D-type cylins. These cyclins are partners of cdk4 or cdk6, and they together phosphorylate retinoblastoma protein (pRb). In late G_1, cyclinE-cdk2 activity increases and completes pRb phosphorylation. From then on, cells are irreversibly committed to enter division process. When cells are in S phase (DNA sythesis), increased cyclinA-cdk2 activity enables DNA replication and cells enter G_2 phase (second gap). Then cyclinA-cdk1 regulates G_2 and M phase cycle proteins together with cyclinB-cdk1. CyclinB-cdk1 complex has a role in late G_2 and G_2/M transition. Finally, in M phase (mitosis), cells divide and form two daughter cells (Currais, 2009).

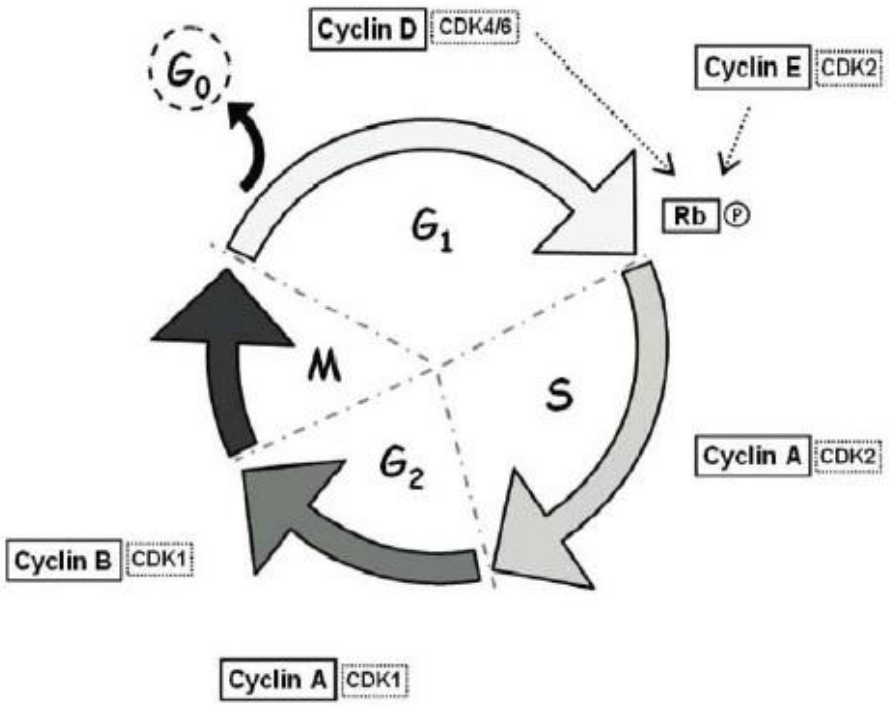

Figure 1.3 : Schematic representation of the eukaryotic cell cycle. (Currais, 2009)

There are two important checkpoints that control whether order and time of the cell cycle transitions are correct or not, G_1/S and G_2/M. These checkpoints ensure that DNA is already replicated and chromosomes are correctly segregated, and cell can decide between going through the cell cycle and arresting the cell growth or inducing apoptosis (Currais, 2009; Arendt, 2003). Under normal physiological circumstances, neurons are expected to reside in G_0 phase of the cell cycle (Figure 1.3) by down regulating their mitotic proteins.

1.1.1.1 Cell cycle markers in neurodegeneration

Although neurons are expected to reside in G_0 phase of the cell cycle, recent studies showed that in neurodegenerative diseases such as Alzheimer's disease (AD), neurons exit G_0, bypass G_1/S checkpoint and continue cell cycle, and they even replicate their DNA (Figure 1.4) (Nagy, 2007; Yang, 2001).

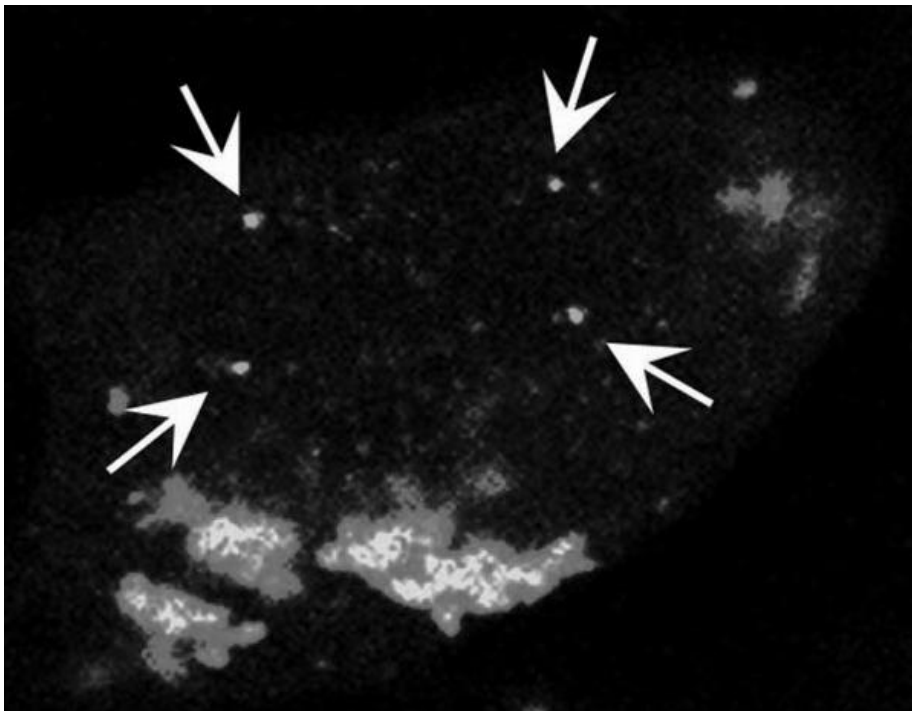

Figure 1.4 : FISH applied to AD brain neurons for chromosome 11. Confocal image of a hippocampal neuron from an AD brain. Arrows indicate the presence of four bright spots of fluorescence in the nuclei, suggesting a doubling of the number of chromosomes 11 in this cell. (Yang 2001)

Neurons down regulate their mitotic proteins under normal conditions. However, in degenerating neurons of AD patients, it has been found that cdk1-cyclinB1 complex was re-activated. Ordinarily, cdks are inactivated by cdk- inhibitors through the progression of the cell cycle and then reactivated when needed. However, similar as cyclin abnormalities, cdk-inhibitors are in their inactive state in neurons of AD patients. Hence, although required for neurons, in this case, cdks will not be able to be down regulated through the cell cycle as it would normally occur in otherwise healthy neurons (Nagy, 2007).

Another reason that gives rise to cell cycle reactivation in Alzheimer's neurons is increased activity of cyclinD1. Reactivation of cyclinD1 results in activation of its partner cdk4, and then neurons in AD re-enter G_1 phase of the cell cycle (Nagy, 2007).

1.1.1.2 Cell cycle markers in differentiation

Although most of the studies attribute neurodegenerative effects for cell cycle related proteins in neurons, recent evidence from different groups demonstrates the constitutive expression of cdks and cyclins indicating that expression of these

proteins might be correlated with differentiation (Schmetsdorf, 2005; Schmetsdorf, 2007; Schwartz, 2007; Matsunaga, 2000; De Falco, 2004). As already indicated, terminally differentiated neural cells are arrested in the G_0 phase and some key cell cycle regulatory proteins are down-regulated. However, cyclinD1, has been found to increase in some neural differentiation models (Hayes, 1991; Okano, 1993; Yan and Ziff, 1995; van Grunsven, 1996). *In vivo* analysis of cyclinD1 showed that reduced cyclinD1 expression correlates with neural development delay induced by nutritional deprivation (Tamaru, 1993; Tamaru, 1994; Shambaugh, 1996). Similarly, disruption of the cyclinD1 gene in mice revealed neurological defects (Sicinski, 1995). Yan and Ziff (1995) demonstrated that cyclinD1 was highly increased by inducers of differentiation, such as NGF and FGF, and not by inducers of proliferation (EGF and insulin) in PC12 cells. In agreement with those, Xiong et al. (1997) have found that bFGF treatment caused 10-fold increase in cyclinD1 protein that was localized primarily in nucleus (Xiong, 1997). However, none of the above studies were able to explain the reason of increase in cyclinD1 during neuronal differentiation.

Furthermore, Schmetsdorf *et al.* (2009) showed that cell cycle related proteins interact with microtbule network in neurons. They also showed that these proteins have tau phosphorylation ability and have roles in neurite outgrowth regulation. According to these results, cell cycle related proteins are attributed dual functions: proliferation control in mitotic cells and structural plasticity control in post-mitotic neurons.

1.1.2 Amyloid beta in physiological neurons

AD is a progressive brain disorder characterized by intracellular neurofibrillary tangles (NFTs) which contain primarily tau protein, extracellular deposition of amyloid beta (Aβ) peptide, and synaptic and neuronal loss (Iwata, 2005). How Aβ contributes to development of AD is not exactly defined and studies mostly have focused on the neurotoxic effetc of Aβ, but physiological roles of Aβ were relatively less defined. There are some cellular functions attributed to Aβ.

Aβ is produced by sequential proteolysis of the amyloid precursor protein (APP) (De Strooper, 2000; Haass, 2005) and production and subsequent release of Aβ positively correlate with the level of neuronal and synaptic activity (Kamenetz, 2003; Cirrito, 2005) and consistent with this, recent study that was published in 2009 by Abramov

et.al, indicated that both elevation and reduction in Aβ levels attenuated short-term synaptic facilitation during bursts in excitatory synaptic connections and suggested a role for endogenous Aβ in the regulation of synaptic vesicle release and concluded that this role of Aβ might be associated with the pathological events that lead to synapse loss in Alzheimer's disease.

In another study (Morley, 2010) low doses of Aβ were applied in the hippocampus *in vivo* and memory retention and enhanced acetylecholine production were enhanced in two tasks. Same study has tested whether endogenous Aβ had a role in learning and memory in young. For this purpose they blocked endogenous Aβ in healthy 2-month-old cognitively intact mice. Results indicated impaired learning in T-maze foot-shock avoidance. They also revealed that $A\beta_{(1-42)}$ facilitated induction and maintenance of long term potentiation (LTP) in hippocampal slices, whereas antibodies to Aβ inhibited hippocampal LTP. In conclusion, this study indicated that Aβ is important for learning and memory in normal healthy young animals.

1.1.2.1 Amyloid beta and PKC interaction

In addition to these functions attributed to Aβ, another role of Aβ might be through Protein Kinase C (PKC) signaling, since Aβ was found to contain a putative PKC pseudosubstrate site in $A\beta_{(28-30)}$ (KGA) which is responsible for direct Aβ – PKC interaction (Chauhan, 1991; Lee, 2004). There are two proposed model for this interaction as illustrated in Figure 1.5. According to the first model, very similar to PS motif, Aβ binding changes conformation of PKC and keeps protein in its inactive state. According to the second model, Aβ bind to C4 domain of PKC and prevents the binding of PKC substrates. The exact binding mechanism of PKC - Aβ is still unclear.

There are several alterations observed in PKC signaling pathways in AD cases. For instance, PKC activity has been consistently found to be reduced in AD fibroblasts, decreased PKC activity and translocation have also been demonstrated in the brain of AD patiens (Lee, 2004; Gasparini, 1998). Furthermore, Aβ has been shown to degrade PKC-α in normal human fibroblasts and PKC-γ in AD patient fibroblasts (Favit, 1998); to reduce PKC-mediated phosphorylation of several soluble brain proteins in a liposome system (Chauhan, 1991) and moreover, to induce translocation of PKC from membrane fraction to cytosol in cultured brain endothelial cells

(Pakaski, 2002). All these studies address an inhibitory role for Aβ on PKC activity besides its role in contributing to the progress of AD.

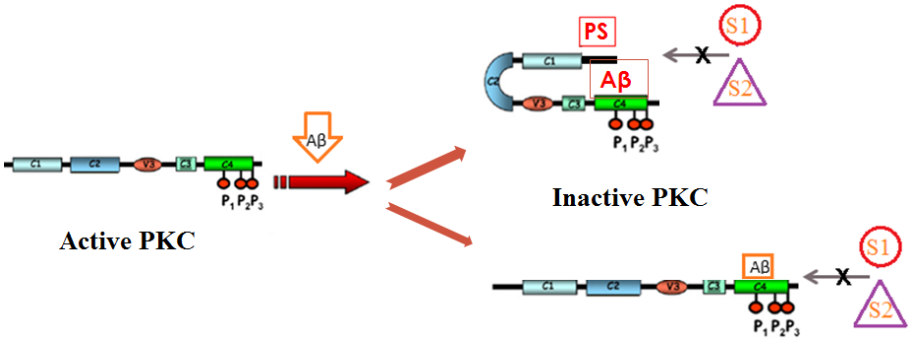

Figure 1.5 : Illustration of PKC – Amyloid interaction.

1.2 Protein Kinase C (PKC) Protein Family

Protein Kinase C (PKC) is a member of Ser/Thr family of phosphorylating enzymes and it was originally discovered in 1977 as a histone protein kinase activated by calcium and diacylglycerol (DAG), phospholipids, and/or phorbol esters (Takai, 1977). These kinases have roles in wide range of cellular events such as ion flux, receptor modulation, cell proliferation, synaptic re-modelling, gene expression, etc. (Figure 1.6).

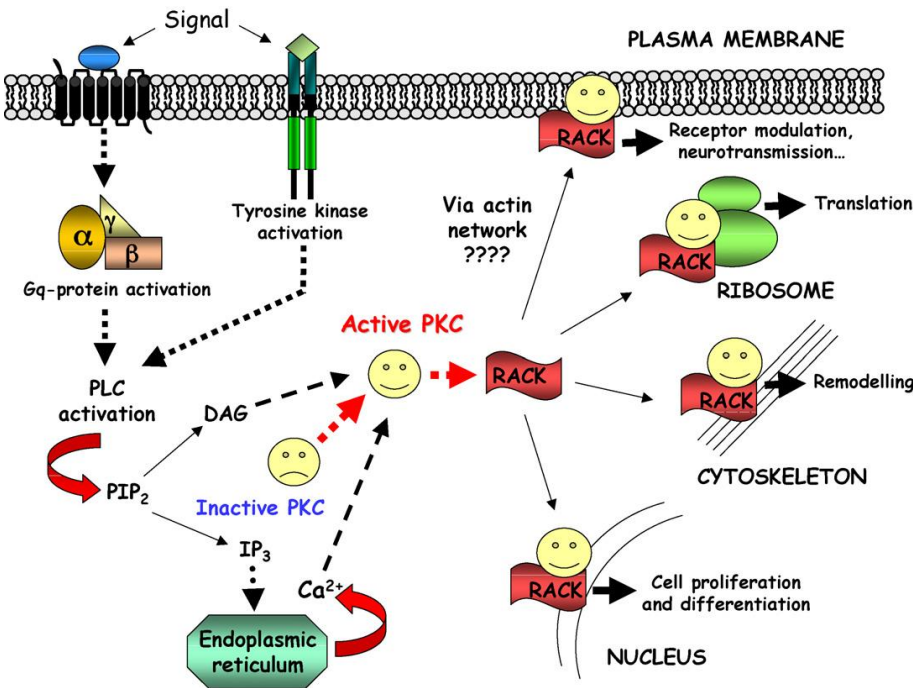

Figure 1.6 : PKC translocation dependent pathways. (Amadio, 2006)

At least 10 PKC isoforms have been described based on sequence homology and activator sensitivity, and these isoforms are clasified in three classes (Figure 1.7): The first class is calcium-dependent or conventional cPKCs (α, βI, βII, γ); the second class is calcium-independent or novel nPKCs (δ, ε, μ, η, θ); and finally the third class is atypical aPKCs (ζ, λ, ι) (Amadio, 2006; Newton, 2003; Nishizuka, 2001; Giorgi, 2010).

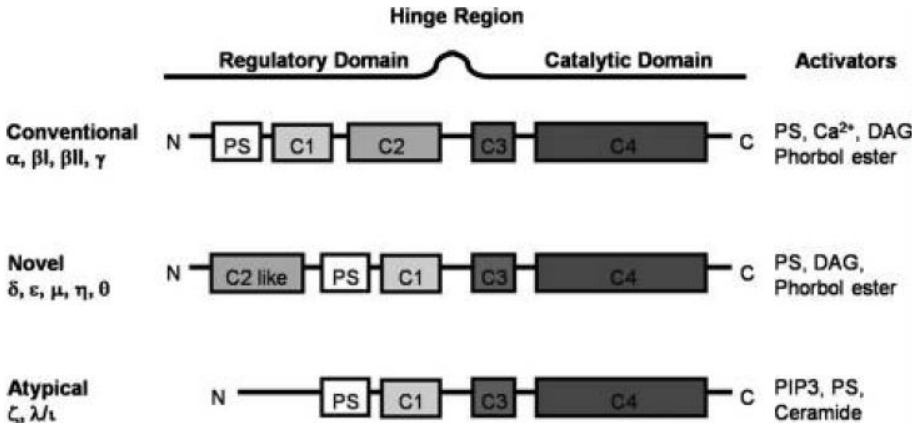

Figure 1.7 : Classification and structure of PKC isoforms. (Giorgi, 2010)

PKC polypeptide consists of a C-terminal catalytic domain and an N-terminal regulatory domain (Figure 1.7). cPKCs have four conserved domains: C1, C2, C3 and C4, and these domains are separated by regions composed of variable sequences V1, V2, V3, V4 and V5. Specific PKC activators interact with the enzyme via regulatory domains (Amadio, 2006; Giorgi, 2010). The C1 domain is composed of one or two cysteine-rich domains which also serve as docking sites for PKC activators such as physiological activator DAG and its analog phorbol esters (such as PMA). The C2 domain contains Ca^{+2} binding site and it is present in both cPKC and nPKC. C1 domain is a putative membrane binding domain (Giorgione, 2006). Finally, C3 contains the ATP binding region, while C4 bears the substrate docking sequence (Newton, 1998). There is a pseudosubstrate (PS) or autoinhibitory region localized close to the C1, and this region keeps PKC in an inactive form (Figure 1.8). Upon interaction with its specific activators, folded conformation of PKC is opened. These activators decrease the affinity of autoinhibitory domain for the catalytic site, and hence, PKC becomes active. Activation of PKC can be described as a shift in the equilibrium between two states of the catalytic domain; PS-bound and PS-unbound (Kraft, 1983; Giorgi, 2010). Ca^{+2} and DAG can sequentially activate cPKC. Ca^{+2} acts rapidly but the binding of DAG to the active site of PKC is initially prevented by PS

and delays kinase activation (Oancea, 1998). Upon DAG binding to the regulatory domain of PKC, PKC increases its affinity for membrane lipids and tranlocates to the plasma membrane. Other lipids such as arachidonic acid, phosphatidylinositol (PI) 4,5-bisphosphate, and phosphatidylinositol 3,4,5-trisphosphate (PIP3) can also stimulate PKC activity. Phorbol esters such as PMA, mimic DAG by binding to the same site in the regulatory domain (Giorgi, 2010). Whenever PKC translocates to the plasma membrane of the cell, PS releases and PKC becomes active (Figure 1.8).

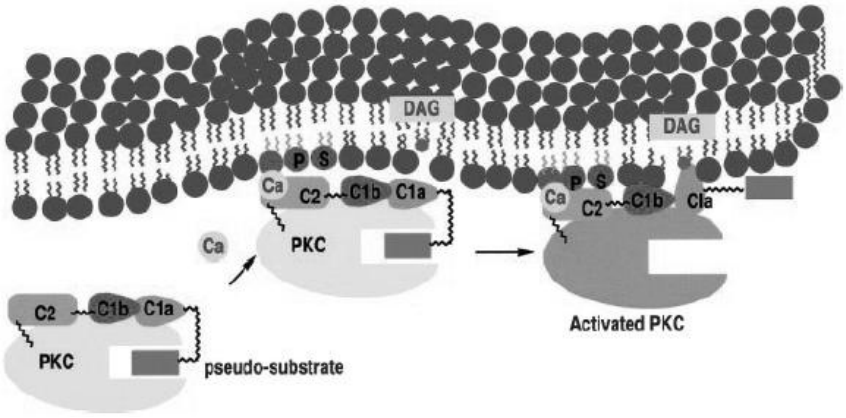

Figure 1.8 : Proposed activation model for PKC. (Medkova and Cho, 1999)

1.2.1 Nuclear activities of PKC

Most of the functions of PKC have been associated to events that occur within the membrane – cytoplasm compartments of the cells. However, there is a growing body of evidence indicating that PKC has functions in nuclear compartments of the cells such as DNA replication, RNA synthesis and processing, gene expression (Martelli, 2006), and some studies link nuclear PKCs with cell proliferation as it was also observed in investigations on the laminin B, a nuclear envelope component and a major PKC substrate in HL60 cells (Hocevar, 1993). In the study by Hocevar et. al. (1993), following DAG-mimicking compound treatment, PKC-βII was found to translocate to the nucleus and phosphorylate laminin B. This phosphorylation leads to laminin disassembly and entry into mitosis. There are some other substrates for nuclear PKCs identified over the years. These proteins are: histone (H1, H2B, H3), lamins (A/C), DNA topoisomerase I and IIα, DNA polymerase β, DNA methyltransferase, etc ... (Martelli, 2006; Omri, 1987; Ajiro, 2000; Huang, 2004; Haas, 1993; Eggert, 1991; Pommier, 1990; Sahyoun, 1986; Tokui, 1991; DePaoli-Roach, 1986). Nevertheless, these findings are still unclear, since investigators

cannot surely decide whether or not PKC-dependent phosphorylation of some of these substrates takes place within the nucleus or elsewhere in the cell.

Similar to situation in cell proliferation, there is a body of evidence that suggests role in differentiation regulation for nuclear PKC isoforms, especially in hematolymphopoietic cell line (Martelli, 1999). Although there is a lack of functional studies that would clarify the issue of how nuclear PKC may influence differentiation, there are speculations that PKC, once in the nucleus, may influence transcription of the genes essential for cell differentiation.

Although information in the field of nuclear PKCs is accumulating in the literature, more detailed studies are still needed to be designed in order to better understand the mechanism of phosphorylation events by PKCs that take place in the nucleus.

1.2.2 PKC-α

Mammalian PKC-α is composed of 672 amino acids and is distributed throughout all tissue types. It is activated by a variety of stimuli such as guanine-nucleotide-binding protein-coupled receptor signaling, tyrosine kinase receptor signaling (Nishizuka, 1992; Dempsey, 2000; Newton, 2001; Nishizuka, 1995; Parekh, 2000), physical stress like hypoxia (Lo, 2001) and mechanical stress (Cheng, 2001). Hence, PKC-α isotype has important functions in various cellular events such as proliferation, apoptosis, differentiation, motility and so on (Figure 1.9).

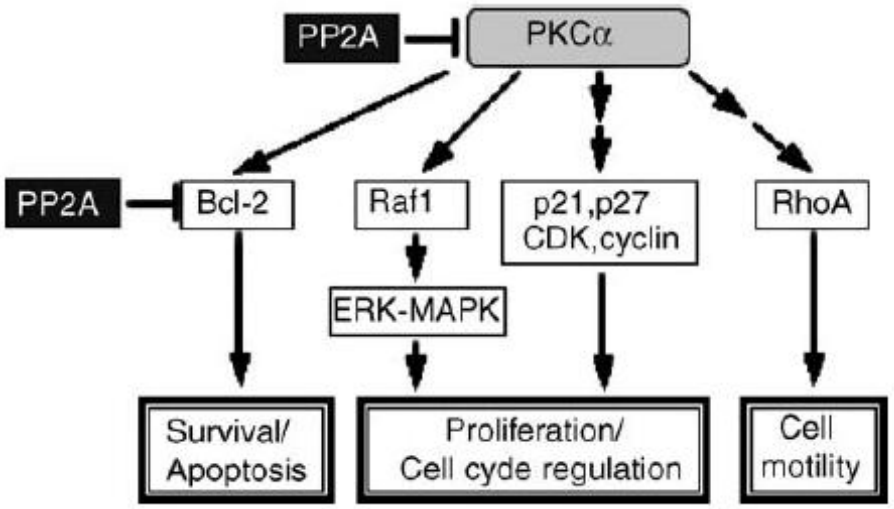

Figure 1.9 : Possible interactions of PKC-α with other signaling pathways. (Michie and Nakagawa, 2005)

Depending on its activation time and activation type, the substrate that takes role in activation, response of PKC-α can vary. However, complete lists of these cell – specific factors are still unavailable (Nakashima, 2002).

1.2.2.1 PKC-α regulation

PKC-α is regulated in the cell by three mechanisms: phosphorylation, co-factor binding and intracellular localization (Parekh, 2000; Newton, 2001).

A. Phosphorylation

PKC-α has to be serially phosphorylated to attain its active form. There are three proposed phosphorylation sites localized in catalytic domain of PKC-α (Figure 1.10); Thr497 (in the activation loop), Thr638 (in the turn motif) and Ser657 (in the C-terminal motif) (Parekh, 2000). Phosphorylation of Thr497 is independent from internal PKC-α activity and was shown to be prerequisite to full phosphorylation of PKC-α and subsequent activation; however, phosphorylation of Thr638 and Ser657 are autophosphorylation-mediated and promoted by Thr497 phosphorylation (Pears, 1992; Cazaubon, 1993; Cazaubon, 1994).

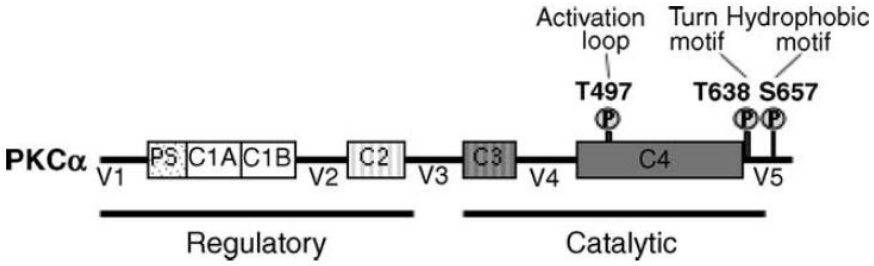

Figure 1.10 : Phosphorylation sites of PKC-α. (Michie and Nakagawa, 2005)

B. Co-factor binding

Phosphorylated PKC-α resides in the cytoplasm and requires additional regulatory mechanisms to be fully active. As already mentioned, there is a PS domain in the N-terminal of PKC-α that prevents catalytic domain – substrate interaction, therefore phosphorylation of substrate (Nishizuka, 1995). Upon receptor – ligand binding, phosphatidylinositol-specific phospholipaseC (PLC) cleaves phosphatidylinositol-4,5-bisphosphate (PIP2) into the calcium mobiliser, inositol-1,4,5-triphosphate (IP3) and DAG (Figure 1.8) (Nishizuka, 1995). Following serial activation events and co-factor bindings to C1 and C2 domains, PKC-α binds to plasma membrane and changes its conformation, which also enables release of PS domain from substrate

binding site (Newton, 2001). Therefore, co-factor binding is especially important in plasma membrane localization and subsequent activation of PKC-α.

1.2.3 Roles of PKC-α

1.2.3.1 Roles of PKC-α in proliferation and differentiation

Studies on the role of PKC-α showed that thymocyte cells isolated from transgenic mice over-expressesing wild-type PKC-α display higher proliferation rate upon stimulation compared to the response of control cells upon stimulation (Iwamoto, 1992). Furthermore, studies with PKC-α MCF-7 breast cancer and malignant U87 glioma cells confirmed increase in proliferation upon over-expression of PKC-α (Mandil, 2001; Ways, 1995). In contrast, there are studies that showed inhibition of proliferation by PKC-α. For instance, in IEC-18 intestinal crypt cells, PKC-α activation appeared to lead to cell cycle arrest by accumulation of the ppRb and induction of the cyclin-dependent kinase inhibitors (Frey, 2000). When it comes to differentiation, studies with T-cells demonstrated PKC-α mediated differentiation and proliferation of pre-T cells via ERKMAPK-and cyclic AMP response element binding protein mediated pathways (Grady, 2004; Michie, 2001).

1.2.3.2 Roles of PKC-α in cell cycle regulation

Studies on the role of PKC-α in cell cycle regulation demonstrated that expression of catalytically active PKC-α constructs enhance cell cycle progression by increasing cyclinD1 expression through AP-1 element of cyclinD1 promoter (Soh and Weinstein, 2003). PKC-α activation was also found to promote cell cycle progression in glioma cells by up-regulating cdk inhibitor p21waf1/cip1 (Besson and Yong, 2000). However, PKC-α can also have inhibitory function in cell cycle regulation. In intestinal epithelial cells, PKC-α signaling results in cell cycle withdrawal into G_0 phase by down-regulation of cyclinD1 and up-regulation of cdk inhibitors p21waf1/cip1 and p27kip1 (Frey, 2000). Similary, in pancreatic cancer cells PKC-α signaling inhibited cell growth by arresting the cells in G_1 phase through increased p21waf1/cip1 expression and hence inhibition of cdk2 and ppRb (Detjen, 2000).

1.3 Aim of the Study

PKC is one of the proteins that have altered expression and activation levels in neurodegenerative disease, such as AD. Decreased activity and expression of particular PKC isoforms have been demonstrated in post-mortem brain cortex of AD patients. Furthermore, amyloid beta was found to directly interact with PKC and decrease its activity. PKC is also an upstream effector of signaling pathways such as Erk, GSK3β that have role in tau hyper-phosphorylation.

In this content, the purpose of the thesis was to investigate the effects of PKC activation by PMA, a general PKC activator which mimics DAG, on cell cycle re-activation in neurons under non-degenerative (in physiological) and degenerative (Aβ treated) conditions. Seeing differential effects of PKC-α in different mitotic cell types, PKC activation studies in neurons' physiological condition would also provide information about the effects of PKC on cyclins in post-mitotic hippocampal neurons to gain insights into understanding the role of PKC-α in neurons. This study would provide an opportunity to observe discrepancies in PKC signaling pathway between physiological (non-degenerative) and Aβ treated (degenerative) neurons in terms of changes in protein level and distribution of cyclins and PKC-α itself. To reveal downstream effects of PMA mediated PKC activation in neurons in terms of differentiation or de-differentiation, changes in pRb and ppRb protein levels were also determined in order to understand how PKC activation would affect them in the pendulum of proliferation and differentiation in case of deviation of neurons from their normal physiological state upon PKC activation. Since differentiation and de-differentiation states in neurons would be related to re-organization of cytoskeletal structure, microtubule structures were also analyzed in PMA treated neurons. Since they are important players of microtubule integrity and crucial factors in neuronal branching, changes in hyper-phosphorylated tau and p60-katanin protein levels were also analyzed. Finally, all experimental conditions were analyzed for any potential activation of apoptosis or changes in proliferation upon PKC activation.

2. MATERIALS AND METHODS

2.1 Materials

2.1.1 Animals

Post-natal 0 (PN0) Sprague-Dawley rats were used for hippocampal neuron culturing. All the animals were handled according to appropriate animal care and utilization procedures. Ethical approval was obtained from Marmara University, 05/09/2008. The procedures involving experimentation on animal subjects were done in accordance with both the guidelines provided by the local authorities and the National Research Council's guidelines for the care and use of laboratory animals.

2.1.2 Antibodies used in this study

Primary antibodies used in this study are listed in Table 2.1.

Table 2.1 : Primary antibodies.

Antibody name	Producer	Catalog number
Goat anti PKC-α	Santa Cruz	sc-208
Rabbit anti cyclinD1	Santa Cruz	sc-717
Rabbit anti cyclinA	Santa Cruz	sc-596
Rabbit anti cyclinB1	Santa Cruz	sc-595
Rabbit anti cyclinE	Santa Cruz	sc-198
Mouse βIII tubulin	Promega	G-7121
Mouse anti β-actin	Santa Cruz	sc-47778
Rabbit anti Histone3	Cell Signaling	9715
Goat anti phospho pRb Ser807/811	Santa Cruz	sc-16670
Rabbit anti pRb	Santa Cruz	sc-50
Rabbit anti phospho tau Ser199	Invitrogen	44-734G
Mouse anti p60-katanin	Akkor & Karabay	
Rabbit anti phosphor GSK3β Ser9	Cell Signaling	9323
Mouse anti GSK3β	Cell Signaling	9832
Rabbit anti Bax	Cell Signaling	2772
Rabbit anti caspase 3	Cell Signaling	9665
Rabbit anti Bcl-2	Cell Signaling	2870

Secondary antibodies used in this study are listed in Table 2.2.

Table 2.2 : Secondary antibodies.

Antibody name	Producer	Catalog number
anti rabbit HRP	Promega	w401b
Donkey anti goat HRP	Promega	v805a
anti mouse HRP	Promega	w402b
Alexa Fluor® 488 goat anti-mouse	Invitrogen	A11029
Alexa Fluor® 647 goat anti-rabbit	Invitrogen	A21245

2.1.3 Buffers and solutions

2.1.3.1 Tris buffer saline

10X stock solution of tris buffer saline (TBS) was prepared by dissolving 87.66 g NaCl and 12.1 g Tris in 1 lt ddH_2O. pH was adjusted to 8.0. Working solution (1X TBS) was prepared by diluting 10X TBS by 10 times.

2.1.3.2 Tris buffer saline – Tween20

Tris buffer saline – Tween20 (TBS-T) was prepared by dissolving 0.1% (v/v) Tween20 in 1X TBS. TBS-T was used as washing buffer in Western blot experiments throughout the study.

2.1.3.3 Towbin buffer

Towbin buffer was prepared by dissolving 1.5 g (25 mM) Tris, 7.5g (192 mM) Glycine and 20% (v/v) Methanol in 500 mL ddH_2O. Towbin was used as transfer buffer in Western blot experiments throughout the study.

2.1.3.4 Immunofluorescence blocking buffer

Blocking buffer application is important to reduce nonspecific antibody bindings. To prepare 1 mL blocking buffer 100 µl (10%) Goat (or Donkey, depending on the type of secondary antibody) serum and 10 mg (10 mg/mL) BSA were dissolved in 1X PBS and filtered with 0.8 µm Nalgene filter. This blocking buffer was used in immunofluorescence staining procedure throughout the study.

2.1.3.5 Western blotting blocking buffer

To prepare 100 mL blocking buffer, 1 g (1%) BSA and 5 g (5%) skim milk were dissolved in 1X TBS. This blocking buffer was used in Western blotting procedure throughout the study.

2.1.3.6 Western blotting stripping buffer

To prepare 100 mL stripping buffer, 200 mM Glycine was dissolved in ddH_2O and pH was adjusted to 2.5 with HCl. Prior to use 0.5% Tween20 was added into Glycine solution. This stripping buffer was used in Western blotting procedure for reprobing experiments throughout the study.

2.1.3.7 PMA solution

To prepare 100 µM stock PMA solution, 1mg PMA was dissolved in 16.2 mL DMSO. Working concentration was diluted in hippocampal serum free plating medium prior to treatment.

2.1.3.8 Gö6976 solution

To prepare 500 µM stock Gö6976 solution, 1mg Gö6976 was dissolved in 5.3 mL DMSO. Working concentration was diluted in hippocampal serum free plating medium prior to treatment.

2.1.3.9 Amyloid beta $_{(1-42)}$ solution

To prepare amyloid beta $_{(1-42)}$ (Aβ) peptide for neurotoxicity studies, peptide aggregation has to be induced since peptide is supplied in a non-neurotoxic form. Pre-incubation is required to obtain aggregated peptide structure. For this purpose; Lyophilized peptide was dissolved in HPLC grade water to obtain 6 mg / mL concentration. Peptide was diluted with Ca^{2+} free PBS to 1 mg / mL and incubated at 1000 rpm 37°C for 24 hours. Neurotoxicity is usually observed at 30 - 100 µg / mL which correspond to ~ 6.5 – 22 µM.

2.1.4 Primary hippocampal neuron culture media

2.1.4.1 Hippocampus dissection medium

Hippocampus dissection medium was prepared with 10 ml 10X HBSS, 1 ml 1M HEPES and 1 ml Penicillin-Streptomycin (Pen/Strep). Final volume was brought to 100 ml by addition of 88 ml ddH_2O. Medium was filter sterilized with 0, 2 µm Nalgene filter.

2.1.4.2 Hippocampal plating medium

Hippocampal medium was prepared by dissolving 1 mL B27 Supplement, 0.33 mL 45% D-Glucose, 0.25 mL L-Glutamine and 2.5 mL FBS in 45.92 mL Neurobasal medium. Medium was filter sterilized with 0.2 µm Nalgene filter. Hippocampal medium was used in wash steps during hippocampi dissection procedure.

2.1.4.3 Hippocampal serum free plating medium

Hippocampal serum free medium was prepared by dissolving 1 mL B27 Supplement, 0.33 mL 45% D-Glucose and 0.25 mL L-Glutamine in 48.42 mL Neurobasal medium. Medium was filter sterilized with 0.2 µm Nalgene filter.

2.1.5 Cell line media

2.1.5.1 Mouse 3T3 fibroblast medium

Fibroblast medium was prepared by dissolving 1 mL L-Glutamine (4mM), 5 mL FBS, 100 µl pen/Strep in 44 mL DMEM (low glucose). Medium was filter sterilized with 0.2 µm Nalgene filter. Medium was used during cultivation of 3T3 mouse fibroblast cells.

2.1.5.2 SH-SY5Y neuroblastoma medium

Neuroblastoma medium was prepared by dissolving 1 mL L-Glutamine (4mM), 10 mL FBS, 200 µl pen/Strep in 89 mL DMEM (low glucose). Medium was filter sterilized with 0.2 µm Nalgene filter. Medium was used during cultivation of SH-SY5Y neuroblastoma cells.

2.1.6 Chemicals

Chemicals used in this study are listed in Table 2.3.

Table 2.3 : Chemicals.

Chemical	Producer
B27	Gibco
DNase	Sigma
2.5% Trypsin	Invitrogen
D-Glucose	L-glutamine
Poly-L-lysine	Sigma
HEPES	Gibco
HBSS	Gibco
FBS	Gibco
Penicillin / Streptomycin	Sigma
PMA	Calbiochem
Gö6976	Calbiochem
DMSO	Sigma
Methanol	Merck
Mounting Medium	Sigma
BSA	Sigma
Skim milk	Fluka
SeeBlue® Plus2 Protein Ladder	Invitrogen
Goat Serum	Gibco
Donkey Serum	Gibco
Ethanol	Merck
Paraformaldehyde	Sigma
Triton X100	Sigma

2.1.7 Commercial kits

Commercial kits used in this study are listed in Table 2.4.

Table 2.4 : Commercial kits.

Kit name	Producer
High Pure RNA Isolation Kit	Roche
Quant-iT™ RNA, BR Assay Kit	Invitrogen
RevertAid™ First Strand cDNA Synthesis Kit	Fermentas
LightCycler® 480 Probes Master Kit	Roche
NE-PER™ Nuclear and Cytoplasmic Protein Extraction Kit	Pierce
Mammalian Cell Extraction Kit	Biovision
BCA Protein Assay Kit	Pierce
SDS Gel Preparation Kit	Fluka
ECL plus HRP Detection Kit	GE Healthcare
SuperSignal® West Femto HRP Detection Kit	Thermo

2.1.8 Primer and probe sets used in quantitative real time PCR

Primer and probe sets used in qRT-PCR in this study are listed in Table 2.5. Probes and primers were designed by using Roche Universal Probe Library software. Probes were purchased from Roche Universal Probe Library, and primers were purchased from Integrated DNA Technologies, Inc.

Table 2.5 : Primer and probe sets.

Gene name	Accession number	Primer sequence	Probe number
cyclinA	NM_001011949.1	gagagggaaattgcagcttg gggcgggtatatctcttcgt	2
cyclinB1	NM_171991.2	tgtgaaagatatctatgcttacctcag cccagtaggtattttggtctaactg	65
cyclinD1	NM_171992.4	gcacaacgcactttctttcc tccagaagggcttcaatctg	16
cyclinE	NM_001100821.1	ctgagagatgagcactttctgc tggagcttatagacttcacacacc	108
cdk1	NM_019296.1	tcatggattcttcgctcgtt tcgggagtgacaaaacacaa	65
cdk2	NM_199501.1	gcatctttgccgaaatggt gatccggaagagttggtcaat	80
cdk4	NM_053593.2	gtcagtggtgccggagat ggattaaaggtcagcatttcca	50
p27	NM_031762.3	agacagtccggctgggtta ttctgttctgttggcccttt	130

2.1.9 Gene assays used in quantitative real time PCR

Gene assays that were used as internal controls for normalization of gene expression levels in qRT-PCR were purchased from Roche Universal Probe Library and are listed in Table 2.6. Gene assays are used as housekeeping for normalization of qRT-PCR results throughout the study.

Table 2.6 : Gene assays.

Gene assay	Catalog number
Rat ACTB	05046203001
Rat GAPD	05046220001

2.1.10 Laboratory equipment

Laboratory equipment that were used in this study are listed in Table 2.7.

Table 2.7 : Laboratory equipment.

Laboratory equipment	Producer
Autoclave	NüveOT 4060 Steam Sterilizer
Deep freezers and refrigerators	-80˚C Heto Ultrafreeze 4410 -20˚C Arçelik +4˚C Arçelik
Electrophoresis tank	Midicell PrimoTM EC 330
Fluorometer	Qubit Invitrogen Q32857
CO2 Incubator	Shel Lab
Laminar flow cabinet	Faster BH-EN
Light microscope	Olympus CH30
Microfuge	Beckman® Coulter Microfuge
Centrifuge	Eppendorf Centrifuge 5424
Micropipettes	Eppendorf 2.5 µl 10 µl, 20 µl, 200 µl, 1000 µl
pH meter	Mettler Toledo MP220
Power supply	BioRad
Real time PCR	LightCycler 480 II Roche
Thermomixer	Eppendorf
Ultrapure water system	TKA Wasseraufbereitungssysteme
Water baths	Memmert
Hemacytometer	Fisher Scientific
Filters	Nalgene
Confocal microscope	Leica, TCS SP2 SE
Dissection microscope	Olympus
Spectrophotometer	PerkinElmer Lambda25 UV/VIS
Densitometer	BioRad
Semi-dry blot system	BioRad
Dumont-style forceps (no:5)	EMS
Plastic culture dishes	TPP
Falcon tubes	BD

2.2 Methods

2.2.1 Primary hippocampal neuron culture

When the cultures started from cells, tissues or organs taken directly from organisms, it is named “primary culture”. Upon dissociated and plated into culture dish, neurons that have completed their division *in situ* start to extend processes, form synapses

with one another, etc. Neurons also retain their individual identities in culture dish and each different type of neurons expresses its own properties.

2.2.1.1 Dissection of the hippocampus

To obtain dissociated primary neuron culture from hippocampi, first hippocampi from PN0 Sprague – Dawley rat brains were dissected. Hippocampus disection procedure is indicated below:

- PN0 rats were transferred on ice bucket to obtain anaesthesia. To minimize any contamination risk, rats were briefly rinsed in 70% ethanol prior to dissection procedure.
- Heads were transferred to a culture dish containing hippocampus dissection medium pre-warmed to 37°C.
- Brains were removed under a dissection microscope. For this procedure Dumont-style forceps (no:5) were used.
    - The cerebral hemispheres were separated from diencephalon and brain stem (Figure 2.1 A, B). Diencephalon and brain stem were discarded.
    - Meninges were carefully removed (Figure 2.1 C).
    - Figure 2.1 D shows one of the hemispheres after removal of meninges. Arrowheads indicate the boundary between the hippocampus and cortex; small arrows mark the free edge of the hippocampus.
    - Figure 2.1 E shows the removal of hippocampus. The hemisphere was stabilized with forceps and another forceps was used to cut the hippocampus and to take it out of the hemisphere.
    - Figure 2.1 F shows the hippocampus after it has been removed.
- Following dissection, hippocampi were transfered to a dish containing hippocampus dissection medium. The hippocampi were cut into small pieces and transferred into 15 mL conical centrifuge tube.
- The volume was brought to 4.5 mL with hippocampus dissection medium.
- 0.5 mL 2.5% Trypsin and 0.25 mL (10 mg/ mL) DNase were added into the tube. Tube was gently mixed and incubated in 37°C water bath for 35 minutes.

- Hippocampi pieces were settled to the bottom of the tube. At the end of incubation step, trypsin and DNase were pipetted off.
- Hippocampi pieces were rinsed 2 times for 5 minutes each with 5 mL hippocampal plating medium.
- Finally 1 mL of warm (37°C) hippocampal plating medium was added into the tube.
- Trituration was performed 6 – 7 times against the side of the tube with a fire-polished Pasteur pipette. The medium was especially pushed out against the side of the tube to prevent frothing since the cells at the air-liquid interface can be lysed.
- Dissociation was completed, and the cell density was determined by using hemacytometer. Neurons were plated onto 200 μg / mL poly-L-lysine coated culture dishes at a density of $1x10^6$ cells / 34 mm culture dish for RNA isolation experiments, and $2.5x10^6$ cells / 60 mm culture dish for Western blot experiments. For immunofluorescence analysis, neurons were plated onto 1 mg / mL poly-L-lysine coated 18 mm glass coverslips at a density of $3x10^4$ cells / coverslip. Cultures were maintained in 37°C, 5% CO2 environment.

2.2.2 Cultivation of mouse 3T3 fibroblast or SH-SY5Y neuroblastoma cells

3T3 fibroblast and SH-SY5Y neuroblastoma cell stocks were taken out from -80°C freezer. Tubes containing cell lines were shaken very carefully in 37°C waterbath and cells were transferred into 10 ml of 37°C warmed apropriate growth medium. Cells were centrifuged at 3000 rpm for 5 minutes. Supernatant was removed, 1 ml fresh 37°C warmed medium was added into the tube and the pellet was resuspended. Since these cells were used in immunofluorescence studies, they were plated on poly-L-lysine coated (for neuroblastoma cells) or non-coated (for fibroblasts) coverslips and maintained in 37°C, 5% CO2 environment.

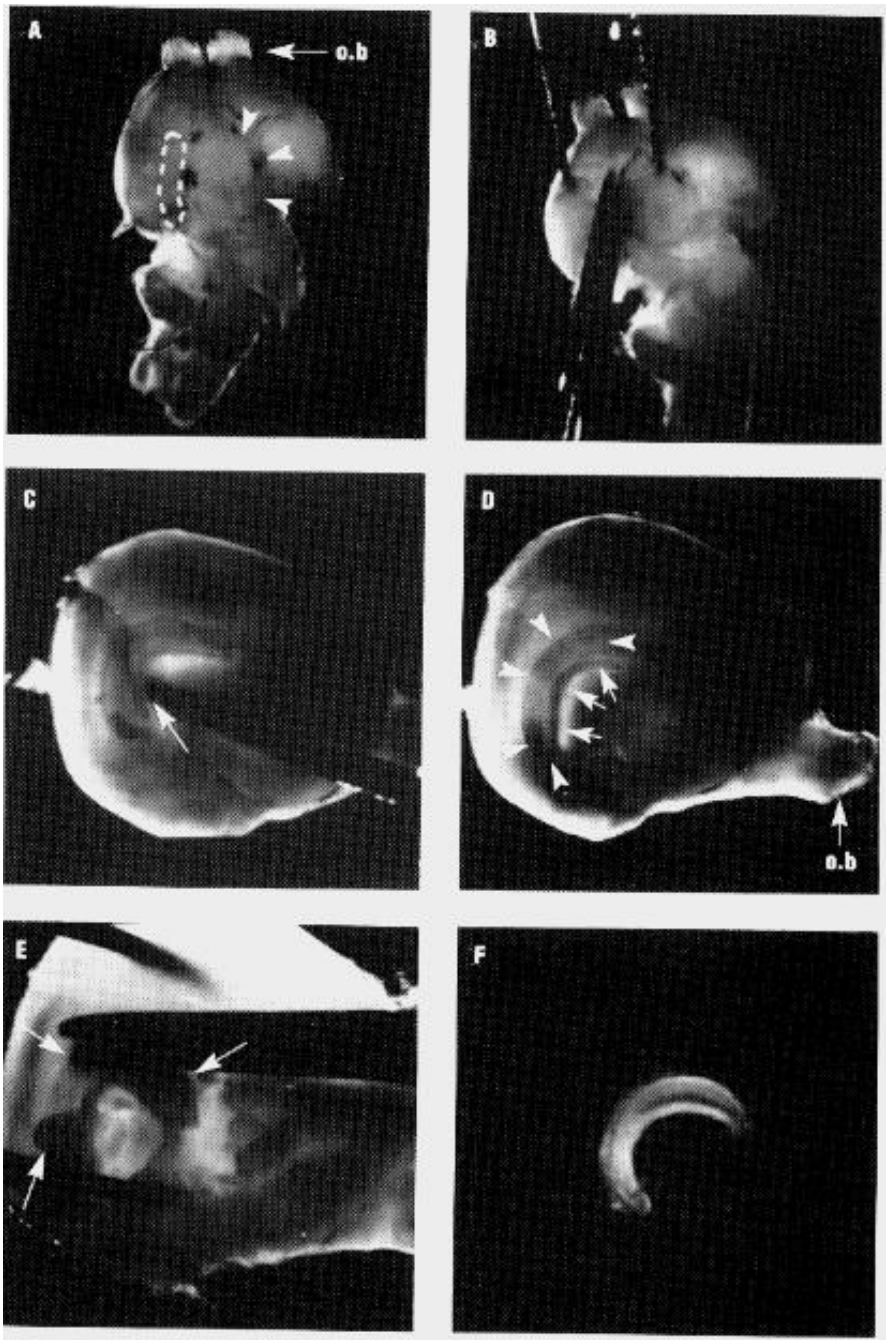

Figure 2.1 : Hippocampus dissection. (Banker & Goslin, 1998)

2.2.3 Culture dish and coverslip coating

Culturing neurons and neuroblastoma cells require using substrates, like poly – L – lysine which enhances cell adhesion. To prepare the coating substrate, 10 mg poly – L – lysine was dissolved in 10 mL ddH_2O (1 mg / mL) and filter sterilized by using 0.2 μm Nalgene filter.

- Culture dishes were coated with 200 μg / mL; whereas glass coverslips were coated with 1 mg/ mL poly – L – lysine solution for 1 hour at room temperature.

- Culture dishes were washed 6 times for 5 minutes each with sterile ddH_2O.
- At the final step, ddH_2O was taken off and culture dishes were dried.

2.2.4 PKC activation and inhibition

PKC activation and inhibition studies were performed by using both mouse 3T3 fibroblast cells and primary hippocampal neurons. PKC activation studies were performed by treatment of mouse 3T3 fibroblast cells with 100 nM PMA for 24 hours and treatment of hippocampal cultures with 100 nM PMA for 24 hours at 1 DIV. Inhibition of PKC-α activity was achieved by 30 minutes or 24 hours treatment of fibroblasts with 500 nM Gö6976 and by 24 hours Gö6976 treatment of hippocampal neurons. Pre-inhibited condition, performed only in hippocampal neurons, was achieved by the end of 1 hour 500 nM Gö6976 treatment followed by 23 hours PMA treatment. Control groups were incubated in 0.1% DMSO containing media.

2.2.5 Amyloid beta $_{1\text{-}42}$ pre-incubation

Amyloid beta $_{(1\text{-}42)}$ peptide was shown to be neurotoxic in its beta sheet structure (Simmons, 1994) and pre-incubation of peptide provides formation of this neurotoxic beta sheet structure. Neurotoxicity is usually observed at ~ 6.5 – 22 μM.

Pre-incubation procedure is indicated below:

- Lyophilized peptide was dissolve in HPLC grade water to obtain final concentration 6 mg / mL.
- Peptide was diluted to 1 mg / mL with PBS (in which Ca^{2+} was omitted).
- Diluted peptide was incubated at 37°C for 24 hours.

2.2.6 Amyloid beta $_{1\text{-}42}$ treatment

Aβ studies were performed by treatment of 1 DIV hippocampal cultures with 7 μM pre-incubated Aβ peptide dissolved in hippocampal serum free medium for 24 hours. Since peptide was dissolved in water and diluted in PBS in pre-incubation procedure, control cells were incubated in hippocampal serum free medium.

2.2.7 Quantitative real time PCR and relative quantification of expression

Specific probe and primers for the genes of interests were purchased from Roche Universal Probe Library. Probes and primers used in this study were listed in Table 2.5. To perform quantitative Real Time Polymerase Chain Reaction (qRT-PCR), total RNA was isolated from cultured hippocampal neurons with High Pure RNA isolation kit according to the manufacturers' instructions. RNA concentrations were measured by Qubit® Fluorometer using Quant-iT™ RNA, BR Assay Kit. cDNA was generated from total RNA using a random hexamer primer and RevertAid™ H minus reverse transcriptase (RevertAid™ First Strand cDNA Synthesis Kit) according to the manufacturers' instructions. Gene expression analysis was performed by using Roche LightCycler® 480 Real-Time PCR System. All reactions contained cDNA, 2X LightCycler® 480 Probes Master Mix, 2 µM primer sets and 100 nM probe sets. PCR reactions were run using the LightCycler® program, 95°C for 10 minutes followed by 45 cycles of 95°C for 10 seconds, 60°C for 30 seconds and 72°C for 1 second.

For relative quantification of gene expressions, each primer-probe set was standardized (Appendix A) to obtain reaction efficiency values between 1.8 - 2.2 and error rate below 0.2 that allows the use of $\Delta\Delta C_T$ method in data analysis (Livak, 2001). This method requires the assignment of one or more housekeeping genes (GAPD and actin in this case), which are assumed to be uniformly and constantly expressed in all samples. Obtained C_T values were normalized against housekeeping gene expression levels. This method uses an equation (2.1) to calculate and present data as 'fold change' (expression level of treated sample / expression level of control sample). Each data point is the average of at least two independent samples with two replicates.

$$2^{-\Delta\Delta CT} = [(C_T \text{ gene of interest} - C_T \text{ internal control}) \text{ treated sample} - (C_T \text{ gene of interest} - C_T \text{ internal control}) \text{ control sample})] \quad \textbf{(2.1)}$$

2.2.8 Immunofluorescence staining of neurons and confocal microscopy

Primary hippocampal neurons which were grown on poly-L-lysine coated coverslips and used for different experimental conditions throughout the study were briefly washed with PBS at 37°C. Then, they were simultaneously fixed and extracted with

cold 100% methanol at -20°C for 10 minutes. For immunofluorescence staining, fixed neurons were blocked in immunofluorescence blocking buffer (10 mg / mL BSA, 10% serum) for 1 hour. Neurons were exposed to particular primary antibodies [PKC-α (1:500), cyclinD1 (1:1000), cyclinA (1:1000), cyclinB1 (1:1000), cyclinE (1:1000), p-tau^{ser199}(1:500) and βIII tubulin (1:1000). Primary antibodies were diluted in immunofluorescence blocking buffer and neurons were incubated with appropriate primary antibodies at 4°C overnight. On the following day, neurons were washed with PBS 3 times for 5 minutes each and were blocked in immunofluorescence blocking buffer for 1 hour and finally incubated in secondary antibodies [Alexa-Fluor®488 (1:1000) or Alexa-Fluor®647 (1:1000)] at 37°C for 1 hour. Secondary antibodies were also diluted in immunofluorescence blocking buffer. Neurons were then washed with PBS 3 times and stained with DAPI for 5 minutes. Cells were again washed with PBS and mounted with mounting medium. Cells were examined with Leica TCS SP2 SE Confocal Microscope with the 63X oil objective. All images were obtained by using same gain, brightness-contrast, and exposure time settings.

2.2.9 Congo red staining of neurons and light microscopy

Congo red staining was performed to visualize Aβ fibrils in primary hippocampal cultures. This procedure was applied to live cells, without any fixation. Basic protocol followed was:

- Cells were washed carefully with PBS.
- 1 mL of 0.1% congo red which was already dissolved in H_2O was applied on the cells for 20 seconds. Cells were then carefully washed with PBS 2 times.
- Cells were examined with light microscope module of Olympus Fluorescent Microscope with the 20X objective.

2.2.10 Protein extraction, subcellular fractionation and Western blot

Before starting the procedure for protein extraction, cells were briefly washed with PBS and harvested with the help of cell scraper. As it was previously indicated, $2.5x10^6$ cells / 60 mm culture dish were used for protein extraction and subsequently for Western blot. Extraction of the total proteins was performed by using BioVision mammalian cell extraction kit according to the manufacturers' instructions. Nuclear

and cytoplasmic fractionation of the lysates was performed with Pierce NE-PER™ nuclear and cytoplasmic protein extraction kit according to the manufacturers' instructions. Protein concentrations were measured by using Pierce BCA protein assay kit and particular BSA standarts.

For the Western blot analysis, amounts of proteins loaded were 2 μg for nuclear / cytoplasmic fractions; 10 μg for total protein samples. Before loading was performed, protein samples were mixed with 5X loading buffer and subsequently were subjected to denaturation by heating to 99°C for 5 minutes. Then, samples were separated on 12.5% denaturing SDS-polyacrylamide gel and separated proteins were transferred to nitrocellulose membranes by using a semi-dry blot system. Membranes were blocked in the blocking buffer (1% BSA – 5% skim milk in TBS-T) at room temperature for 2 hours, then blotted with appropriate primary antibodies [anti PKC-α (1:500), anti cyclinD1 (1:250), anti pRb (1:100), anti phospho pRb Ser807/811(1:100), anti actin (1:100), anti Histone3 (1:1000), anti phospho tau Ser199 (1:500), anti p60-katanin (1:100), anti GSK3β (1:500), anti phospho GSK3β Ser9 (1:500), anti Bax (1:500), anti Bcl-2 (1:100) and anti-caspase3 (1:500)] diluted in blocking buffer at 4°C overnight. Membranes were washed with TBS-T 6 times for 5 minutes and then incubated with appropriate HRP conjugated secondary antibodies diluted in TBS-T (1:5000) for 1 hour at room temperature. For revealing the presence of the protein bands, membranes were treated with ECL Plus or SuperSignal® West Femto Western blotting detection reagents and films were exposed and developed. Developed films were scanned with densitometer, and the densities of the specific bands were quantified and normalized against actin (for cytoplasmic fractions and total protein) and Histone3 (for nuclear fractions).

For reblotting, membranes were washed several times with TBS-T and then stripped in stripping buffer for 20 minutes at 80°C. Membranes were washed with TBS-T 3 times for 5 minutes and blocked in blocking buffer. Same blotting protocol as described in detail above was followed for reblotting.

2.2.11 Proliferation and apoptosis analysis

To reveal any activated proliferation or apoptosis upon applied treatmens in neurons, the PathScan® Apoptosis and Proliferation Multiplex IF kit was used. This kit contains primary cocktail composed of 3 primary antibodies which are specific for

cleaved PARP Asp214, phospho Histone3 Ser10 and α-tubulin. Cleavage of PARP facilitates cellular disassembly and serves as marker for cells undergoing apoptosis. Phosphorylation of Histone3 is correlated with chromosome condensation that occurs both in mitosis and meiosis. In addition to primary hippocampal neurons, SH-SY5Y neuroblastoma cells were also used for this procedure to serve as positive control for either proliferation or naturally occuring apoptosis.

For this purpose, cells were grown on poly-L-lysine coated coverslips and treated with appropriate chemicals depending on the experimental condition. Prior to the procedure, growth medium was aspirated and cells were briefly washed with 37°C PBS. Cells were then fixed with 4% paraformaldehyde (pre-warmed to 37°C) for 15 minutes at room temperature. Fixative was aspirated and cells were washed with PBS 3 times for 5 minutes each. For immunofluorescence staining, cells were incubated in blocking solution (5% goat serum, 0.3% Triton X-100) for 1 hour at room temperature. Then, cells were incubated in primary cocktail, which contains primary antibodies for cleaved PARP Asp214, phospho Histone3 Ser10 and α-tubulin, at 4°C overnight. Primary coctail was diluted (1:100) in dilution buffer (1% BSA, 0.3% Triton X-100). Cells were again washed with PBS 3 times for 5 minutes each and incubated in detection cocktail at room temperature for 2 hours in dark. Detection coctail was also diluted (1:100) in dilution buffer. Cells were finally washed with PBS 3 times for 5 minutes each and mounted with mounting medium. Samples were examined with Leica TCS SP2 SE Confocal Microscope with the 63X oil objective. All images were obtained using same gain, brightness-contrast, and exposure time settings.

2.2.12 Integrative pixel analysis

Band densities of Western blot images were analysed by using Photoshop CS4 Software. Band intensity of each protein blot was calculated by measuring area and pixel values. Each calculated value was normalized against actin (for cyctoplasmic fraction and total lysate) or Histone3 (for nuclear fraction).

2.2.13 Neuronal process analysis

Neurons were analyzed morphologically for their processes. Image-Pro Express (Meyer Instruments) software was used to obtain average total process length and number values. Sum of total process (axon and dendrites) lengths was obtained for

all neurons and then the number was divided by the number of the measured neurons and average total process length value per neuron was calculated. Average process number values were determined by counting all process numbers and dividing by the number of measured neurons.

2.2.14 Statistical analysis

Statistical method used in this study was "paired-2 tailed student's t test". Test was performed with the help of Statistical Package for the Social Sciences (SPSS) software. P value under 0.05 was considered statistically significant and indicated with "*" in graphs. Relative mRNA expression values were calculated with Relative expression software tool (REST, 2009) software, Qiagen. Error bars in the graphs were generated using ± SEM values for qRT-PCR and ± SD values for immunofluorescence and Western blotting analysis.

3. RESULTS

3.1 Effects of PKC Activation in Hippocampal Neurons

3.1.1 PMA and Gö6976 treatments in 3T3 fibroblast cells

Since it was difficult to observe translocation of PKC upon activation in neurons because of specialized and globular morphology of neurons, PKC activation and inhibition studies were initially performed with flat cells, mouse 3T3 fibroblast by treating the cells with either PMA or Gö6976 for 24 hours (Figure 3.1).

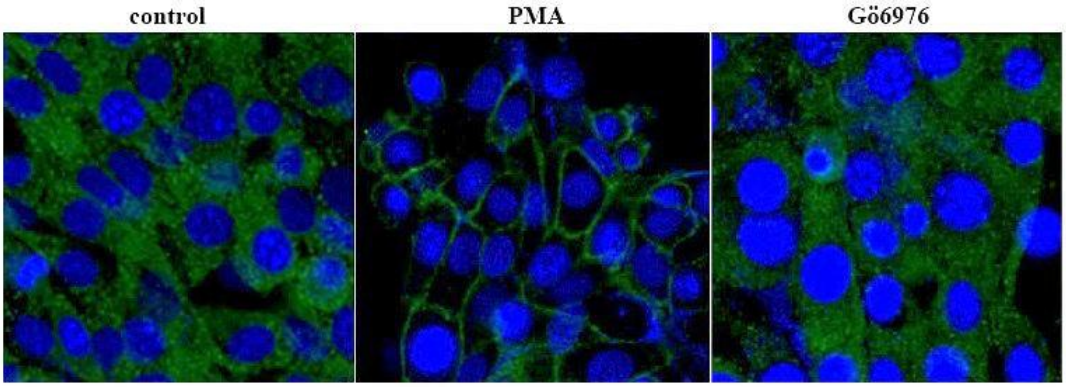

Figure 3.1 : PKC activation and inhibition studies in mouse 3T3 fibroblasts. Immunofluorescence labeling was performed for PKC-α (green) and nucleus (DAPI, blue).

According to the immunofluorescence results PKC-α was distributed throughout the fibroblast cells in control and Gö6976 treated cells, however, results indicated membrane translocation of PKC-α upon 24 hours PMA treatment. This results was expected as an indication of PKC activation under normal conditions.

3.1.2 PKC-α distribution analysis in PKC activated hippocampal neurons

The aim of this study was to reveal effects of PKC activation on cell cycle re-activation in neurons under non-degenerative and degenerative conditions in terms of cyclins, Cdks and other cell cycle related proteins such as pRb and p60-katanin. For this purpose PKC activation was achieved by PMA treatment in physiological neurons, as a non-degenerative condition, and in amyloid beta (Aβ) treated neurons, as a degenerative condition and changes in cell cycle related proteins were analyzed.

Since PKC distribution upon activation was not clear enough in neurons, studies were started up with PKC-α distribution analysis (Figure 3.2) As a common known knowledge, PKC is normally localized in the cytoplasm of the cell and usually translocates to the cell membrane upon activation under normal circumstances. However, different PKCs have been shown in the nucleus in various tissues (Amadio, 2006). When immunofluorescence analysis was performed, results showed that PKC-α was prominently localized in the nuclear regions in PMA treated (PKC activation) neurons (Figure 3.2a, middle panel). Whereas in control (Figure 3.2a, left panel) and Gö6976+PMA treated (pre-inhibition) neurons (Figure 3.2a, right panel), if at all, PKC-α was faintly localized in the nucleus, but mostly throughout the cell body and processes of the neurons.

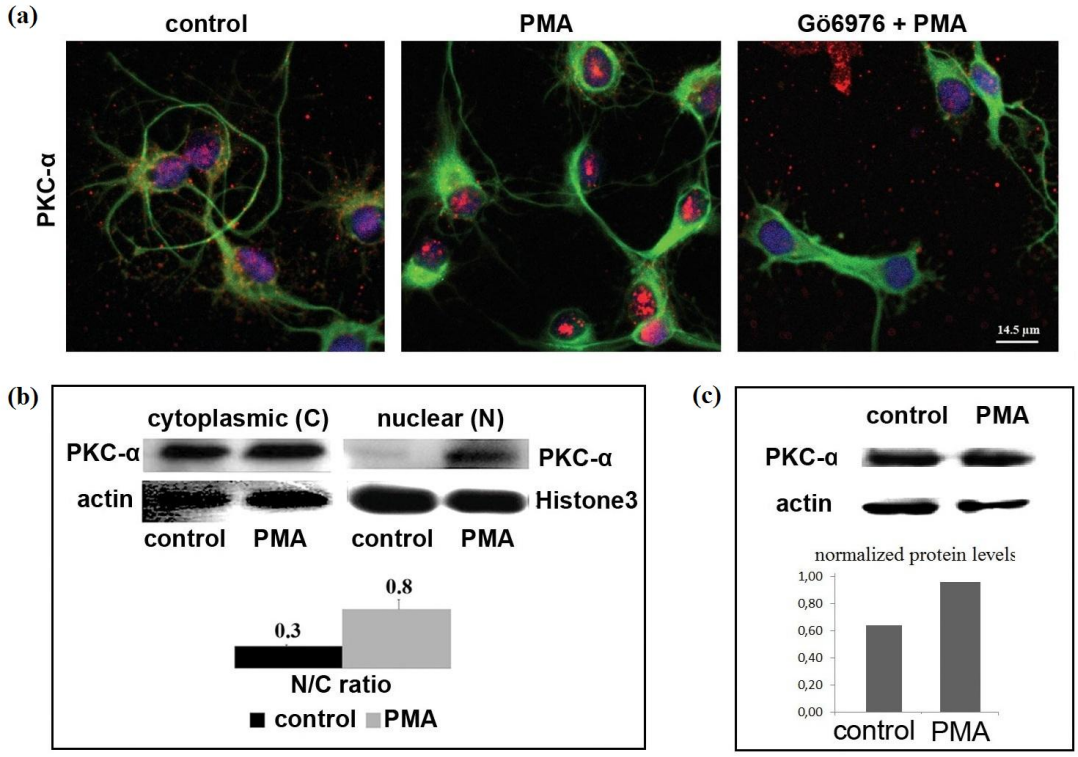

Figure 3.2 : PKC-α analysis of hippocampal neurons after PMA and Gö6976 + PMA treatments. Neurons were treated with either PMA for 24 hours or pre-inhibited with Gö6976 for 1 hour and then activated for 23 hours (Gö6976 + PMA). **(a)** Immunofluorescence analysis of neurons. Cells were labeled with PKC-α (red), DAPI (blue) and neuron specific βIII tubulin (green). Scale Bar, 14.5 µm. **(b)** Western blot of cytoplasmic and nuclear protein fractions of control and PMA treated hippocampal and quantitative analysis of the blots. **(c)** Western blot of total cell lysate. Bar represents mean values ± SD.

Consistent with these immunofluorescence results, Western blot analysis of cytoplasmic (C) and nuclear (N) fractions also indicated nuclear translocation of

PKC-α upon PMA treatment. Band intensities of PKC-α (Figure 3.2b) were quantified and normalized against actin for cytoplasmic fraction and Histone3 for nuclear fraction. Quantitation results revealed that nuclear/cytoplasmic (N/C) ratio of PKC-α was 0.3 for control neurons; whereas the ratio was 0.8 under activation by PMA. Nuclear/cytoplasmic ratio was nearly 2.5-fold higher in PMA treated neurons compared to control, indicating a translocation of PKC-α into the nucleus. Furthermore, Western blot results indicated an increase in expression level of PKC-α in PMA treated hippocampal neurons. Bar represents mean values ± SD.

3.1.3 Effects of PKC activation in mRNA levels of cyclins and cdks

As previously indicated, when changes in expression level and distribution of PKC-α were analyzed, an increase was observed in nuclear localization of PKC-α upon PMA treatment. Since PKC-α has also roles in the regulation of cell cycle machinery and some cell cycle markers were known to alter in degenerative diseases like AD, this study aimed to reveal any possible effets of nuclear PKC-α on the mRNA levels of hippocampal neurons in terms of cell cycle markers (Figure 3.3) upon over-activation.

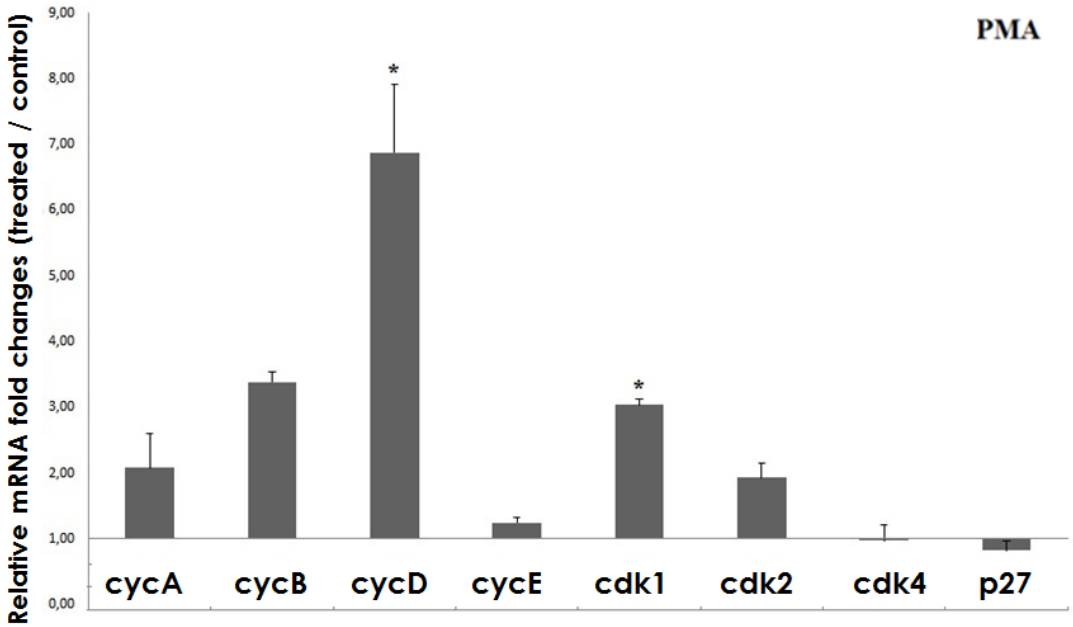

Figure 3.3 : Changes in relative mRNA levels of cell cycle proteins upon PKC activation. Bar represents mean values ± SEM. * $p < 0.05$.

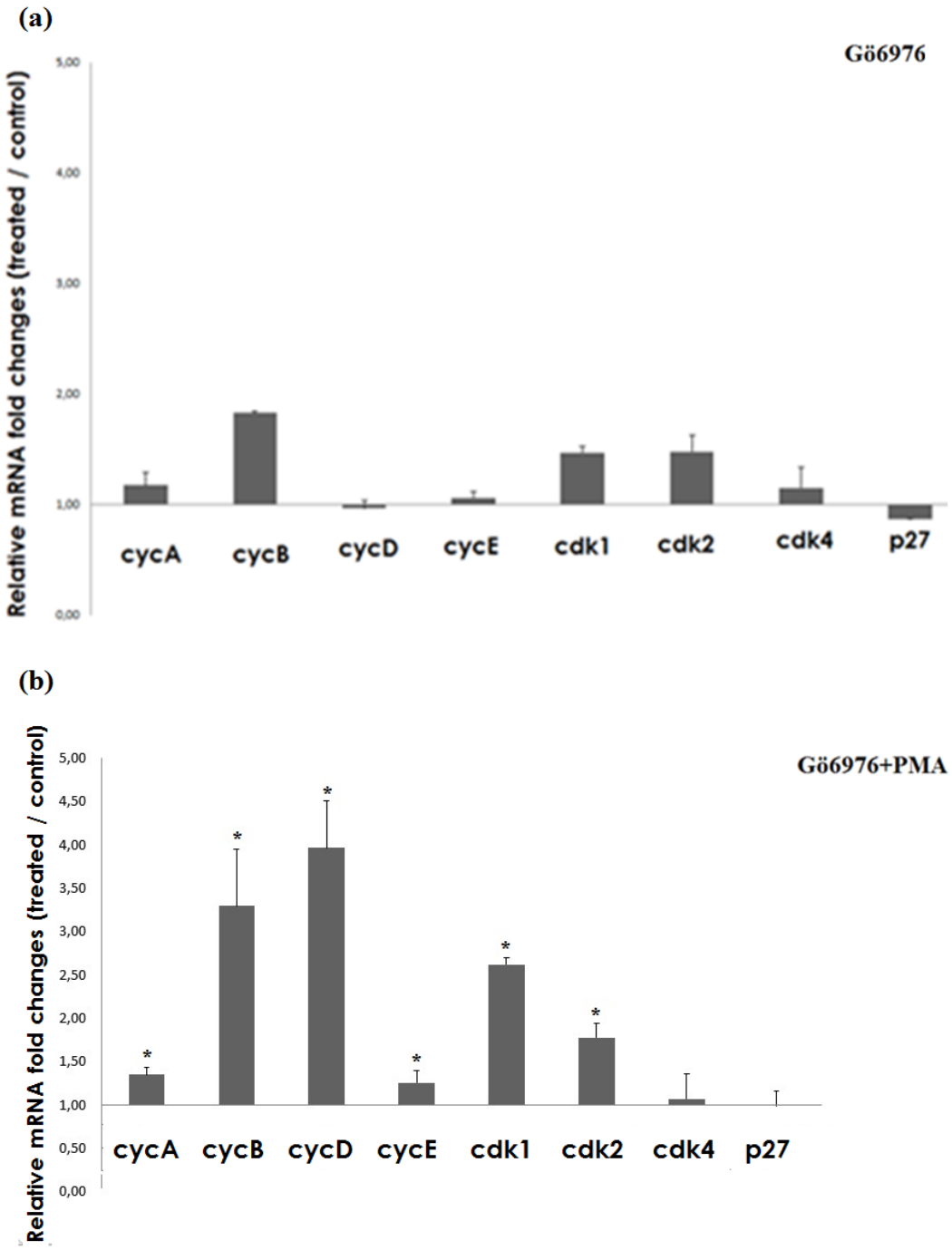

Figure 3.4 : Changes in relative mRNA levels of cell cycle proteins upon Gö6976 and Gö6976 + PMA treatments. **(a)** Changes in relative mRNA levels of cell cycle proteins upon 24 h Gö6976 treatment and **(b)** 1 h Gö6976 treatment followed by 23 h PMA treatment. Bar represents mean values ± SEM. * $p < 0.05$.

In addition to PMA treatment, changes in mRNA levels of hippocampal neurons upon PKC inhibition (Figure 3.4a) and 1 hour inhibiton followed by 23 hours activation conditions were also analyzed (Figure 3.4b) since we did not know how would PKC activation act on the regulation of cell cycle markers. Results indicated a

significant increase in cyclinD1 (6.88-fold) and cdk1 (3.04-fold) mRNA levels for PMA treated hippocampal neurons ($p < 0.05$, Figure 3.3). However, under inhibitory conditions triggered by Gö6976, there was no significant change in mRNA levels of cell cycle proteins ($p > 0.05$) (Figure 3.4a). In 1 hour pre-inhibiton followed by 23 hours activation conditions (Figure 3.4b), all analyzed cell cycle markers (except cdk4 and p27) were up-regulated compared to control neurons. When cyclinD1 mRNA was analyzed, a ~ 4-fold increase was observed. However, in PMA treated condition, the increase was ~ 8-fold. One hour pre-inhibition of PKC with Gö6976 down-regulated effect of PKC on cyclinD1 expression.

3.1.4 Analysis of protein levels and distibutions of cyclins in PMA treated neurons

When mRNA analysis was performed results indicated elevated mRNA levels in couple of cell cycle markers only under PMA treatment. For instance, there was no significant change in mRNA levels of only Gö6976 treated hippocampal neurons (Figure 3.4a). Altough changes in mRNA levels are important for the cells, changes in protein levels and distributions are also important since translation of mRNA into protein determines the functionality of the protein. For this reason, changes in protein levels were also analyzed for cyclinA, cyclinB, cyclinD1 and cyclinE with immunofluorescence analysis.

When immunofluorescence analysis was performed for cyclinA (Figure 3.5a) it was seen that besides being expressed under all of the three experimental conditions, cyclinA was also present in control neurons. When integrative pixel analysis was performed for the immunofluorescence image of cyclinA (Figure 3.5b), it could be seen that cyclinA levels were similar in PMA and Gö6976 + PMA treated neurons. However, in Gö6976 treated cells where PKC inhibition was performed for 24 hours, there was a decrease in cyclinA levels compared to control neurons.

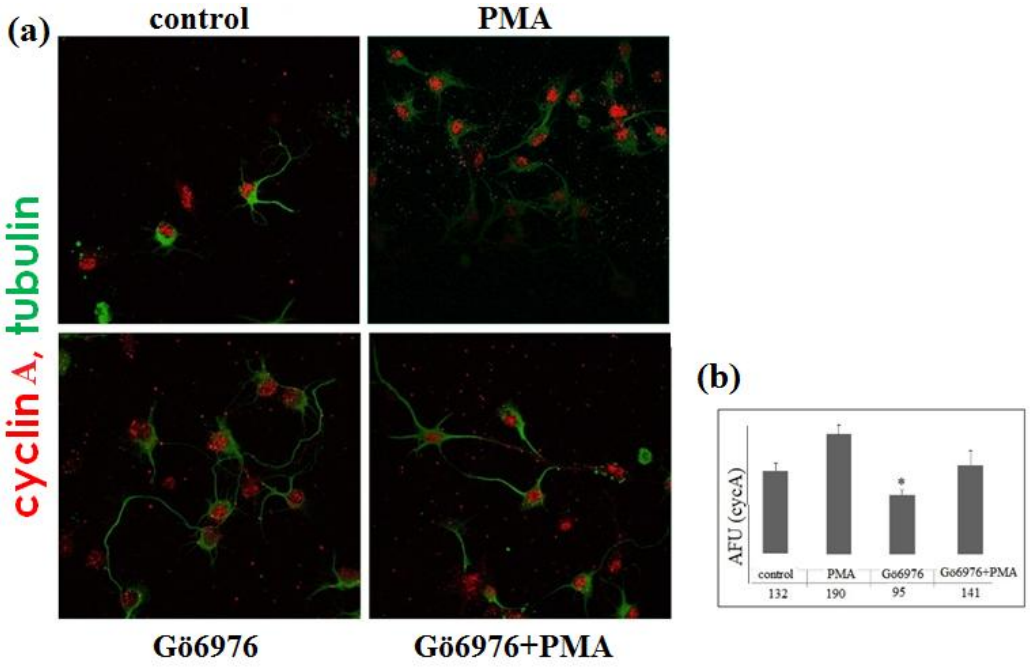

Figure 3.5 : Immunofluorescence analysis of cyclinA protein levels after PMA and Gö6976 treatments. **(a)** Neurons were treated for 24 hours with either 0.1% DMSO (control) or PMA or Gö6976 (PKC inhibition) or differently neurons were pre-inhibited with Gö6976 for 1 hour and then PMA treated for 23 hours (Gö6976+PMA). Cells were labeled with cyclinA (cycA, red) and neuron specific βIII tubulin (green). **(b)** Arbitrary fluorescence units (AFU) analysis of immunofluorescence image of cyclinA. Bar represents mean values ± SD. * $p < 0.05$.

When immunofluorescence analysis was performed for cyclinB1 (Figure 3.6a), low level of protein was faintly seen in all experimental conditions including control group. Integrative pixel analysis for immunofluorescence image of cyclinB1 (Figure 3.6b) revealed that cyclinB1 levels did not change much depending on the different treatments. All four conditions contained similar amounts of expressed cyclinB1 protein.

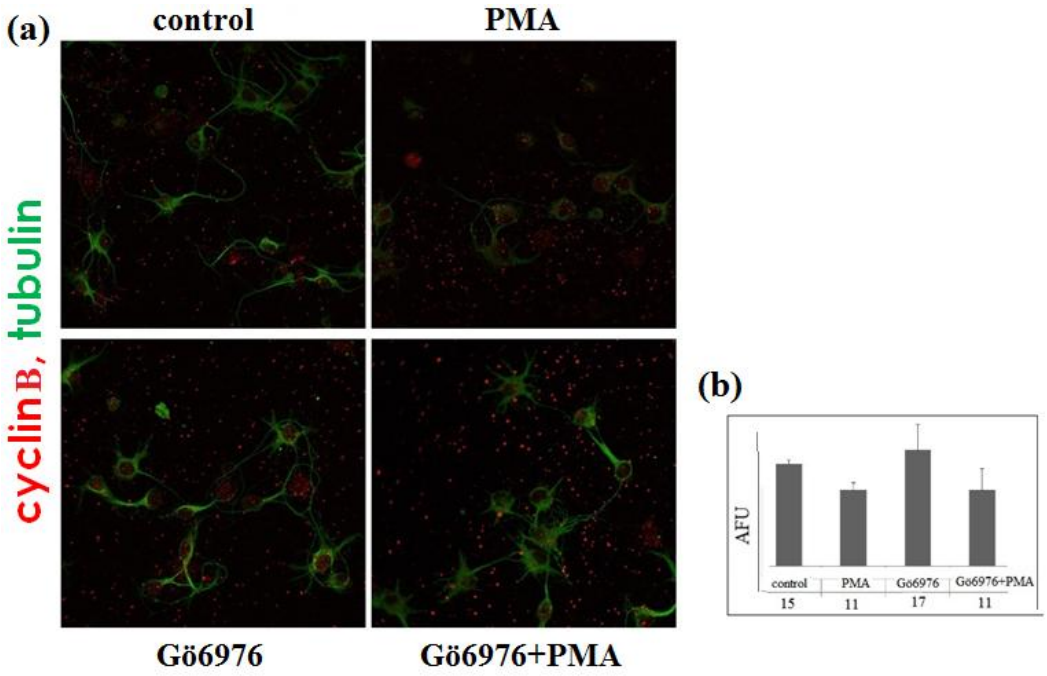

Figure 3.6 : Immunofluorescence analysis of cyclinB1 protein levels after PMA and Gö6976 treatments. **(a)** Neurons were treated for 24 hours with either 0.1% DMSO (control) or PMA or Gö6976 (PKC inhibition) or differently neurons were pre-inhibited with Gö6976 for 1 hour and then PMA treated for 23 hours (Gö6976+PMA). Cells were labeled with cyclinB1 (cycB, red) and neuron specific βIII tubulin (green). **(b)** Integrative pixel analysis as arbitrary fluorescence units (AFU) for immunofluorescence image of cyclinB1.

CyclinD1 immunofluorescence analysis (Figure 3.7a) revealed completely different results compared to cyclinA and cyclinB. Integrative pixel analysis for immunofluorescence image of cyclinD1 (Figure 3.7b) indicated similar results as changes in mRNA levels, cyclinD1 levels were elevated in PMA treated neurons. cyclinD1 was found to be localized in the cell body, or even in the nuclear regions of neurons.

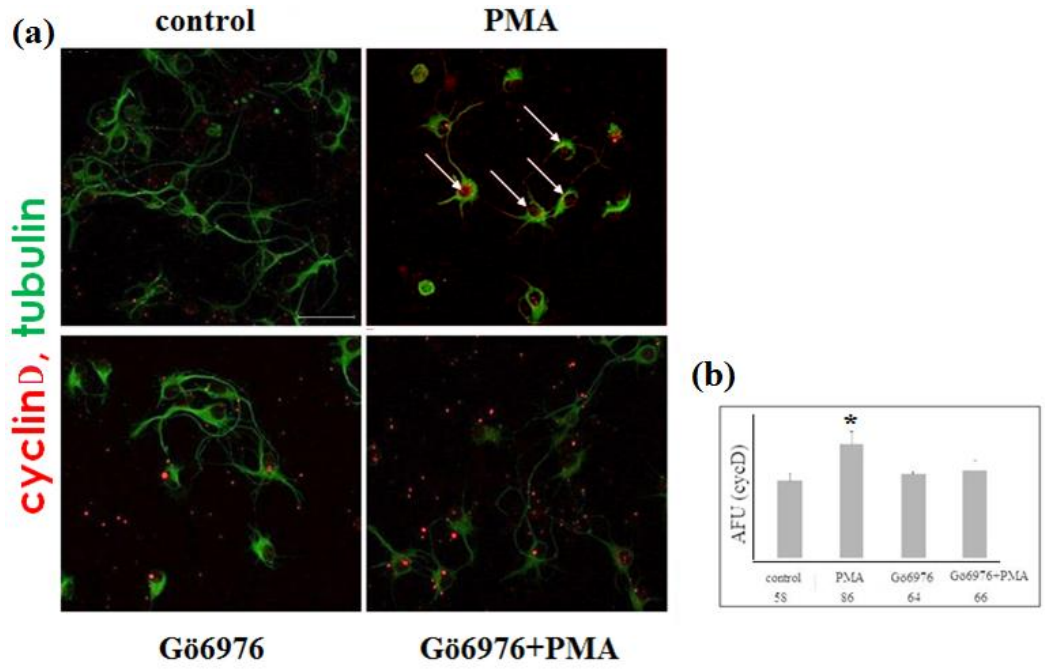

Figure 3.7 : Immunofluorescence analysis of cyclinD1 protein levels after PMA and Gö6976 treatments. **(a)** Neurons were treated for 24 hours with either 0.1% DMSO (control) or PMA or Gö6976 (PKC inhibition) or differently neurons were pre-inhibited with Gö6976 for 1 hour and then PMA treated for 23 hours (Gö6976+PMA). Cells were labeled with cyclinD1 (cycD, red) and neuron specific βIII tubulin (green). Arrows indicate nuclear cyclinD1. **(b)** Integrative pixel analysis as arbitrary fluorescence units (AFU) for immunofluorescence image of cyclinD1. Bar represents mean values ± SD. * $p < 0.05$.

Finally, when cyclinE protein levels were checked (Figure 3.8a), cyclinE was found to be expressed in all four experimental conditions. Integrative pixel analysis showed that (Figure 3.8b), cyclinE levels were increased in PMA and Gö6976 + PMA treated neurons; however, in Gö6976 treated cells cyclinE level was similar to control neurons.

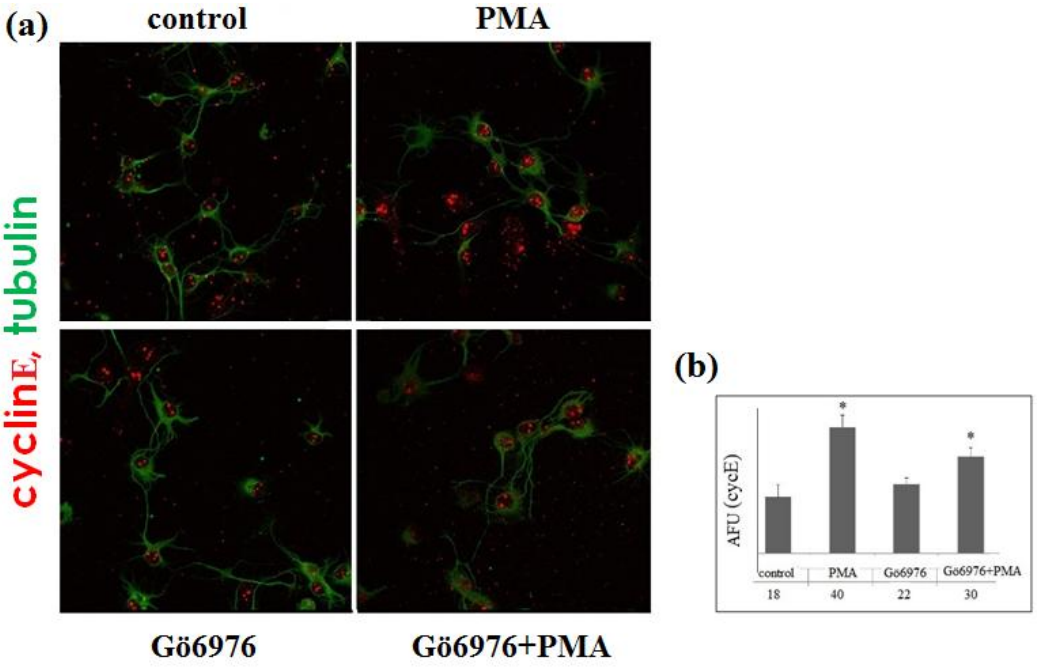

Figure 3.8 : Immunofluorescence analysis of cyclinE protein levels after PMA and Gö6976 treatments. **(a)** Neurons were treated for 24 hours with either 0.1% DMSO (control) or PMA or Gö6976 (PKC inhibition) or differently neurons were pre-inhibited with Gö6976 for 1 hour and then PMA treated for 23 hours (Gö6976+PMA). Cells were labeled with cyclinE (cycE, red) and neuron specific βIII tubulin (green). **(b)** Integrative pixel analysis as arbitrary fluorescence units (AFU) for immunofluorescence image of cyclinE. Bar represents mean values ± SD. * $p < 0.05$.

3.1.5 CyclinD1 analysis in hippocampal neurons upon PMA mediated PKC activation

Since increase was specifically observed in both mRNA and protein levels of cyclinD1 upon PKC activation, cyclinD1 was chosen for further detailed analysis. PKC-α was shown to be a negative regulator of cyclinD1 in intestinal epithelial cells (Frey, 2000), and a positive regulator of cyclinD1 in gliomal cells (Besson and Yong, 2000). Results in this study showed that PKC-α was condensed in the nuclei of neurons upon activation (Figure 3.2, middle panel). To reveal whether this nuclear PKC-α had any possible effects on cyclinD1, detailed analysis for cyclinD1 was performed in PKC activated and inhibited neurons (Figure 3.9).

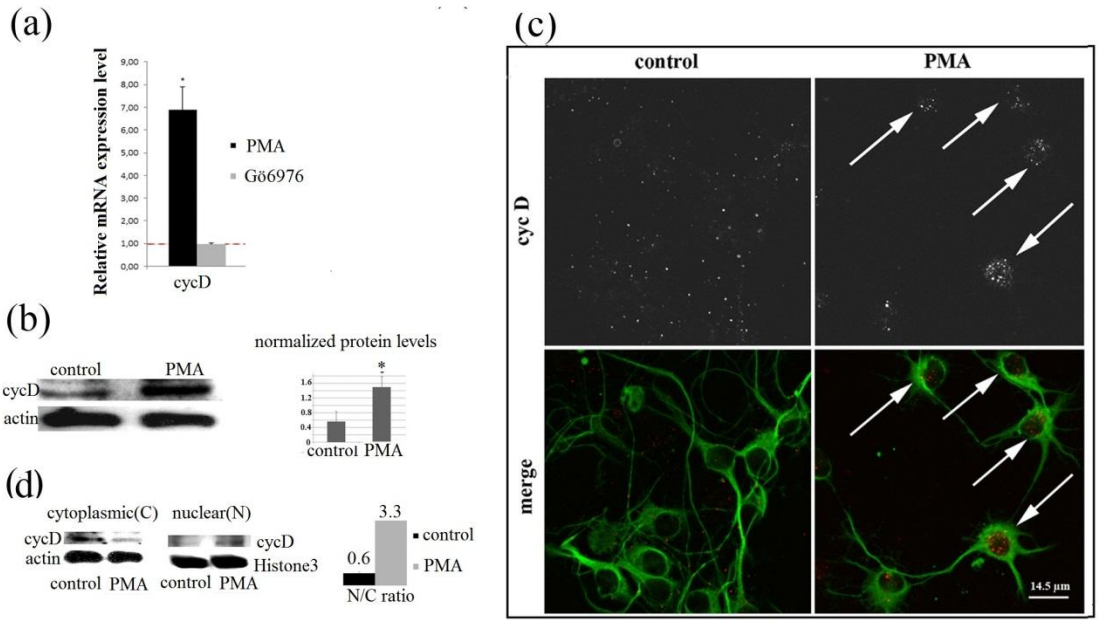

Figure 3.9 : CyclinD1 analysis in hippocampal neurons upon PMA treatment. **(a)** mRNA levels of cyclinD1 (cycD) in PKC activated (PMA) and inhibited (Gö6976) hippocampal neurons were quantified by qRT-PCR. Calculations were performed according to $\Delta\Delta C_T$ method, where expression of control is accepted 1 (red line). Bar represents mean values ± SEM. * $p < 0.05$**. (b)** Western blot of total protein lysate of control and PKC activated (PMA) hippocampal neurons (b, left). Lysates were separated with SDS-PAGE and probed with cycD and actin antibody. Quantitative analysis of the blots (b, right). Band intensities were normalized against actin. Bar represents mean values ± SD. * $p < 0.05$. **(c)** Treated hippocampal neurons immunolabeled for cycD (red in the lover panel; grey in the upper panel) and neuron specific βIII tubulin (green). Scale Bar, 14.5 µm. **(d)** Western blot of cytoplasmic and nuclear protein fractions of control and PKC activated (PMA) hippocampal neurons (left). Membrane was probed with cycD antibody and Histone3 or actin antibodies as an internal control. Quantitative analysis of the blots (right). Band intensities of cycD were normalized against actin for cytoplasmic fraction, and Histone3 for nuclear fraction. Bar represents mean values ± SD.

Results indicated a significant, 6.88-fold increase in cyclinD1 mRNA levels of PMA treated hippocampal neurons ($p < 0.05$); whereas under inhibitory conditions triggered by Gö6976, mRNA levels of cyclinD1 were 0.96 ($p > 0.05$), similar to control groups (Figure 3.9a). Given that a significant change in mRNA levels of cyclinD1 was observed only in PMA treated hippocampal neurons, hence, further studies were performed to determine whether this increase was corresponding to an increase in the protein level, too. To reveal that, Western blot analysis was performed for total protein lysate in PKC activated hippocampal neurons. Blot results also indicated nearly a 3-fold increase in cyclinD1 protein level (Figure 3.9b).

Since protein localization is as crucial as its expression level for its function, immunofluorescence analysis was also performed in order to observe localization of cyclinD1 within the neurons (Figure 3.9c). PKC activated hippocampal neurons were labeled for cyclinD1 (cycD) and neuron specific βIII tubulin simultaneously. Immunofluorescence results pointed out a remarkable nuclear accumulation of cyclinD1 in PKC-α activated condition (Figure 3.9c). In order to further analyze and quantify the shuttling of cyclinD1, nuclear/cytoplasmic fractioning of PKC activated hippocampal neurons was performed and fractions were analyzed with Western blotting (Figure 3.9d, left). Results indicated that nuclear/cytoplasmic ratio of cyclinD1 was 0.6 for control neurons, while under activation condition by PMA, the ratio was 3.3 (Figure 3.9d, right). Nuclear/cytoplasmic ratio was increased 5-fold compared to control group upon PKC activation, which also confirmed nuclear translocation of cyclinD1.

3.1.6 Analysis of pRb and ppRb protein levels upon PKC activation and inhibition

Since pRb is one of the best characterized substrate of cyclinD1, changes in pRb and ppRb levels were investigated. In addition, loss of pRb was found to interfere with differentiation and can re-activate cell cycle machinery even in terminally differentiated cells (Endo and Goto 1992). Increase in both mRNA and protein levels of cyclinD1 was observed in PKC activated cells. Therefore changes on pRb and ppRb protein levels were also investigated by immunofluorescence (Figure 3.10a) and Western bloting (Figure 3.10c). Quantitation results indicated nearly 50% decrease in pRb protein level upon PKC activation (Figure 10.b, d – left), and this decrease was accompanied by nearly 50% increase in ppRb protein level (Figure 3.10d – right).

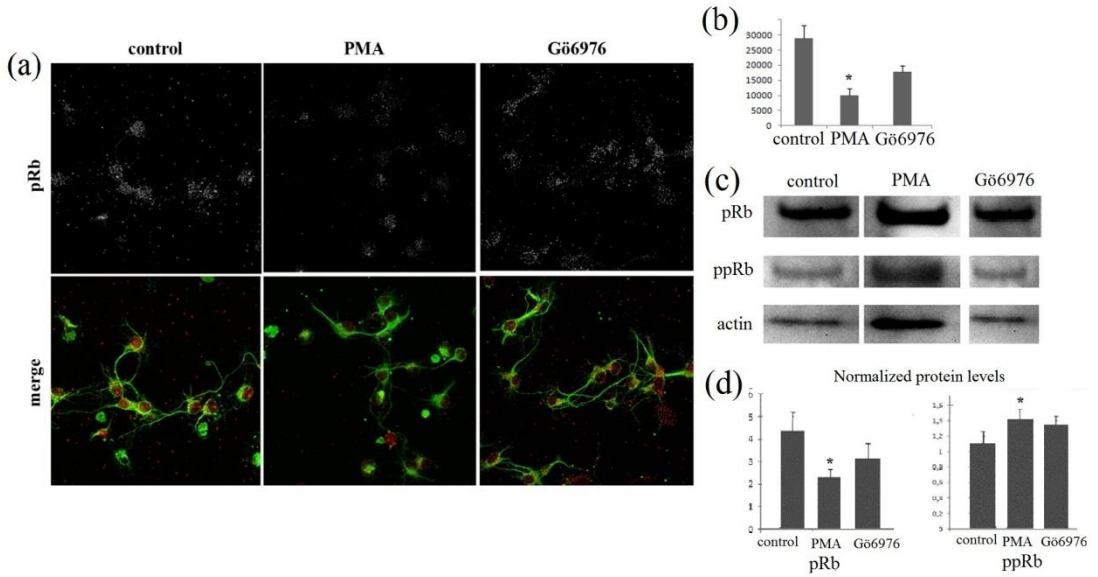

Figure 3.10 : Analysis of pRb and ppRb protein levels in hippocampal neurons after PMA and Gö6976 treatments. **(a)** Treated hippocampal neurons immunolabeled for pRb (red in the lover panel; grey in the upper panel) and neuron specific βIII tubulin (green). **(b)** Integrative pixel analysis of the blots. **(c)** Total protein lysate of control and PKC activated (PMA) hippocampal neurons were separated with SDS-PAGE and probed with pRb, ppRb and actin antibody. **(d)** Quantitative analysis of the blots was performed by normalizing band intensities against actin. Bar represents mean values ± SD. * $p < 0.05$.

3.1.7 Morphological analysis of hippocampal neurons

Visual observations indicated that PMA treated neurons had shorter process formations which led me to analyze the morphology and quantify the differences between the groups (Figure 3.11a). To this aim, process lengths of neurons were measured by using Image-Pro Express (Meyer Instruments) software. To assess whether pre-inhibition of PKC with Gö6976 would reverse the effects of activated PKC in terms of neuronal process features, sequential inhibition-activation condition of PKC was performed. Measurement results showed that average total process lengths of PMA treated neurons decreased nearly 25% ($p < 0.05$) compared to control neurons, whereas average total process lengths of neurons in which PKC was pre-inhibited with Gö6976 were similar to control neurons ($p > 0.05$) (Figure 3.11b). Yet, average process numbers of PMA treated neurons increased nearly 50% ($p < 0.05$) compared to control neurons, while in Gö6976 pre-treated neurons process numbers were even less than control neurons ($p < 0.001$) (Figure 3.11c). Therefore, under PKC activation, neuronal processes were shortened, while process numbers were increased

significantly. Moreover, microtubule density was condensed in the cell body of PMA treated neurons.

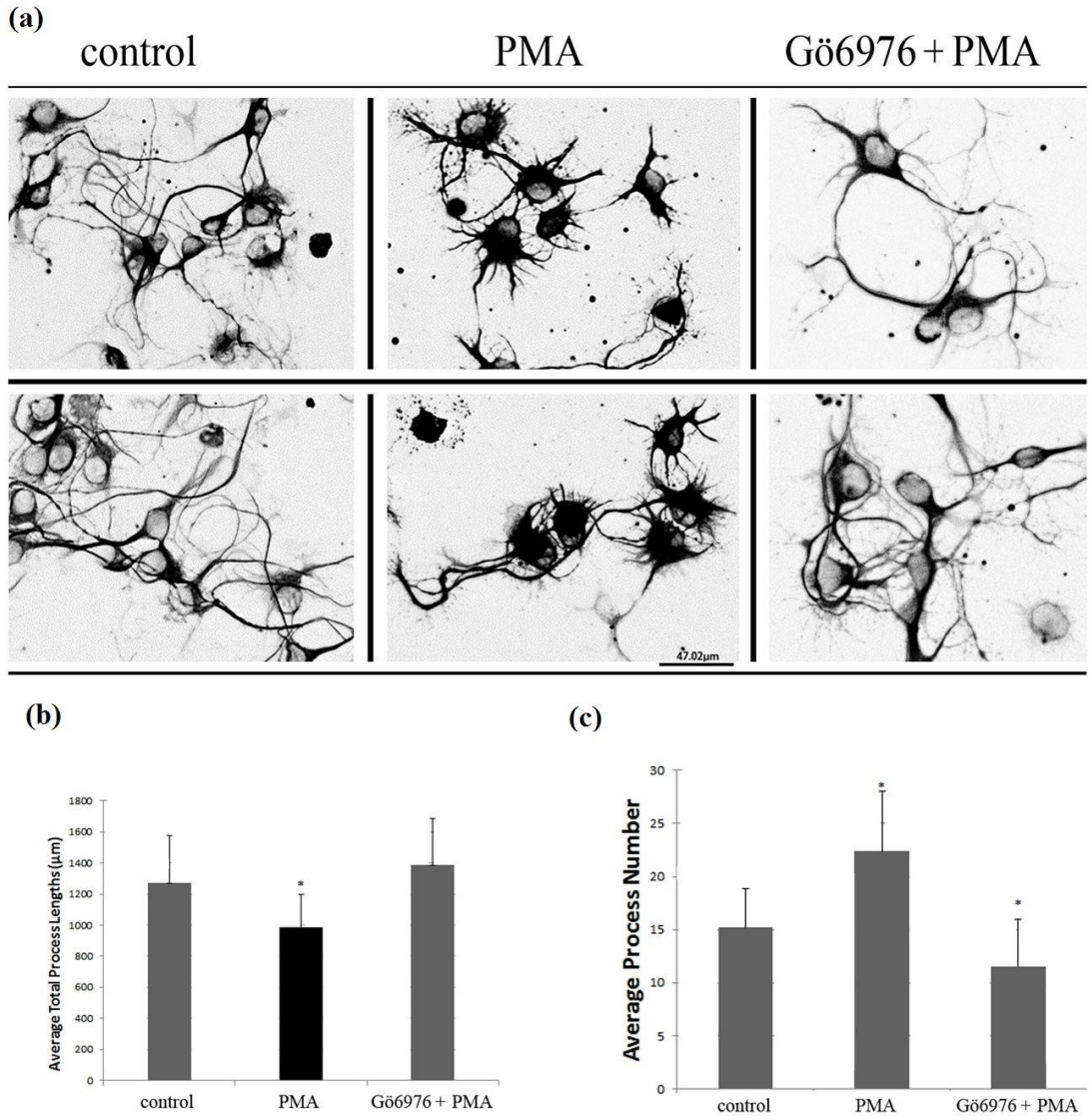

Figure 3.11 : Morphological analysis of hippocampal neurons. Morphological analysis of hippocampal neurons after PMA and Gö6976 treatments. Analysis was performed by using Image-Pro Express (Meyer Instruments) software. **(a)** Hippocampal neurons were immunolabeled for neuron specific βIII tubulin. **(b)** Average total process lengths analysis of hippocampal neurons in control, PMA treated and 1 hour Gö6976 + 23 hours PMA treated conditions. **(c)** Average process number analysis of hippocampal neurons in control, PMA treated and 1 hour Gö6976 + 23 hours PMA treated conditions. Scale Bar, 47.02µm. Bar represents mean values ± SD. * $p < 0.05$.

3.1.8 Determination of p-tau and p60-katanin levels upon PKC activation

Microtubule re-organization differences were observed in PKC activation conditions. Hence, p-tau and p60-katanin protein levels were also analyzed since they are important players of neuronal microtubule organization (Baas and Qiang, 2005; Johnson and Stoothoff, 2004). Therefore, changes in protein level of p-tau (Figure 3.12a) was also analyzed in PMA treated neurons and results were compared with control neurons. Western blot results indicated 2.6-fold increase ($p< 0.05$) in p-tau protein levels upon PMA treatment (Figure 3.14b). Since p-tau dissociates from microtubules, increase in p-tau levels would result in more accessible microtubules, which would serve as substrates for microtubule severing protein p60-katanin (Baas and Qiang, 2005). Hence, changes in p60-katanin levels in PMA treated neurons (Figure 3.12a) were quantified and 1.5-fold increase was observed ($p< 0.05$) in PMA treated neurons compared to control neurons (Figure 3.14b).

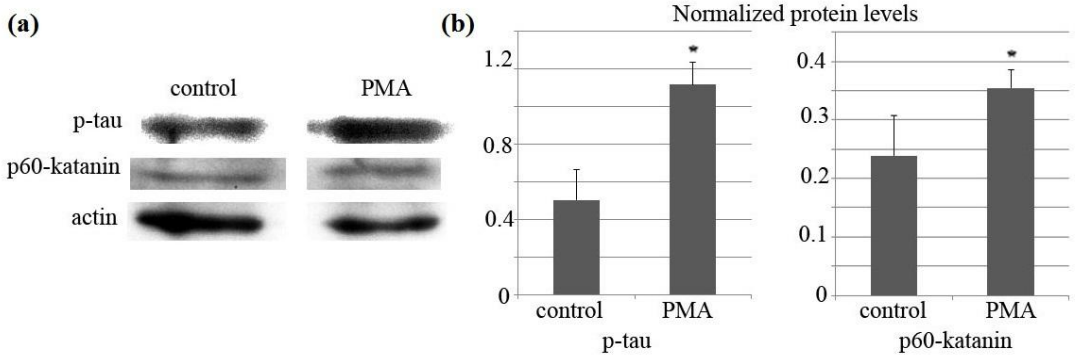

Figure 3.12 : P-tau and p60-katanin protein levels in PMA treated hippocampal neurons. **(a)** Western bloting analysis of p-tau and p60-katanin protein lysates in control and PMA treated neurons. Control and PKC activated hippocampal neurons were immunolabeled for p-tau (Ser^{199}) and p60-katanin proteins. **(b)** Quantitative analysis of the blots were achieved by normalizing band intensities of p-tau and p60-katanin against actin. Bar represents mean values ± SD. * $p< 0.05$.

3.1.9 Phosphorylation analysis of GSK3β upon PMA treatment

For proliferating cells, cyclinD1, marker for G_0 exit, needs to be up-regulated so that cells could proceed through G_1 phase. CyclinD1 accumulates in the nucleus throughout G_1 phase, and re-localizes to the cytoplasm as cells proceed to S phase. Orchestration of cyclinD1 translocation is carried out by GSK3β. Activated GSK3β is one of the main players for the transport of cyclinD1 back to the cytoplasm that takes place when cells exit G_1 to proceed through S phase (Baldin, 1993; Diehl,

1998). GSK3β is also one of the substrates of PKC and has a role in tau phosphorylation. Findings in this study demonstrated that PKC activation increased nuclear accumulation of cyclinD1, phosphorylation of Rb and tau. Hence, phosphorylation analysis for GSK3β was performed in total protein lysates of PMA treated hippocampal neurons (Figure 3.13).

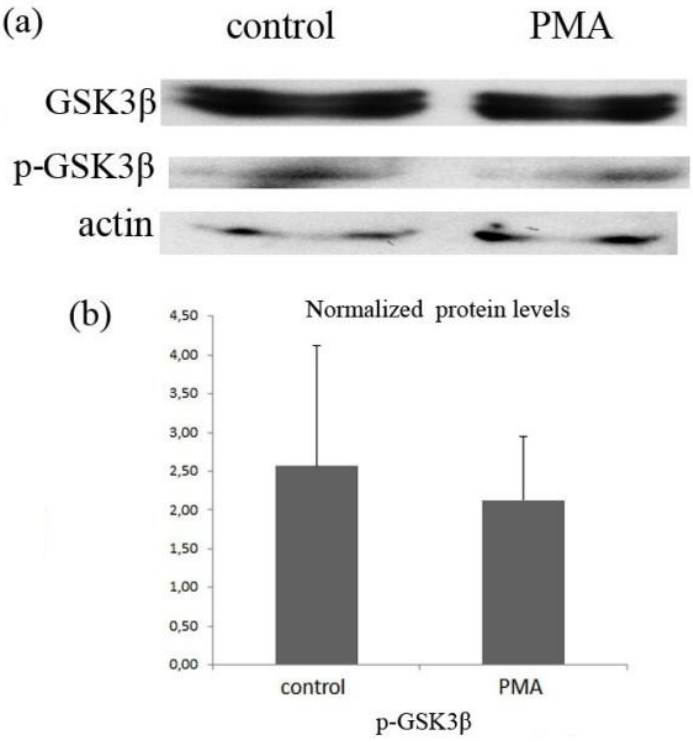

Figure 3.13 : GSK3β and p-GSK3β analysis in PMA treated hippocampal neurons. **(a)** Western blot analysis of GSK3β and p-GSK3β protein lysates in control and PMA treated neurons. Control and PKC activated hippocampal neurons were immunolabeled for GSK3β and p-GSK3β (Ser9). **(b)** Quantitative analysis of the blots were achieved by normalizing band intensities of GSK3β and p-GSK3β against actin. Bar represents mean values ± SD.

When phorsphorylation of GSK3β was analyzed by Western blotting, there was no significant change ($p > 0.05$) observed between control and PMA treated neurons.

3.1.10 Proliferation and apoptosis analysis in PMA treated neurons

Increase in nuclear cyclinD1 is associated with proliferation in mitotic cells; while in neurons increase in nuclear cyclinD1 (Nagy, 2007; Herrup and Yang, 2007; Atabay and Karabay, 2011) and p-tau (Lee, 2001; Atabay and Karabay, 2011) evoke neurodegeneration. To reveal any possible activation of proliferation or apoptosis upon PKC activation, ThePathScan® Apoptosis and Proliferation Multiplex IF kit

was used. The kit contains primary cocktail composed of three primary antibodies specific for α-tubulin, phospho Histone3 Ser10 and cleaved PARP Asp214 (Figure 3.14a). Cleavage of PARP facilitates cellular disassembly and serves as a marker for cells undergoing apoptosis, while phosphorylation of Histone3 is correlated with chromosome condensation that occurs both in mitosis and meiosis. Results indicated that PMA treatment triggered neither proliferation nor apoptosis in neurons (Figure 3.14a, middle). Whereas, in physiological mitotic cells, both proliferation and naturally occurring apoptosis were observed (Figure 3.14a, right).

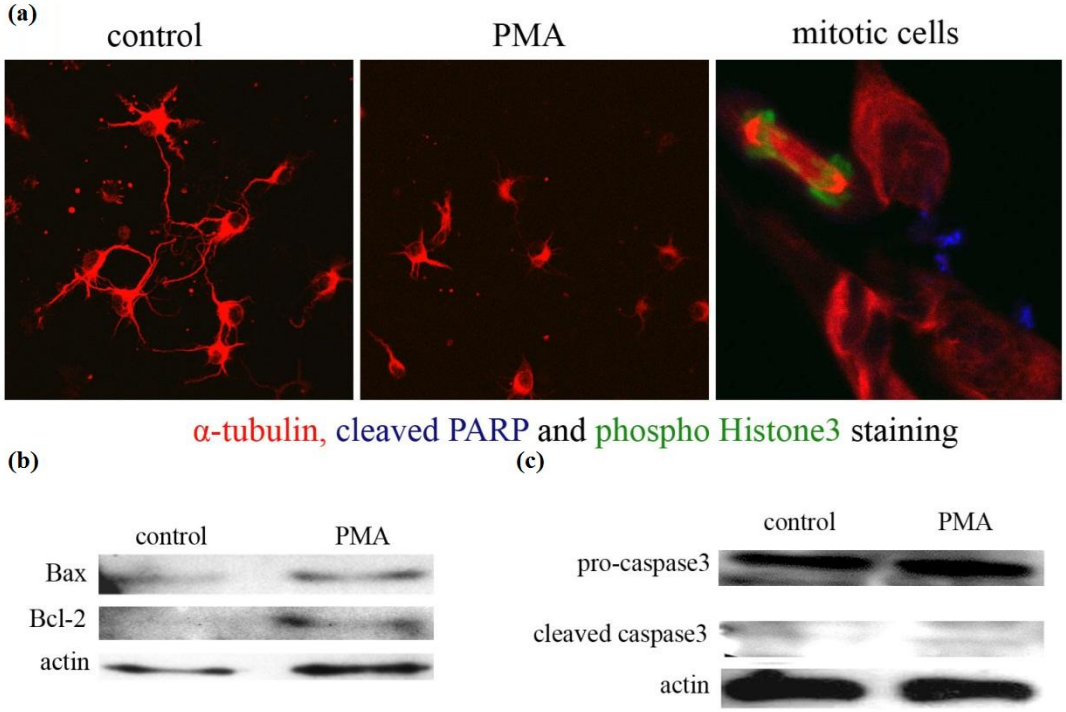

Figure 3.14 : Apoptosis and proliferation analysis of hippocampal neurons after PMA treatment. **(a)** Apoptosis and proliferation analysis of hippocampal neurons and mitotic cells. Cells were immunolabeled for cleaved PARP (blue, indication of apoptosis), phospho Histone3 (green, indication of proliferation) and α-tubulin (red). **(b, c)** Western blot image of total protein lysate of control and PKC activated (PMA) hippocampal neurons. Lysates were separated with SDS-PAGE and probed with Bax, Bcl-2 (b), caspase3 (c) and actin (b, c) antibodies.

PMA treated cells were also analyzed for Bax pro-apoptotic protein, Bcl-2 anti-apoptotic protein (Figure 3.14b) and caspase3 protease (Figure 3.14c). There was no significant difference in Bax protein levels between control and PMA treated neurons (Figure 3.14b, upper) ($p > 0.05$). When Bcl-2 levels were analyzed (Figure 3.14b, middle), there was no protein band observed in control neurons, while it was obvious in PMA treated neurons. Immunoblotting for caspase3 protein was performed for

both control and PMA treated neurons (Figure 3.14c). Findings indicated that pro-caspase3 levels were increased in PMA treated cells, but there was no indication for increase in cleaved caspase3.

3.2 Effects of PKC Activation in Amyloid Beta Treated Hippocampal Neurons

3.2.1 Observation of amyloid beta plaques in hippocampal neurons

The aim of this study was to reveal effects of PKC activation on cell cycle re-activation in neurons under non-degenerative and degenerative condition. In this part of the study, hippocampal neurons were treated with Aβ in order to trigger amyloid based degeneration. It is known that concentrations between 6.5 – 22 μM of Aβ causes neurodegeneration, hence, 7 μM final concentration of Aβ was chosen in this study since the aim was to only initiate degeneration rather than obtain totally degenerated neurons. Aβ plaques that were observed were monitored with congo red staining by light microscopy (Figure 3.15).

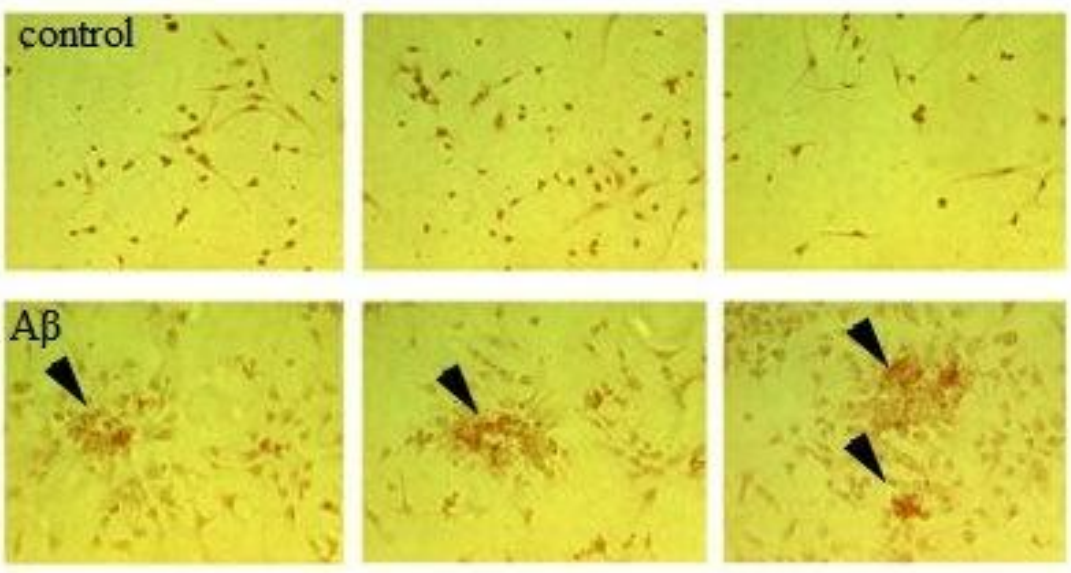

Figure 3.15 : Congo red staining of hippocampal neurons for Aβ plaques. Congo red staining was performed for hippocampal neurons following 24 hours 7 μM Aβ treatment. Image was obtained by using light microscopy. Arrowheads show plaque depositions.

3.2.2 Expression level and subcellular distribution analysis of PKC-α upon PKC activation in amyloid beta treated neurons

PKC is one of the proteins that have altered expression levels in AD and its activity and translocation has been consistently found to be reduced in AD patients' fibroblasts and brains (Battaini, 1999; Gasparini, 1998). In the previous section of the study, the aim was to investigate the effects of PKC activation in hippocampal neurons under their physiological conditions. In this part of the study, the aim was to reveal the effects of PKC under neurodegenerative condition such as AD. For this purpose, PKC activation studies were performed in Aβ treated neurons in order to compare discrepancies in PKC signaling pathway between physiological and Aβ treated neurons in terms of changes in protein levels and distributions of cyclins, specifically cyclinD1 and PKC-α itself.

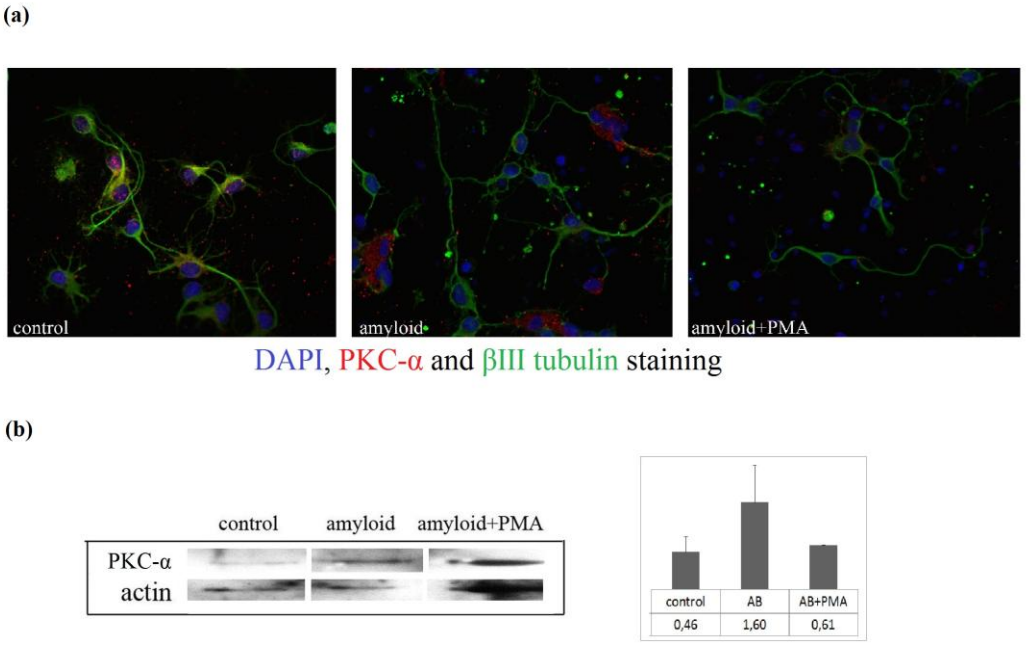

Figure 3.16 : Immunofluorescence and Western blot analysis of PKC-α protein levels after Aβ and PMA treatments. Neurons were treated for 24 hours with either 0.1% DMSO (control) or Aβ (amyloid) or neurons were pre-treated with Aβ for 24 hours and then PMA treated for an additional 24 hours (amyloid + PMA). **(a)** Cells were labeled with PKC-α (red), neuron specific βIII tubulin (green) antibodies and DAPI (blue). **(b)** Western blot analysis of PKC-α (b,left) and quantitation of the blots (b, right). Bar represents mean values ± SD.

For this purpose, protein expression and subcellular distribution of PKC-α were analyzed in Aβ treated hippocampal neurons (Figure 3.16). According to immunofluorescence analysis (Figure 3.16a), PKC-α was distributed throughout the

cell (cell body and processes) in control neurons (Figure 3.16a, left panel). When neurons were treated with 7 μM Aβ for 24 hours (Figure 3.16a, middle panel), distribution of PKC-α was not changed prominently. When neurons were sequencially treated with Aβ and PMA for 24 hours each, PKC-α level was faintly decreased (Figure 3.16a, right panel). When Western blot analysis was performed for the same experimental conditions (Figure 3.16b, left), quantitation results showed that there was no significant change in PKC-α protein levels between control and experimental neurons (Figure 3.16b, right).

3.2.3 Effects of PKC activation on mRNA levels of cyclins in amyloid beta treated hippocampal neurons

As indicated in the previous part, PMA mediated PKC activation significantly increased mRNA level of cyclinD1 and cdk1 (Figure 3.3). qRT-PCR analysis was again performed to reveal effects of PKC activation under Aβ treated condition in hippocampal neurons (Figure 3.17). When qRT-PCR results were analyzed, it was seen that there was no significant change in mRNA levels of cell cycle proteins in Aβ treated hippocampal neurons (Figure 3.17a). Furthermore, mRNA levels of cell cycle proteins in 24 h Aβ and 24 hours PMA treated hippocampal neurons were similar to control neurons (Figure 3.17b). Differently from only PMA treated neurons (Figure 3.3), Aβ treated neurons did not response to PMA mediated PKC activation, in terms of increase in cyclinD1 mRNA level.

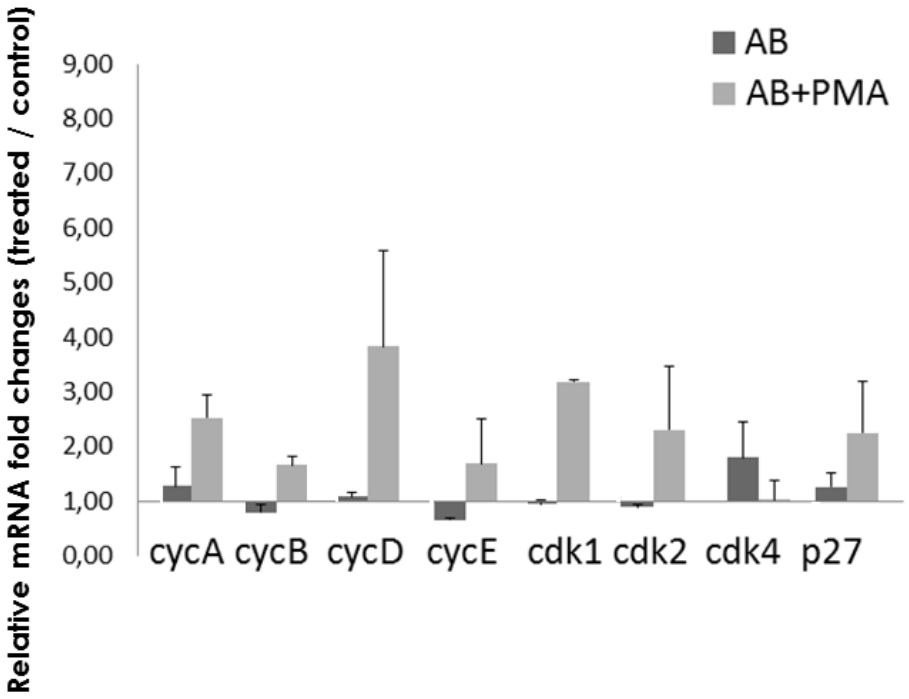

Figure 3.17 : Changes in relative mRNA levels of cell cycle proteins upon Aβ and PMA treatments. **(a)** Changes in relative mRNA levels of cell cycle proteins upon 24 h Aβ treatment and **(b)** 24 h Aβ treatment followed by 24 hours PMA treatment. Boxes represents the interquartile range of observations. The dotted line shows the median gene expression. Line represents relative gene expression level for control cells which is accepted 1. Bar represents mean values ± SEM. * $p < 0.05$.

3.2.4 Analysis of protein levels and distibutions of cyclinD1 in amyloid beta treated hippocampal neurons

mRNA analysis did not indicate any significant change in mRNA levels neither in Aβ treated nor in Aβ + PMA treated neurons (Figure 3.17). Though, immunofluorescence analysis was performed to see whether protein level or distribution of cyclinD1, which has been found to be up-regulated in PMA treatment, was changed upon amyloid treatment.

When immunofluorescence analysis was performed for cyclinD1 (Figure 3.18), integrative pixel analysis results indicated increase only in PMA condition. CyclinD1 levels in Aβ and Aβ + PMA condition were similar to control neurons (Figure 3.18b). Nuclear localization of cyclinD1 was not observed in control, Aβ and Aβ + PMA treated neurons but clearly observed in only PMA treated ones (Figure 3.18a).

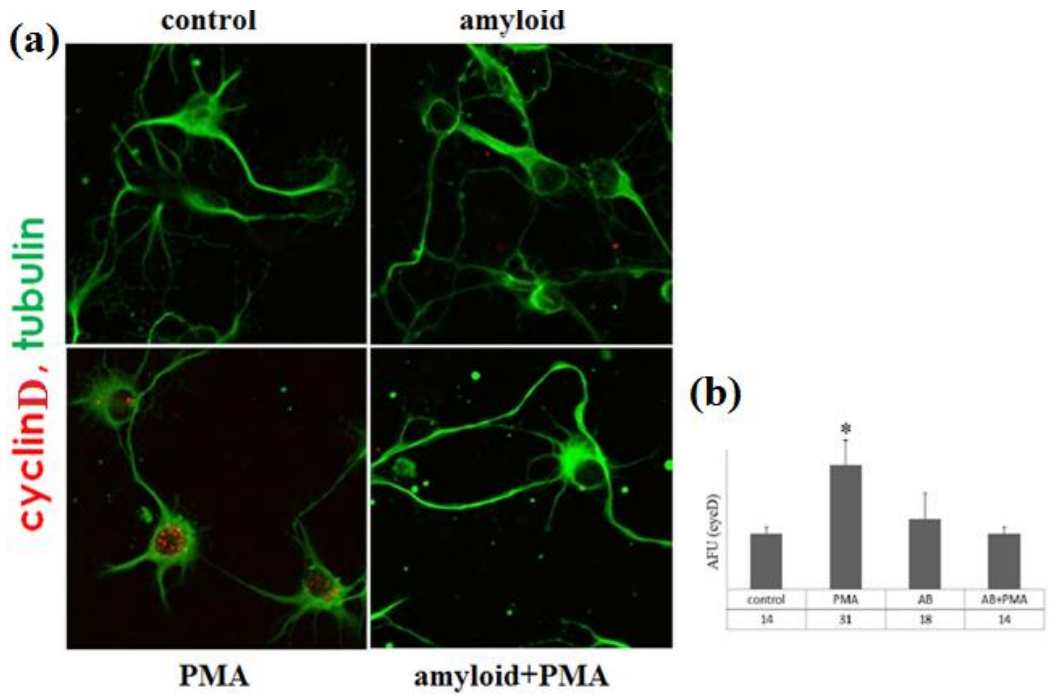

Figure 3.18 : Immunofluorescence analysis of cyclinD1 protein levels after Aβ and PMA treatments. **(a)** Neurons were treated for 24 hours with either 0.1% DMSO (control) or PMA or Aβ or neurons were pre-treated with Aβ for 24 hours and then PMA treated for an additional 24 hours (Aβ + PMA). Cells were labeled with cyclinD1 (cycD, red) and neuron specific βIII tubulin (green) antibodies. **(b)** Integrative pixel analysis as arbitrary fluorescence units (AFU) for immunofluorescence image of cyclinD1. Bar represents mean values ± SD. * $p < 0.05$.

3.2.5 Analysis expression level and subcellular distribution of pRb upon PKC activation in amyloid beta treated neurons

As indicated in the first part of the study, pRb is one of the best characterized substrate of cyclinD1 and loss of pRb was found to interfere with differentiation (Endo and Goto, 1992). In the first part of the study, quantitation results indicated a nearly 50% decrease in pRb protein level upon only PKC activation (Figure 3.10). Here, in the second part of the study, immunofluorescence analysis was performed for pRb in amyoid or amyloid+PMA treated neurons (Figure 3.19a) in addition to control and only PMA treated cells. Integrative pixel analysis results indicated more than 50% decrease in pRb protein level upon only PKC activation (PMA). pRb levels were similar between conrol and Aβ or Aβ + PMA treated neurons (Figure 3.19b).

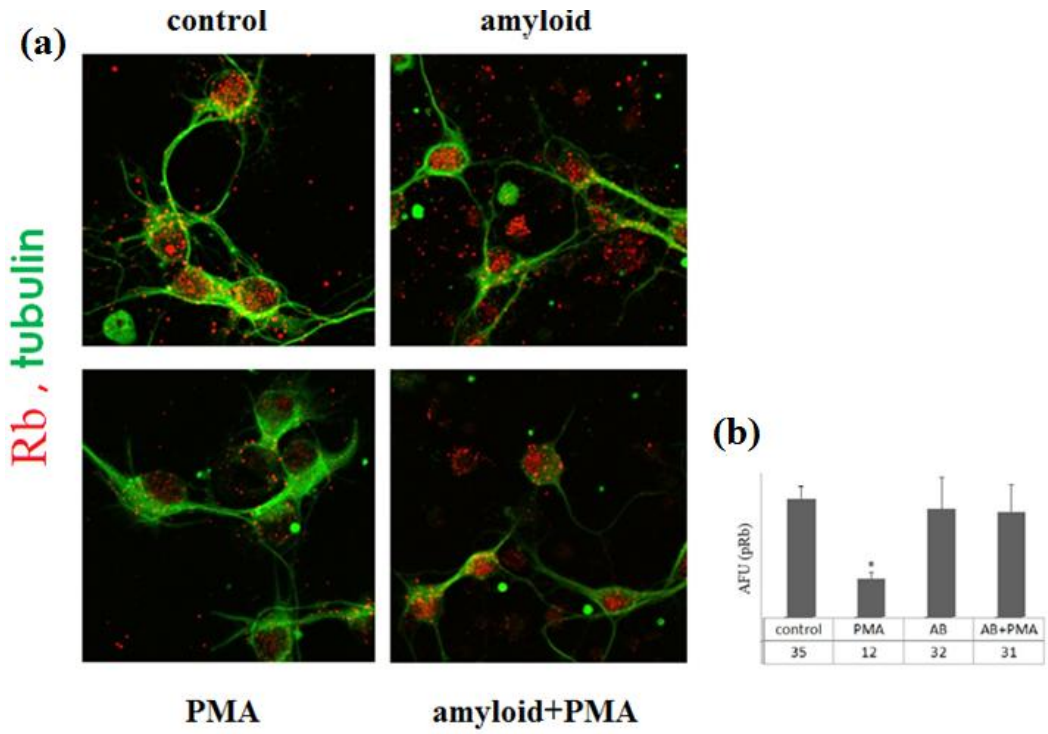

Figure 3.19 : Immunofluorescence analysis of pRb protein levels after Aβ and PMA treatments. **(a)** Neurons were treated for 24 hours with either 0.1% DMSO (control) or PMA or Aβ or neurons were pre-treated with Aβ for 24 hours and then PMA treated for an additional 24 hours (Aβ + PMA). Cells were labeled with pRb (red) and neuron specific βIII tubulin (green) antibodies. **(b)** Integrative pixel analysis as arbitrary fluorescence units (AFU) for immunofluorescence image of pRb. Bar represents mean values ± SD. * $p < 0.05$.

3.2.6 Morphological analysis of amyloid beta treated hippocampal neurons

Morphological analysis of the neurons has revealed that under PKC activation, neuronal processes were shortened, while process numbers were increased significantly (Figure 3.11). Similar morphological analysis was performed for amyloid beta treated neurons to reveal effects of amyloid on neuronal processes. Results indicated that average total process lengths of amyloid and amyloid+PMA treated neurons were similar to control neurons ($p > 0.05$) (Figure 3.20b), however, there was a nearly 50% decrease in average process number of amyloid and amyloid+PMA treated neurons ($p < 0.001$) (Figure 3.20c).

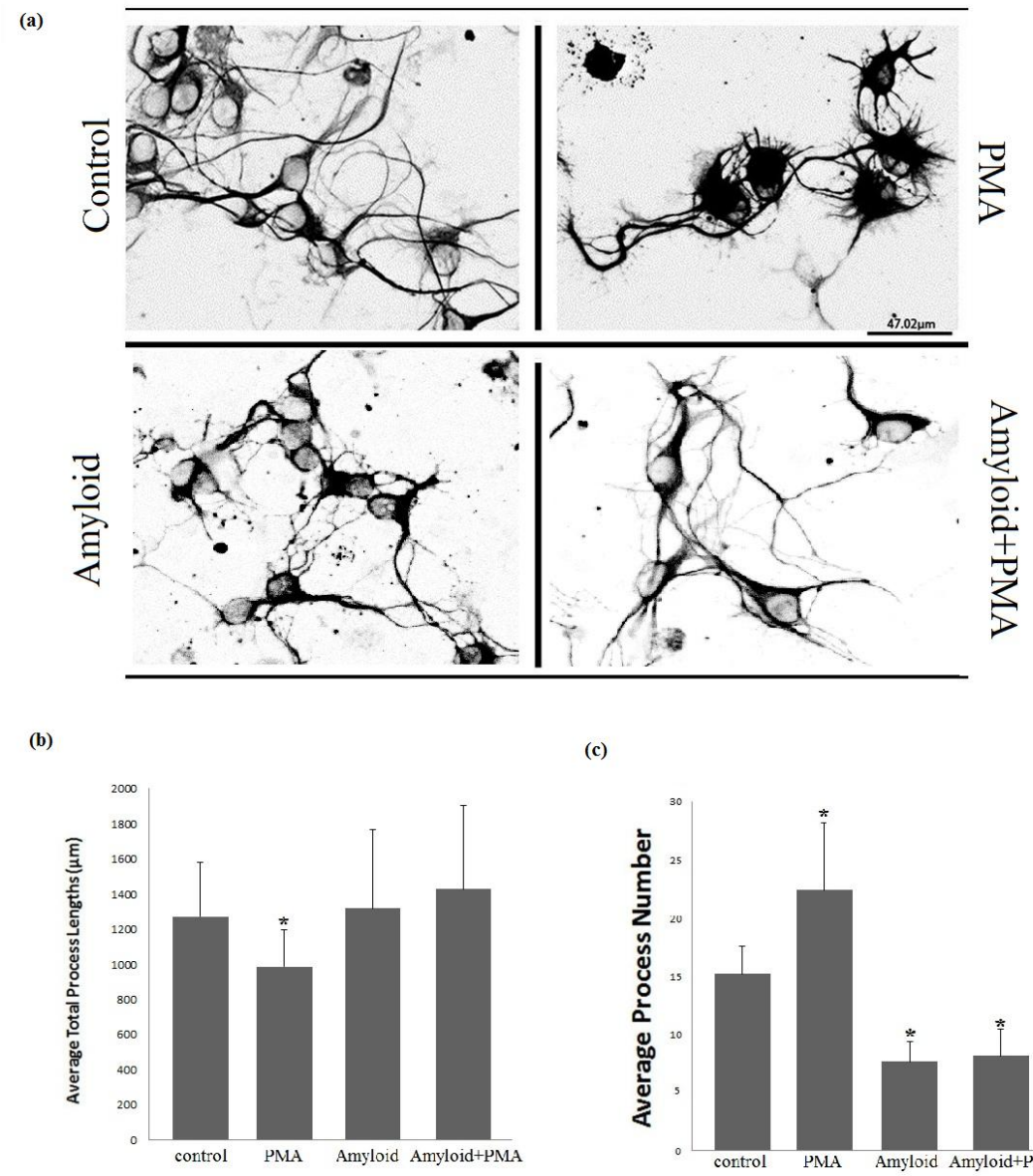

Figure 3.20 : Morphological analysis of amyloid beta treated hippocampal neurons. **(a)** Hippocampal neurons were immunolabeled for neuron specific βIII tubulin. **(b)** Average total process lengths analysis of hippocampal neurons in control, PMA, Aβ, Aβ + PMA treated conditions. **(c)** Average process number analysis of hippocampal neurons in control, PMA, Aβ, Aβ + PMA treated conditions. Scale Bar, 47.02µm. Bar represents mean values ± SD. * $p < 0.05$.

3.2.7 Analysis expression level and subcellular distribution of p-tau, p60-katanin and GSK3β upon PKC activation in amyloid beta treated neurons

Microtubule re-organization differences were observed in PKC activation conditions and hence, p-tau and p60-katanin protein levels were analyzed (Figure 3.12). In this part of the study, changes in protein level of p-tau (Figure 3.21a) and p60-katanin (Figure 3.21b) were also analyzed. Western blot quantitation did not reveal

significant differences between control and treated neurons for p-tau (Figure 3.21a) and p60-katanin levels were similar between all three conditions ($p > 0.05$) (Figure 3.21b).

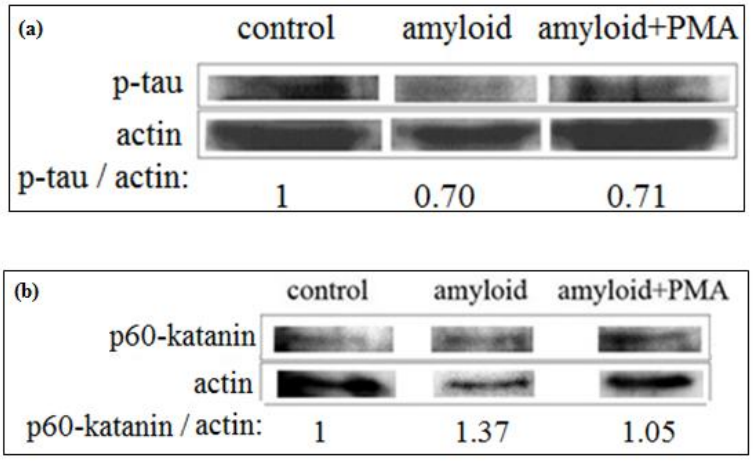

Figure 3.21 : Western blot analysis of p-tau and p60-katanin protein levels after Aβ and PMA treatments. Neurons were treated for 24 hours with either 0.1% DMSO (control) or Aβ or neurons were pre-treated with Aβ for 24 hours and then PMA treated for an additional 24 hours (Aβ + PMA). **(a, b)** Western blot analysis and quantitation of the blots for p-tau (a) and p60-katanin (b). Bar represents mean values ± SD.

3.2.8 PKC activation triggered neither proliferation nor apoptosis in amyloid beta treated neurons

To reveal any possible activation of proliferation or apoptosis upon Aβ treatment ThePathScan® Apoptosis and Proliferation Multiplex IF kit was used. There was no indication for either proliferation or apoptosis under these experimental conditions (Figure 3.22a). Aβ treated cells were also analyzed for Bax pro-apoptotic protein and Bcl-2 anti-apoptotic protein by Western blot (Figure 3.22b). Quantitation of Western blot indicated a significant increase in Bax/Bcl-2 ratio between control and Aβ treated and between control and Aβ + PMA treated neurons ($p < 0.05$) (Figure 3.22c).

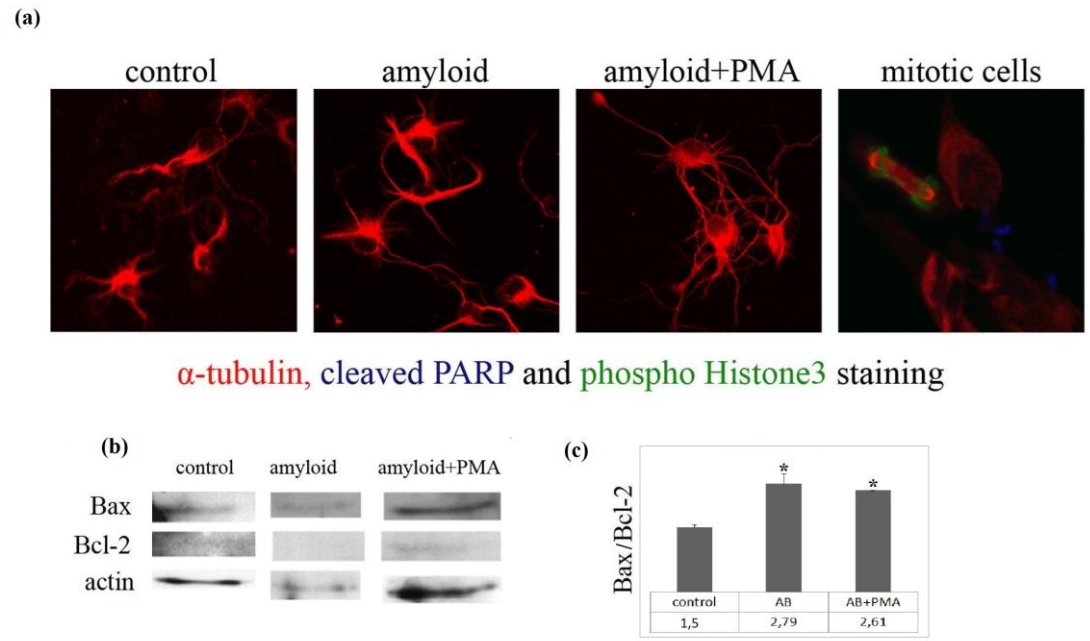

Figure 3.22 : Apoptosis and proliferation analysis of hippocampal neurons after Aβ treatment. **(a)** Apoptosis and proliferation analysis of neurons and mitotic cells. Cells were immunolabeled for cleaved PARP (blue), phosphor Histone3 (green) and α-tubulin (red). **(b)** Western blot image of total protein lysate of control, amyloid treated and sequencially amyloid teated and PKC activated (amyloid+PMA) hippocampal neurons. Lysates were probed with Bax, Bcl-2 and actin antibodies. **(c)** Quantitation of Western blot image in terms of Bax/Bcl2 ratio. Bar represents mean values ± SD. * $p < 0.05$.

4. DISCUSSION AND CONCLUSIONS

Since neurons are terminally differentiated cells that are restricted from reverting back to the cell cycle, stringent set of control mechanisms are required to keep them at G_0 phase. Revealing the effects of PKC activation on cyclins, especially cyclinD1 is crucial in terms of understanding whether it would lead neurons to cell cycle re-activation as indicated by PKC's involvement with neurodegeneration. For instance, PKC activity has been consistently found to be reduced in AD patients' fibroblasts; decreased activity and expression of particular PKC isoforms have also been demonstrated in postmortem brain cortex of AD subjects. Here, it was shown that PKC activation changed distribution of both PKC-α and cyclinD1 in neurons under their physiological condition. PKC activation also increased phosphorylation of pRb, triggered microtubule re-organization and increased protein levels of p-tau and p60-katanin. Yet, it did not activate any apoptotic or proliferative signaling pathway via up-regulation of cyclinD1 which has been shown to be involved in degeneration of neurons. Experimental results indicated that cyclinD1 might also be related with neuronal differentiation as suggested by a number of increasing contemporary studies.

Since it was not clear enough in neurons, the effects of PKC activation on distributional and expressional orchestration of PKC-α was investigated in physiological conditions. Although PKC-α usually functions in cytoplasm and membrane fractions of the cells, there has been evidence indicating a role for PKC-α in nuclear compartments such as in replication and transcription (Martelli, 2006). Consequently, it was found that PKC-α was prominently translocated to the nuclei of hippocampal neurons upon activation, indicating a possible nuclear role for neuronal PKC-α. However, when neurons were treated with Aβ for 24 hours, as a degenerative condition, they did not response to PMA treatment in terms nuclear localization of PKC-α. It is possible that direct Aβ – PKC interaction was observed through PKC pseudosubstrate domain of Aβ (Lee, 2004) and prevented activation by PMA.

As cytoplasmic PKC-α could serve either activating or inhibitory functions, it is also likely that nuclear PKC-α could either up- or down-regulate transcription of the

target genes, such as cyclinD1, in this case. For instance, in hippocampal neurons, it was found that cyclinD1 was up-regulated both in mRNA and protein levels upon PMA mediated PKC activation. Yet, pre-inhibition of PKC with Gö6976 before activation caused a reduction in the expression level of cyclinD1 supporting the specificity of the effect of PKC activation on cyclinD1 expression. However, exact mechanism of cyclinD1 up-regulation by PKC in neurons is still elusive and detailed mechanism for transcriptional control needs to be elucidated in further studies. Yet, changes in mRNA level did not correspond exactly to the changes in protein level. For instance mRNA increase in cyclinD1 upon PMA treatment was observed to be ~8-fold, however, changes in protein level of cyclinD1 was nearly 3-fold. Yet, it is known that mRNA levels cannot be always used to predict protein levels. There are many factors such as RNA secondary structure, 3' UTR (Un-Translated Region), post translational modification, protein-protein interactions, other protein stabilizing molecules, etc… effecting rate of mRNA and protein turnover. There may also be miRNAs (micro RNAs) that have roles in affecting cyclinD1 mRNA stability, as well.

Differently from only PMA treated neurons, in Aβ treated and Aβ + PMA treated neurons neither mRNA nor protein level and distribution of cyclinD1 was changed. It can be speculated that although Aβ treatment did not initiate a full neurodegeneration, it probably caused impairments in PKC signaling pathway as a results of direct Aβ – PKC interaction and prevented nuclear accumulation of PKC-α upon activation and its subsequent influences on cyclinD1.

It is widely accepted that, for proliferating cells, cyclinD1, a marker for G_0 exit, needs to be up-regulated so that cells could proceed through G_1 phase. According to the known model, cyclinD1 accumulates in the nucleus throughout G_1 phase, and re-localizes to the cytoplasm as cells proceed to S phase (Baldin, 1993; Diehl 1998). According to conventional knowledge, cell cycle proteins are thought to be silenced in terminally differentiated neurons. However, there are many recent studies indicating expression of cyclinD1, cyclinA and other cell cycle related proteins in neurons and attributing cell cycle independent roles for them such as participating in synaptic plasticity and differentiation (Schmetsdorf, 2007; Richter, 2001; Bowser and Smith, 2002; Ross and Risken, 1994; Ross, 1996). Based on findings in this study which demonstrated that PKC activation increased nuclear accumulation of

cyclinD1, it could be tempting to predict that neurons attempted to leave G_0 phase to proceed through G_1 phase. However, there was no up-regulation of cell cycle progression indicator downstream cyclin, cyclinA, in either transcriptional or translational level. These findings may also contribute to the information of cell cycle independent role for nuclear cyclinD1 in neurons.

pRb is one of the substrates of cyclinD1. Hyper-phosphorylated pRb (ppRb) is inactive form of pRb and present in late G_1, S, G_2, and M phases of cycling cells (Nagy, 2007). Furthermore, loss of pRb was found to interfere with differentiation and can re-activate cell cycle machinery even in terminally differentiated cells (Herrup and Yang, 2007). Results showed a decrease in pRb level and it is compensated by an increase in ppRb level. In dividing cells, increase in ppRb levels is accompanied by an increase in S phase cyclin, cyclinA. However, in this study, neither mRNA (Figure 3.3) nor protein levels or subcellular distributions of cyclinA (Figure 3.5) were changed upon PKC activation. Thus, unlike mitotic cells, increase in ppRb level in neurons did not result in further progress in cell cycle. Yet, decrease in pRb level appeared together with retraction of neuronal processes (Figure 3.11a, middle), and this is consistent with the role of pRb in differentiation (Ezhevsky, 1997). Decreased pRb level caused shorter process formation towards more globular structure in neurons.

Observations indicated changes in morphology of neurons in terms of microtubule lengths and process numbers. Hence, neurons were analyzed to obtain average total process lengths and average process numbers (Figure 3.11b and 3.11c, respectively). Results indicated that average total process lengths were decreased in PKC activated neurons (Figure 3.11a, middle and Figure 3.11b). However, in neurons that PKC was pre-inhibited with Gö6976 before activation (Figure 3.11a, right and Figure 3.11b), average total process lengths were similar to control neurons (Figure 3.11a, left and Figure 3.11b). In addition to this, average process number was increased nearly 50% in PKC activated neurons, and there was a slight decrease in the number of processes per neuron in pre-inhibition condition (Figure 3.11c). Morphological changes in neuronal branches occur as a result of microtubule re-organization, and in this study, PKC activated neurons also exhibited re-organization in neuronal processes. Furthermore, when neurons were treated with Aβ and Aβ + PMA, average total process lengths were similar to control neurons (Figure 3.20b) while in PMA treated

neurons process lengths were decreased (Figure 3.11b, 3.20b) as an indication of microtubule re-organization. It can be concluded that Aβ prevented microtubule re-organization upon PMA treatment probably as a result of Aβ – PKC interaction, as previously indicated. Despite the fact that average total process lengths did not changed upon Aβ treatments, average process numbers were decreased in both Aβ and Aβ + PMA treated neurons implying amyloid caused impairments in minor process formations which may lead to neurodegeneration in further timepoints.

The main players taking part in microtubule re-organization in terms of neuronal differentiation are p-tau and p60-katanin (Vale, 2000; Baas and Qiang, 2005). In this content, Western blot results indicated 2.6-fold increase in p-tau protein levels upon PMA treatment (Figure 3.12a). tauSer199 has been shown to be phosphorylated (p-tauSer199) by GSK3β of which PKC is an upstream effector. As there was no increase observed in the phosphorylation level of GSK3β upon activation of PKC (Figure 3.13) under this experimental conditions, it could be likely that tau phosphorylation was achieved by GSK3β which is still in an active form in de-phosphorylated state. Since PKC showed nuclear localization rather than being localized in membrane/cytosolic compartments upon activation, it could not either phosphorylate cytosolic tau or inactivate cytosolic GSK3β. Therefore, instead of a direct phosphorylation by PKC, tau was more likely to be phosphorylated by active GSK3β, and phosphorylation of tau caused retraction of axons. Besides its role in axonogenesis (Johnson and Stoothoff, 2004), p-tau takes role in microtubule re-organization, for instance, p-tau dissociates from microtubules and these microtubules become more accessible and serve as substrates for microtubule severing protein p60-katanin (Baas and Qiang, 2005). p60-katanin's severing activity is already known to increase upon tau hyper phosphorylation in terms of easier access onto microtubules. Consistent with morphological observations in this study on neuronal processes, increase was seen in the protein level of p60-katanin which was also in correlation with an observed increase in p-tau levels, as expected.

In dividing cells, during the transition from interphase to mitosis, p60-katanin is known to increase (Karabay, 2004). Based on cyclinD1 increase upon PKC activation, neurons might be thought as being tricked by unconfirmed signals of division and therefore, they are increasing their p60-katanin level. In addition to be known as an indisputable marker of coming out of cell cycle, cyclinD1 also seems to

have a role in neuronal morphology. On the other hand, in addition to cyclinD1 increase, whether or not PKC could transcriptionally activate p60-katanin remains to be further investigated. Based on our previous studies on microtubule severing protein p60-katanin, it is known that long microtubules are cut into shorter microtubules by up-regulation of p60-katanin. Besides, in neurons, p60-katanin gives rise to side branch increase by cutting long microtubules into shorter pieces (McNally and Vale, 1993). All of observations indicating the increase in process number and accumulation of microtubules in the cell body are consistent with p60-katanin's known functions in neurons.

When it comes to p-tau and p60-katanin protein levels of neurons in Aβ treated conditions, phosphorylation levels were similar to control groups. Although only PMA treatment increased p-tau levels together with p60-katanin levels (Figure 3.12), there was no increase in phosphorylation state of Aβ treated neurons upon PMA induction (Figure 3.20). Although results inicated that Aβ did not trigger neurodegeneration totally under these experimental conditions, it is possible for Aβ to cause impairments in PKC signaling pathway and prevent activatory effect of PMA, consequently elevation in p-tau and p60-katanin protein levels.

As up-regulation of cell cycle markers in neurons has been shown to ultimately cause apoptosis (Johnson and Stoothoff, 2004; Gasparini, 1998; Atabay and Karabay, 2011), it was important to see if there would be any increase in apoptosis regulatory proteins. Balance between these proteins is thought to determine the cell fate in terms of death or survival. Thus, it was specifically concentrated on pro-apoptotic Bax, anti-apoptotic Bcl-2, and apoptotic caspase3 (Oltvai, 1993). Changes in cleaved PARP level that takes part in downstream of apoptotic signaling pathway was also analyzed. Although up-regulation of cell cycle markers in neurons has been associated with an increase in apoptotic proteins, findings in this study indicating an increase in nuclear cyclinD1 did not actually produce any considerable change in Bax, cleaved PARP and active caspase3 apoptotic proteins, yet there was an increase in the anti-apoptotic Bcl-2 protein. When Bax/Bcl-2 ratio was analyzed for Aβ conditions, it could be seen that Bax/Bcl-2 ratio was slightly increased indicating an early attempt to neurodegeneration.

In only PMA treated neurons, although there was an increase in pro-caspase3, it could not be cleaved to generate active caspase3. It is likely that pro-caspase3 is

counteracted by the increase in the anti-apoptotic Bcl-2 to inhibit apoptosis. In addition to known roles of caspase3 in apoptotic perspective, recent studies introduced a new and provocative point of view for the roles of caspase3. D'Amelio et al. (2010) have shown that inhibition of caspase3 activation altered proteins that are related to differentiation and has dramatically reduced neurite formation. Morphological changes that were observed in PKC-α activated neurons, indicating stunt processes seem to be consistent with these newly attributed functions of caspase-3.

Surprisingly, previously indicated factors, such as nuclear localization of cyclinD1 and increase in p-tau leading neurons into degeneration did not seem to create a neurodegenerative pattern in PMA treated neurons in this study. For instance, in a previous study from our lab (Atabay and Karabay, 2011) in which Pin1 - a regulator of cell cycle progression - was inhibited, increases were observed in p-tau and cleaved caspase3 levels, and ultimately in apoptosis of neurons. Yet, in PKC activation, even though an increase in p-tau was observed there was no increase in cleaved caspase3; and in addition to this, an increase was observed in the anti-apoptotic protein Bcl-2. Therefore, it is probably not solely the increase in cyclinD1 that would lead neurons into apoptosis; it is rather an accompanying increase in cleaved caspase3 or neutralization of it by anti-apoptotic proteins that would determine the fate of neurons between survival and apoptosis in an emerging degenerative condition. Impinges on which signaling pathways in neurons cause activation of cell cycle related proteins and whether or not they could be modulated remain to be the subject of further research.

In conclusion, in addition to its previously known roles in cell cycle regulation, PKC over-activation may have effects causing withdrawal from differentiation in neurons by increasing nuclear cyclinD1 and promoting microtubule re-organization via increasing p60-katanin and Aβ seems to prevent this attributed function of PKC probably by direct Aβ – PKC interaction through its pseudosubstrate site.

REFERENCES

Abramov E., Dolev I., Fogel1 H., Ciccotosto G.D., Ruff E. and Slutsky I. (2009). Amyloid-β as a positive endogenous regulator of release probability at hippocampal synapses. *Nat Neurosci.,* 12(12), 1567-1576.

Ajiro K. (2000). Histone H2B phosphorylation in mammalian apoptotic cells. An association with DNA fragmentation. *J. Biol. Chem.,* 275, 439-443.

Akkor M. and Karabay A. (2010). Production and characterization of a monoclonal antibody against P60-katanin. *Hybridoma,* 29 (6), 531-7.

Amadio M., Battaini F., Pascale A. (2006). The different facets of protein kinases C: old and new players in neuronal signal transduction pathways. *Pharmacol Res*., 54, 317-325.

Arendt T. (2003) Synaptic plasticity and cell cycle activation in neurons are alternative effector pathways: the 'Dr. Jekyll and Mr. Hyde concept' of Alzheimer's disease or the yin and yang of neuroplasticity. *Prog Neurobiol.,* 71(2-3), 83-248.

Atabay K.D. and Karabay A. (2011). Pin1 inhibition activates cyclinD1 and produces neurodegenerative pathology. *J Neurochem.,* 120 (3), 430-9.

Baas P.W., Black M.M. (1989). The basis of polarity in neurons. *TINS*, 12, 211-214.

Baas P.W. (1999). Microtubules and Neuronal Polarity: Lessons from Mitosis. *Neuron*, 22, 23-31.

Baas p.W. (2002). Neuronal Polarity: microtubules strike back. *Nature Cell Biology*, 4, E194-195.

Baas P.W. and Qiang L. (2005). Neuronal microtubules: when the MAP is the roadblock. *Trends Cell Biol,*. 15(4), 183-187.

Baldin V., Lukas J., Marcote M.J., Pagano M., Draetta G. (1993), CyclinD1 1 is a nuclear protein required for cell cycle progression in G1. *Genes Dev,*. 7, 812-821.

Banker G. and Goslin K., (1998), Culturing Nerve Cells (2nd edition). MIT Press, London.

Battaini F., Pascale A., Lucchi L., Pasinetti G.M., Govoni S. (1999), Protein Kinase C Anchoring Deficit in Postmortem Brains of Alzheimer's Disease Patients, *Experimental Neurology*, 159, 559-564.

Besson A. and Yong V.W. (2000). Involvement of p21Waf1/Cip1 in Protein Kinase C Alpha-Induced Cell Cycle Progression. *Mol Cell Biol.,* 20 (13), 4580-4590.

Borgatti P., Mazzoni M., Carini C., Neri L.M., Marchisio M., Bertolaso L., Previati M., Zauli G., Capitani S. (1996). Changes of nuclear protein kinase C activity and isotype composition in PC12 cell proliferation and differentiation. *Exp Cell Res.*, 224(1), 72-8.

Cazaubon S.M., Parker P.J. (1993). Identification of the phosphorylated region responsible for the permissive activation of protein kinase C. *J Biol Chem.*, 268, 17559-17563.

Cazaubon S., Bornancin F., Parker P.J. (1994). Threonine-497 is a critical site for permissive activation of protein kinase Cα. *Biochem J.*, 301, 443-448.

Chauhan A., Chauhan V.P., Brockerhoff H., Wisniewski H.M. (1991). Action of amyloid beta-protein on protein kinase C activity. *Life Sci.* 49, 1555-1562.

Cheng J-J., Wung B-S., Chao Y-J. and Wang D.L. (2001). Sequential activation of protein kinase C (PKC)-α and PKC-ε contributes to sustained RafERKl/2 activation in endothelial cells under mechanical strain. *J. BioL Chem.*, 276, 31368-31375.

Cirrito J.R., Yamada K.A., Finn M.B., Sloviter R.S., Bales K.R., May P.C., Schoepp D.D., Paul S.M., Mennerick S., Holtzman D.M. (2005). Synaptic activity regulates interstitial fluid amyloid-beta levels in vivo. *Neuron*, 48, 913-922.

Currais A., Hortobágyi T., Soriano S. (2009). The neuronal cell cycle as a mechanism of pathogenesis in Alzheimer's disease. *Aging,* 1(4), 363-371.

D'Amelio M., Cavallucci V. and Cecconi F. (2010). Neuronal caspase-3 signaling: not only cell death. *Cell Death and Differentiation* 17, 1104-1114.

De Falco M., Fedele V., De Luca L., Penta R., Cottone G., Cavallotti I., Laforgia V. & De Luca A. (2004). Evaluation of Cyclin D1 expression and its subcellular distribution in mouse tissues. *J. Anat.*, 205, 405-412.

De Strooper B. and Annaert W. (2000). Proteolytic processing and cell biological functions of the amyloid precursor protein. *J Cell Sci.*, 113, 1857-1870.

Dempsey E.C., Newton A.C., MochJy-Rosen D., Fields A.P., Reyland, M.E., Insel, PA., and Messing, R.O. (2000). Protein kinase C isozymes and the regulation of diverse cell responses. *Am. J. Physiol.* 279, L429-L438.

DePaoli-Roach A., Roach P.J., Zucker K.E., Smith S.S. (1986). Selective phosphorylation of human DNA methyltransferase by protein kinase C. *FEBS Lett.* 197, 149-153.

Detjen K.M., Brembeck F.H., Welzel M., Kaiser A., Haller H., Wiedenmann B., Rosewicz S. (2000). Activation of protein kinase Cα inhibits growth of pancreatic cancer cells via p21cip-mediated G1 arrest. *J Cell Sci.*, 113, 3025-3035.

Diehl J.A., Cheng M., Roussel M.F., Sherr C.J. (1998). Glycogen synthase kinase-3b regulates cyclinD1 proteolysis and subcellular localization. *Genes Dev.*, 12, 3499-3511.

Eggert M., Radomski N., Triepier D., Traub P., Jost E. (1991). Identification of phosphorylation sites on murine nuclear lamin C by RP-HPLC and microsequencing. *FEBS Lett.,* 292, 205-209.

Endo T. and Goto S. (1992). Retinoblastoma Gene Product Rb Accumulates during Myogenic Differentiation and Is Deinduced by the Expression of SV40 Large T Antigen1. *J. Biochem.,* 11(2), 427-430.

Ezhevsky S.A., Nagahara H., Vocero-Akbani A.M., Gius D.R., Wei M.C., Dowdy S.F. (1997). Hypo-phosphorylation of the retinoblastoma protein (Rb) by cyclinD1:cdk4/6 complexes results in active Rb. *Cell Biology*, 94, 10699-10704.

Favit A., Grimaldi M., Nelson T.J., Alkon D.L. (1998). Alzheimer's-specific effects of soluble beta-amyloid on protein kinase C-alpha and -gamma degradation in human fibroblasts. *Proc. Natl. Acad. Sci. U. S. A.*, 95, 5562-5567.

Frey M.R., Clark J.A., Leontieva O., Uronis J.M., Black A.R. and Black J.D. (2000). Protein Kinase C Signaling Mediates a Program of Cell Cycle Withdrawal in the Intestinal Epithelium. *J Cell Biol.*, 151(4), 763-777.

Haas M., Jost E. (1993). Functional analysis of phosphorylation sites in human lamin A controlling lamin disassembly, nuclear transport and assembly. *Eur. J. Cell Biol,*. 62, 237-247.

Haass, C. (2004). Take five–BACE and the gamma-secretase quartet conduct Alzheimer's amyloid β-peptide generation. *EMBO J.* 23, 483–488.

Hayes T.E., Valtz N.L. and McKay R.D. (1991). Downregulation of CDC2 upon terminal differentiation of neurons. *New Biol.*, 3, 259-269.

Huang W., Mishra V., Batra S., Dillon I., Mehta K.D. (2004). Phorbol ester promotes histone H3-Ser10 phosphorylation at the LDL receptor promoter in a protein kinase C-dependent manner. *J. Lipid Res.*, 45, 1519-1527.

Iwata N., Higuchi M., Saido TC. (2005). Metabolism of amyloid-beta peptide and Alzheimer's disease. *Pharmacol Ther.*, 108(2), 129-148.

Iwamoto T., Hagiwara M., Hidaka H., Isomura T., Kioussis D., Nakashima I. (1992). Accelerated proliferation and interleukin-2 production of thymocytes by stimulation of soluble anti-CD3 monoclonal antibody in transgenic mice carrying a rabbit protein kinase Cα. *J Biol Chem.*, 267, 18644-18648.

Galderisi U., Jori F.P. and Giordano A. (2003). Cell cycle regulation and neural differentiation. *Oncogene,* 22, 5208-5219.

Gasparini S.G., Racchi M., Binetti M., Trabucchi M., Solerte S.B., Alkon D., Etcheberrigaray G., Gibson H.G., Blass J., Paoletti R., Govoni S. (1998). Peripheral markers in testing pathophysiological hypotheses and diagnosing Alzheimer's disease. *FASEB J.*, 12(1), 17-34.

Giorgi C., Agnoletto C., Baldini C., Bononi A., Bonora M., Marchi S., Missiroli S., Patergnani S., Poletti F., Rimessi A., Zavan B., Pinton P. (2010). Redox Control of Protein Kinase C: Cell- and Disease-Specific Aspects. *Antioxid Redox Signal.*, 13(7), 1051-1085.

Giorgione J.R., Lin J.H., McCammon J.A., Newton A.C. (2006). Increased membrane affinity of the C1 domain of protein kinase C delta compensates for the lack of involvement of its C2 domain in membrane recruitment. *J Biol Chem.,* 281, 1660-1669.

Grady G.C., Mason S.M., Stephen J., Zuniga-Pflucker J.C., Michie A.M. (2004). Cyclic adenosine 5'-monophosphate response element binding protein plays a central role in mediating proliferation and differentiation downstream of the pre-TCR complex in developing thymocytes. *J Immunol.,* 173, 1802-1810.

Herrup K. and Yang Y. (2007). Cell cycle regulation in the postmitotic neuron: oxymoron or new biology? *Nat Rev Neurosci.,* 8(5), 368-78.

Hocevar B.A., Burns D.J., Fields A.P. (1993). Identification of protein kinase C (PKC) phosphorylation sites on human lamin B. Potential role of PKC in nuclear lamina structural dynamics. *J Biol Chem.,* 268, 7545-7552.

Johnson G.V.W. and Stoothoff W.H. (2004). Tau phosphorylation in neuronal cell function and dysfunction. *J Cell Sci.,* 117(24), 5721-5729.

Kamenetz F., Tomita T., Hsieh H., Seabrook G., Borchelt D., Iwatsubo T., Sisodia S., Malinow R. (2003). APP Processing and Synaptic Function. *Neuron,* 37, 925-937.

Karabay A., Yu W., Solowska J.M., Baird D.H., Baas P.W. (2004). Axonal growth is sensitive to the levels of katanin, a protein that severs microtubules. *J Neurosci.,* 24(25), 5778-88.

Khidr L. and Chen P.L. (2006). RB, the conductor that orchestrates life, death and differentiation. *Oncogene,* 25, 5210-5219.

Kraft A.S., Anderson W.B. (1983). Phorbol esters increase the amount of Ca2+, phospholipid-dependent protein kinase associated with plasma membrane. *Nature,* 301, 621-623.

Lee V.M., Goedert M., Trojanowski J.Q. (2001). Neurodegenerative tauopathies. *Annu. Rev. Neurosci.,* 24, 1121-1159.

Lee W., Boo J.H., Jung M.W., Park S.D., Kim Y.H., Kim S.U, and Mook-Jungb I. (2004). Amyloid beta peptide directly inhibits PKC activation. *Mol. Cell. Neurosci.,* 26, 222-231.

Livak K.J. and Schmittgen T.D. (2001). Analysis of Relative Gene Expression Data Using Real-Time Quantitative PCR and the $2^{-\Delta\Delta CT}$ Method. *Methods*, 25, 402-408.

Lo L-W., Cheng J-J., Ciu J-J., Wung B-S., Liu Y-C. and Wang D.L. (2001). Endothelial exposure to hypoxia induces Rge-1 expression involveing PKCa-mediated Ras/Raf-l/ERKl/2 pathway. *J. Cell. Physwl.,* 188, 304-312.

Lodish H. (2003). Molecular Cell Biology (5th ed.) (Vol.20, pp. 826) W.H. Freeman & Company.

Mandil R., Ashkenazi E., Blass M., Kronfeld I., Kazimirsky G., Rosenthal G., Umansky F., Lorenzo P.S., Blumberg P.M., Brodie C. (2001). Protein kinase Cα and protein kinase Cδ play opposite roles in the proliferation and apoptosis of glioma cells. *Cancer Res.,* 61, 4612-4619.

Martelli A.M., Sang N., Borgatti P., Capitani S., Neri L.M. (1999). Multiple biological responses activated by nuclear protein kinase C. *J. Cell. Biochem,*. 74, 499-521.

Martelli A.M., Evangelisti C., Nyakern M., Manzoli F.A. (2006). Nuclear protein kinase C. *Biochim Biophys Acta.*, 1761, 542-551.

Matsunaga Y. (2000). Expression of Cyclin E in postmitotic cells in the central nervous system. *Kokubyo Gakkai Zasshi.*, 67, 169-181.

McNally F.J. and Vale R.D. (1993). Identification of katanin, an ATPase that severs and disassembles stable microtubules. *Cell,* 75, 419-429.

Medkova M. and Cho W. (1999). Interplay of C1 and C2 Domains of Protein Kinase C-α in Its Membrane Binding and Activation. *J Biol Chem.,* 274(28), 19852-19861.

Michie A.M., Soh J-W., Hawley R.G., Weinstein I.B., Zuniga-Pflucker J.C. (2001). Allelic exclusion and differentiation by protein kinase C mediated signals in immature thymocytes. *Proc Natl Acad Sci USA.,* 98, 609-614.

Michie A.M. and Nakagawa R. (2005). The link between PKCα regulation and cellular transformation. *Immunol Lett.*, 96(2), 155-162.

Morley J.E., Farr1 S.A., Banks W.A., Johnson S.N., Yamada K.A., Xu L. (2010). A Physiological Role for Amyloid-β Protein: Enhancement of Learning and Memory. *J Alzheimers Dis.*,19(2), 441-449.

Nagy Z. (2007). The dysregulation of the cell cycle and the diagnosis of Alzheimer's disease. *Biochim Biophys Acta.*, 1772, 402-408.

Nakashima S. (2002). Protein Kinase Cα (PKCα): Regulation and Biological Function. *J Biochem.*, 132(5), 669-675.

Newton A.C. and Johnson J.E. (1998). Protein kinase C: a paradigm for regulation of protein function by two membrane-targeting modules. *Biochim Biophys Acta.*, 1376, 155-172.

Newton A.C. (2001). Protein kinase C: Structure, function, and regulation. *J. Biol. Chem.*, 270, 28495-28498.

Newton A.C. (2003). Regulation of the ABC kinases by phosphorylation: PKC as a paradigm. *Biochem J.,* 370, 361-371.

Nishizuka Y. (1992). Intracellular signaling by hydrolysis of phoapholipids and activation of protein kinase C. *Science*, 268, 607-614.

Nishizuka Y. (1995). Protein kinase C and lipid signaling for sustained cellular responses. *FASEB J.,* 9, 484-496.

Nishizuka Y. (2001). The protein kinase C family and lipid mediators for transmembrane signaling and cell regulation. *Alcohol. Clin. Exp. Res.* 25(5 Suppl. ISBRA), 3S–7S.

Oancea E and Meyer T. (1998). Protein kinase C as a molecular machine for decoding calcium and diacylglycerol signals. *Cell*, 95, 307-318.

Okano H.J., Pfaff D.W. and Gibbs R.B. (1993). RB and Cdc2 expression in brain: correlations with 3H-thymidine incorporation and neurogenesis. *J. Neurosci.*, 13, 2930-2938.

Oltvai Z.N., Milliman C.L. and Korsmeyer S.J. (1993). Bcl-2 heterodimerizes in vivo with a conserved homolog, Bax, that accelerates programmed cell death. *Cell*, 74, 609-619.

Omri B., Breton M.F., Pavlovic-Hournac M. (1987). Characteristics of thyroid protein kinase C. Different Ca2 requirement for the phosphorylation of endogenous proteins and of H1 histone. *Eur. J. Biochem.*, 165, 83-90.

Pakaski M., Balaspiri L., Checler F., Kasa P. (2002). Human amyloid-β causes changes in the levels of endothelial protein kinase C and it's α isoform in vitro. *Neurochem. Int.* 41, 409- 414.

Parekh D.B., Ziegler W. and Parker P.J. (2000). Multiple pathways control protein kinase C phosphorylation. *EMBO J.*, 19, 496-503.

Pears C., Stabel S., Cazaubon S., Parker P.J. (1992). Studies on the phosphorylation of protein kinase C-α. *Biochem J.*, 283, 515-518.

Pommier Y., Kerrigan D., Hartman K.D., Glazer R.I. (1990). Phosphorylation of mammalian DNA topoisomerase I and activation by protein kinase C. *J. Biol. Chem.*, 265, 9418-9422.

Quarmby L.M. and Lohret T.A. (1999). Microtubule severing. *Cell Motil Cytoskeleton.*, 43, 1-9.

Sahyoun N., Wolf M., Besterman J., Hsieh T., Sander M., LeVine III H., Chang K.J., Cuatrecasas P. (1986). Protein kinase C phosphorylates topoisomerase II: topoisomerase activation and its possible role in phorbol ester-induced differentiation of HL-60 cells. *Proc. Natl. Acad. Sci. U. S. A.*, 83, 1603-1607.

Schmetsdorf S., Gartner U. & Arendt T. (2005). Expression of cell-cycle related proteins in developing and adult mouse hippocampus. *Int. J. Devl. Neurosci.*, 23, 101-112.

Schmetsdorf S., Gartner U. & Arendt T. (2007). Prenatal development of expression of cell-cycle proteins and its persistence in the adult neocortex. *Cereb. Cortex*, 17, 1821-1829.

Schmetsdorf S., Arnold E., Holzer M., Arendt T. and Gartner U. (2009). A putative role for cell cycle-related proteins in microtubule-based neuroplasticity. *Eur J Neurosci.*, 29, 1096-1107.

Schwartz E.I., Smilenov L.B., Price M.A., Osredkar T., Baker R.A., Ghosh S., Shi F.D., Vollmer T.L., Lencinas A., Stearns D.M., Gorospe M. & Kruman I.I. (2007). Cell cycle activation in postmitotic neurons is essential for DNA repair. *Cell Cycle*., 6, 318-329.

Shambaugh III G.E., Lee R.J., Watanabe G., Erfurth F., Karnezis A.N., Koch A.E., Haines III G.K., Halloran M., Brody B.A. and Pestell R.G. (1996). Reduced cyclin D1 expression in the cerebella of nutritionally deprived rats correlates with developmental delay and decreased cellular DNA synthesis. *J. Neuropathol. Exp. Neurol.,* 55, 1009-1020.

Sicinski P., Donaher J.L., Parker S.B., Li T., Fazeli A., Gardner H., Haslam S.Z., Bronson R.T., Elledge S.J. and Weinberg R.A. (1995). Cyclin D1 provides a link between development and oncogenesis in the retina and breast. *Cell,* 82, 621-630.

Simmons L.K., May P.C., Tomaselli K.J., Rydel R.E., Fuson K.S., Brigham E.F., Wright S., Lieberburg I., Becker G.W. and Brems D.N. (1994). Secondary structure of amyloid beta peptide correlates with neurotoxic activity in vitro. *Mol. Pharmacology,* 45(3):373-37.

Soh J.W. and Weinstein I.B. (2003). Roles of Specific Isoforms of Protein Kinase C in the Transcriptional Control of CyclinD1 and Related Genes. *J Biol Chem.,* 278(36), 34709-34716.

Takai Y., Kishimoto A., Inoue M., and Nishizuka Y. (1977). Studies on a cyclic nucleotide-independent protein kinase and its proenzyme in mammalian tissues. I. Purification and characterization of an active enzyme from bovine cerebellum. *J Biol Chem.*, 252, 7603-7609.

Tamaru T., Okada M. and Nakagawa H. (1994). Differential expression of D type cyclins during neuronal maturation. *Neurosci. Lett.,* 168, 229-232.

Tamaru T., Trigun S.K., Okada M. and Nakagawa H. (1993). Identification of cells expressing a D type G1 cyclin in matured brain: implication for its role in neuronal function. *Neurosci. Lett.,* 153, 169-172.

Tokui T., Inagaki M., Nishizawa K., Yatani R., Kusagawa M., Ajiro K., Nishimoto Y., Date T., Matsukage A. (1991). Inactivation of DNA polymerase β by in vitro phosphorylation with protein kinase C. *J. Biol. Chem.,* 266, 10820-10824.

Vale R.D. (2000). AAA proteins. Lords of the ring. *J.Cell Biol.*, 150(1), 13-19.

van Grunsven L.A., Thomas A., Urdiales J.L., Machenaud S., Choler P., Durand I. and Rudkin B.B. (1996). Nerve growth factor-induced accumulation of PC12 cells expressing cyclin D1: evidence for a G1 phase block. *Oncogene,* 12, 855-862.

Ways D.K., Kukoly C.A., deVente J., Hooker J.L., Bryant W.O., Posekany K.J., Fletcher D.J., Cook P.P., Parker P.J. (1995). MCF-7 breast cancer cells transfected with protein kinase C-α exhibit altered expression of other protein kinase C isoforms and display a more aggressive neoplastic phenotype. *J Clin Invest.*, 95, 1906-1915.

Xiong W., Pestell R. and Rosner M.R. (1997). Role of cyclins in neuronal differentiation of immortalized hippocampal cells. *Mol. Cell. Biol.*, 17, 6585-6597.

Yan G.Z and Ziff E.B. (1995). NGF regulates the PC12 cell cycle machinery through specific inhibition of the cdk kinases and induction of cyclin D1. *J. Neurosci.*, 15, 6200-6212.

Yang Y., Geldmacher D.S. and Herrup K. (2001). DNA Replication Precedes Neuronal Cell Death in Alzheimer's Disease. *J. Neurosci.*, 21(8), 2661-2668.

Yu W., Qiang L., Solowska J.M., Karabay A., Korulu S., Baas P.W. (2008). The microtubule-severing proteins spastin and katanin participate differently in the formation of axonal branches. *Mol Biol Cell.*, 19(4), 1485-98.

APPENDICES

APPENDIX A : qRT-PCR efficiency and error rate values.

APPENDIX B : qRT-PCR data generated by relative expression software tool.

APPENDIX C : Data comparison table for the different experimental conditions.

APPENDIX A : qRT-PCR efficiency and error rate values.

Table A.1 : qRT-PCR efficiency and error rate values.

Gene	Efficiency	Error Rate
Beta actin	1.899	0.0547
GAPD	1.968	0.00875
cyclinA	1.973	0.0154
cyclinB1	1.810	0.0141
cyclinD1	1.918	0.06
cyclinE	1.859	0.009
cdk1	1.863	0.0290
cdk2	1.980	00136
cdk4	1.934	0.00980
p27	1.889	0.00219

APPENDIX B : qRT-PCR data generated by relative expression software tool.

Table B.1 : qRT-PCR data for PMA treated neurons generated by relative expression software tool.

Gene	Type	Reaction Efficiency	Expression	Std. Error	95% C.I.	P(H1)	Result
cycA	TRG	1,0	1,995	0,114 - 32,850	0,104 - 40,316	0,487	
cycB	TRG	1,0	3,349	0,446 - 24,475	0,329 - 37,862	0,164	
cycD	TRG	1,0	6,733	2,106 - 21,283	1,649 - 27,039	0,020	UP
cycE	TRG	1,0	1,236	0,261 - 5,619	0,245 - 6,480	0,482	
cdk1	TRG	1,0	3,008	2,219 - 4,440	1,468 - 4,978	0,000	UP
cdk2	TRG	1,0	1,900	0,453 - 7,308	0,434 - 9,227	0,350	
cdk4	TRG	1,0	0,937	0,258 - 2,700	0,223 - 5,026	0,905	
p27	TRG	1,0	0,803	0,180 - 2,872	0,177 - 4,789	0,568	
actin	REF	1,0	0,894				
gapd	REF	1,0	1,118				

Legend:
P(H1) - Probability of alternate hypothesis that difference between sample and control groups is due only to chance.
TRG - Target
REF - Reference

Interpretation

cycA sample group is not different to control group. P(H1)=0,487

cycB sample group is not different to control group. P(H1)=0,164

cycD is UP-regulated in sample group (in comparison to control group) by a mean factor of 6,733 (S.E. range is 2,106 - 21,283).
cycD sample group is different to control group. P(H1)=0,020

cycE sample group is not different to control group. P(H1)=0,482

cdk1 is UP-regulated in sample group (in comparison to control group) by a mean factor of 3,008 (S.E. range is 2,219 - 4,440).
cdk1 sample group is different to control group. P(H1)=0,000

cdk2 sample group is not different to control group. P(H1)=0,350

cdk4 sample group is not different to control group. P(H1)=0,905

p27 sample group is not different to control group. P(H1)=0,568

Table B.2 : qRT-PCR data for Gö6976 treated neurons generated by relative expression software tool.

Gene	Type	Reaction Efficiency	Expression	Std. Error	95% C.I.	P(H1)	Result
cycA	TRG	1,0	1,162	0,081 - 16,363	0,068 - 20,078	0,514	
cycB	TRG	1,0	1,823	0,255 - 13,194	0,188 - 18,256	0,487	
cycD	TRG	1,0	0,958	0,327 - 2,866	0,256 - 3,646	0,843	
cycE	TRG	1,0	1,054	0,221 - 4,810	0,208 - 5,545	0,597	
cdk1	TRG	1,0	1,463	1,074 - 2,147	0,717 - 2,407	0,097	
cdk2	TRG	1,0	1,465	0,342 - 6,089	0,328 - 6,687	0,496	
cdk4	TRG	1,0	1,134	0,283 - 3,592	0,244 - 6,683	0,843	
p27	TRG	1,0	0,864	0,165 - 4,184	0,159 - 5,099	0,512	
actin	REF	1,0	0,972				
gapd	REF	1,0	1,029				

Legend:
P(H1) - Probability of alternate hypothesis that difference between sample and control groups is due only to chance.
TRG - Target
REF - Reference

Interpretation

cycA sample group is not different to control group. P(H1)=0,514

cycB sample group is not different to control group. P(H1)=0,487

cycD sample group is not different to control group. P(H1)=0,843

cycE sample group is not different to control group. P(H1)=0,597

cdk1 sample group is not different to control group. P(H1)=0,097

cdk2 sample group is not different to control group. P(H1)=0,496

cdk4 sample group is not different to control group. P(H1)=0,843

p27 sample group is not different to control group. P(H1)=0,512

Table B.3 : qRT-PCR data for 1 h Gö6976 followed by 23 h PMA treated neurons generated by relative expression software tool.

Gene	Type	Reaction Efficiency	Expression	Std. Error	95% C.I.	P(H1)	Result
cycA	TRG	1,0	1,331	1,200 - 1,478	1,164 - 1,523	0,000	UP
cycB	TRG	1,0	3,188	2,710 - 3,755	2,620 - 3,881	0,000	UP
cycD	TRG	1,0	3,870	3,432 - 4,367	3,374 - 4,440	0,000	UP
cycE	TRG	1,0	1,233	1,147 - 1,328	1,109 - 1,372	0,000	UP
cdk1	TRG	1,0	2,580	2,435 - 2,736	2,387 - 2,789	0,000	UP
cdk2	TRG	1,0	1,744	1,663 - 1,833	1,602 - 1,900	0,000	UP
cdk4	TRG	1,0	1,019	0,747 - 1,393	0,724 - 1,436	0,670	
p27	TRG	1,0	0,961	0,870 - 1,067	0,817 - 1,133	0,337	
actin	REF	1,0	0,839				
gapd	REF	1,0	1,191				

Legend:
P(H1) - Probability of alternate hypothesis that difference between sample and control groups is due only to chance.
TRG - Target
REF - Reference

Interpretation

cycA is UP-regulated in sample group (in comparison to control group) by a mean factor of 1,331 (S.E. range is 1,200 - 1,478).
cycA sample group is different to control group. P(H1)=0,000

cycB is UP-regulated in sample group (in comparison to control group) by a mean factor of 3,188 (S.E. range is 2,710 - 3,755).
cycB sample group is different to control group. P(H1)=0,000

cycD is UP-regulated in sample group (in comparison to control group) by a mean factor of 3,870 (S.E. range is 3,432 - 4,367).
cycD sample group is different to control group. P(H1)=0,000

cycE is UP-regulated in sample group (in comparison to control group) by a mean factor of 1,233 (S.E. range is 1,147 - 1,328).
cycE sample group is different to control group. P(H1)=0,000

cdk1 is UP-regulated in sample group (in comparison to control group) by a mean factor of 2,580 (S.E. range is 2,435 - 2,736).
cdk1 sample group is different to control group. P(H1)=0,000

cdk2 is UP-regulated in sample group (in comparison to control group) by a mean factor of 1,744 (S.E. range is 1,663 - 1,833).
cdk2 sample group is different to control group. P(H1)=0,000

cdk4 sample group is not different to control group. P(H1)=0,670

p27 sample group is not different to control group. P(H1)=0,337

Table B.4 : qRT-PCR data for 24 h amyloid beta treated neurons generated by relative expression software tool.

Gene	Type	Reaction Efficiency	Expression	Std. Error	95% C.I.	P(H1)	Result
cycA	TRG	1,0	1,236	0,924 - 1,466	0,870 - 2,031	0,208	
cycB	TRG	1,0	0,792	0,134 - 4,165	0,093 - 8,130	0,744	
cycD	TRG	1,0	1,090	0,699 - 1,490	0,526 - 1,805	0,751	
cycE	TRG	1,0	0,660	0,425 - 0,961	0,398 - 1,446	0,112	
cdk1	TRG	1,0	0,952	0,378 - 2,248	0,228 - 4,385	0,897	
cdk2	TRG	1,0	0,900	0,520 - 1,407	0,419 - 2,451	0,790	
cdk4	TRG	1,0	1,713	0,789 - 5,346	0,686 - 10,019	0,448	
p27	TRG	1,0	1,256	0,844 - 2,388	0,732 - 3,212	0,601	
actin	REF	1,0	1,271				
gapd	REF	1,0	0,787				

Legend:
P(H1) - Probability of alternate hypothesis that difference between sample and control groups is due only to chance.
TRG - Target
REF - Reference

Interpretation

cycA sample group is not different to control group. P(H1)=0,208

cycB sample group is not different to control group. P(H1)=0,744

cycD sample group is not different to control group. P(H1)=0,751

cycE sample group is not different to control group. P(H1)=0,112

cdk1 sample group is not different to control group. P(H1)=0,897

cdk2 sample group is not different to control group. P(H1)=0,790

cdk4 sample group is not different to control group. P(H1)=0,448

p27 sample group is not different to control group. P(H1)=0,601

Table B.5 : qRT-PCR data for 24 h amyloid beta and 24 h PMA treated neurons generated by relative expression software tool.

Gene	Type	Reaction Efficiency	Expression	Std. Error	95% C.I.	P(H1)	Result
cycA	TRG	1,0	2,518	1,575 - 5,499	1,392 - 6,525	0,129	
cycB	TRG	1,0	1,673	1,065 - 3,121	0,805 - 4,399	0,249	
cycD	TRG	1,0	3,446	2,041 - 10,326	1,954 - 12,258	0,133	
cycE	TRG	1,0	1,503	0,866 - 4,726	0,827 - 5,366	0,741	
cdk1	TRG	1,0	3,232	2,054 - 5,078	1,367 - 7,899	0,082	
cdk2	TRG	1,0	2,031	1,126 - 6,257	1,031 - 8,003	0,327	
cdk4	TRG	1,0	0,971	0,631 - 2,642	0,627 - 3,122	0,969	
p27	TRG	1,0	2,078	1,314 - 5,685	1,129 - 7,220	0,289	
actin	REF	1,0	1,197				
gapd	REF	1,0	0,835				

Legend:
P(H1) - Probability of alternate hypothesis that difference between sample and control groups is due only to chance.
TRG - Target
REF - Reference

Interpretation

cycA sample group is not different to control group. P(H1)=0,129

cycB sample group is not different to control group. P(H1)=0,249

cycD sample group is not different to control group. P(H1)=0,133

cycE sample group is not different to control group. P(H1)=0,741

cdk1 sample group is not different to control group. P(H1)=0,082

cdk2 sample group is not different to control group. P(H1)=0,327

cdk4 sample group is not different to control group. P(H1)=0,969

p27 sample group is not different to control group. P(H1)=0,289

APPENDIX C : Data comparison table for the different experimental conditions.

Table C.1 : Data comparison for the different experimental conditions.

condition / analysis		CONTROL	PMA	Gö6976	Gö6976 + PMA	Aβ	Aβ + PMA
cDNA	cycA	1	1	1	1.3	1	1
	cycB	1	1	1	3.2	1	1
	cycD	1	7x	1	3.9	1	1
	cycE	1	1	1	1.2	1	1
	cdk1	1	3	1	2.6	1	1
	cdk2	1	1	1	1.7	1	1
	cdk4	1	1	1	1	1	1
IF	cycA	1	1	0.7	1	n/a	n/a
	cycB	1	1	1	1	n/a	n/a
	cycD	1	1.5	1	1	1	1
	cycE	1	2.2	1	1.7	n/a	n/a
	pRb	1	0.5	1	n/a	1	1
western	cycD	1	3	n/a	n/a	n/a	n/a
	pRb	1	0.5	1	n/a	n/a	n/a
	ppRb	1	2	1	n/a	n/a	n/a
	p-tau	1	2.6	n/a	n/a	1	1
	p60-katanin	1	1.5	n/a	n/a	1	1
	pGSK3β	1	1	n/a	n/a	1	1
	Bax/Bcl2	1	decrease	n/a	n/a	increase	increase
morphology	Av. Total Process Length	1	0.75	n/a	1	1	1
	Av. Process Number	1	1.5	n/a	0.8	0.5	0.5

CURRICULUM VITAE

Name Surname:	Şirin KORULU KOÇ
Place and Date of Birth:	Bulgaria, 07.07.1980
Address:	I.T.U. Science and Letters Faculty, Department of Molecular Biology and Genetics, 34469, Maslak, Istanbul, Turkey
E-Mail:	sirinkorulu@gmail.com
B.Sc.:	I.T.U. Molecular Biology and Genetics
M.Sc.:	I.T.U. Molecular Biology – Genetics and Biotechnology

PUBLICATIONS/PRESENTATIONS ON THE THESIS

- **Korulu S.**, Yildiz-Unal A., Yuksel M. and Karabay A., Elevated cyclinD1 level causes retraction of processes via katanin increase in hippocampal neurons through protein kinase C signaling. (Submitted to *European Journal of Neuroscience*)
- **Korulu S.,** Yıldız A., Atabay K.D., Karabay A. From Neurodegeneration to Regeration. *The EMBO (European Molecular Biology Organization) Meeting*. 4-7 September 2010, Barcelona, İspanya.
- **Korulu S.** and Karabay A. Understanding the Role of PKC in Neurons and Neurodegeneration. *International Neuropsychological Society 2010 Mid-Year Meeting.* 30 June-3 July 2010, Cracow, Polonya
- Akbalık G., Akkor M., Dilsizoğlu A., Esen D., **Korulu S.,** Yıldız A., Karabay A. Mikrotubul İlişkili proteinler ve Nörodejenerasyon. *İTÜ Moleküler Biyoloji ve Genetik Kulübü, Moleküler Biyoloji ve Genetik Öğrenci Kongresi,* 8-11 Eylül 2007, İTÜ, İstanbul.
- **Korulu S**., Ünal A., Neğiş Y., Atabay K.D., Karabay A. Nöronlarda Hücre Siklüs Belirteçlerinin Aktivasyonu. *Uluslar arası katılımlı IV. İTÜ Moleküler Biyoloji ve Genetik Öğrenci Kongresi*, 27-31 Ağustos 2010, İTÜ, İstanbul.
- **Korulu S.,** Yıldız A., Atabay K.D., Karabay A. Nöronlarda Mitotik Belirteçlerin Aktivasyonunun Kontrolü, *XI. Ulusal Tıbbi Biyoloji ve Genetik Kongresi,* 28-31 Ekim 2009, Bodrum